Institut für Wasserbau · Universität Stuttgart

Mitteilungen

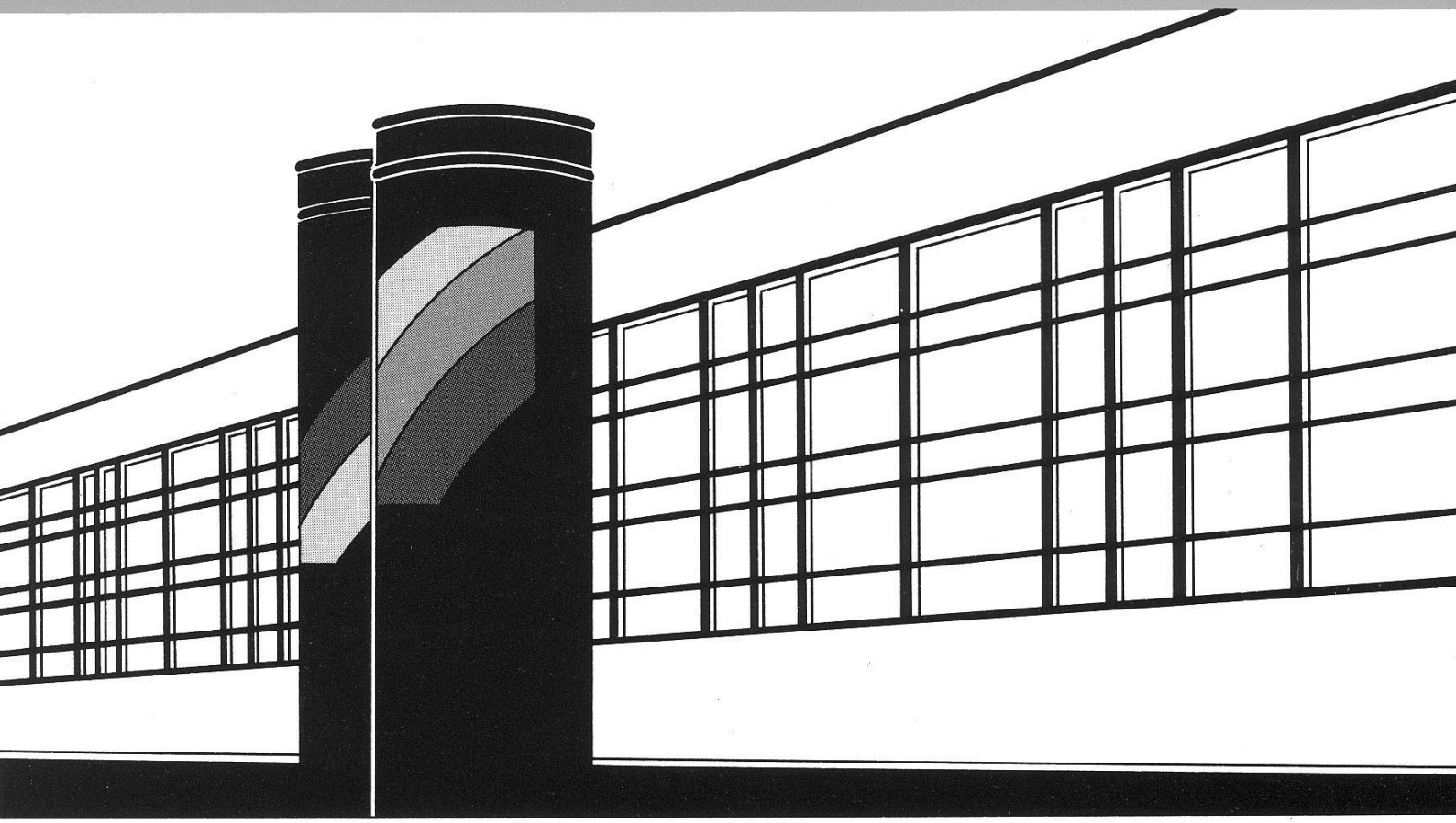

Heft 208 Nguyen Nghia Hung

Sediment dynamics in the floodplain of the Mekong Delta, Vietnam

Sediment dynamics in the floodplain of the Mekong Delta, Vietnam

Von der Fakultät Bau- und Umweltingenieurwissenschaften der Universität Stuttgart zur Erlangung der Würde eines Doktor-Ingenieurs (Dr.-Ing.) genehmigte Abhandlung

Vorgelegt von

Nguyen Nghia Hung

aus Nghe An, Vietnam

Hauptberichter: Prof. Dr. rer. nat. Dr.-Ing. András Bárdossy

Mitberichter: Prof. Dr. rer. nat. Dr.-Ing. Bruno Merz

Tag der mündlichen Prüfung: 16. September 2011

Institut für Wasserbau
der Universität Stuttgart
2011

Heft 208

Sediment dynamics in the floodplain of the Mekong Delta, Vietnam

von
Dr.-Ing.
Nguyen Nghia Hung

Eigenverlag des Instituts für Wasserbau
der Universität Stuttgart
2011

D93 Sediment dynamics in the floodplain of the Mekong Delta, Vietnam

Bibliografische Information der Deutschen Nationalbibliothek
Die Deutsche Nationalbibliothek verzeichnet diese Publikation in der Deutschen Nationalbibliografie; detaillierte bibliografische Daten sind im Internet über http://www.d-nb.de abrufbar

Nguyen Nghia Hung:
Sediment dynamics in the floodplain of the Mekong Delta, Vietnam / von Nguyen Nghia Hung. Institut für Wasserbau,
Universität Stuttgart. - Stuttgart: Inst. für Wasserbau, 2011

(Mitteilungen / Institut für Wasserbau,
Universität Stuttgart: H. 208).
Zugl.: Stuttgart, Univ., Diss., 2011
ISBN 978-3-942036-12-2
NE: Institut für Wasserbau <Stuttgart>: Mitteilungen

Herausgegeben 2011 vom Eigenverlag des Instituts für Wasserbau

Druck: Document Center S. Kästl, Ostfildern

"I am turned into a sort of machine for observing facts & grinding out conclusions"

Charles Darwin

Abstract

The Mekong Delta is one of the largest and most intensively used estuaries in the world. It experiences annual widespread flooding, which provide the basis of livelihood for about 17 million people in the Mekong Delta, but they also pose a considerable hazard when extreme events exceed protection levels. Especially since the Delta in Vietnam is intensively used for agriculture, the pristine natural floodplains have been altered to channel networks, dike rings, paddy fields and aquaculture ponds. Sediment dynamics play an important role in carrying contaminants, bacteria, nutrients, heavy metals, phytoplankton, pesticides, etc. They are the primary source for the productivity of biota in floodplains as well as a sustainable agro-ecosystem within the Delta. However, little is known about the dynamics of these suspended sediments, including multi-processes erosion, deposition, and suspension in the complex channel network of the Delta. In particular, quantitative analyses are lacking, mainly because of lacking data about the inundation processes in the floodplains.

In 2008, therefore, a comprehensive in-situ monitoring scheme to monitor floodplain inundation as well as the dynamics of suspended sediment was established in a study area of the North-Eastern part of the Delta, the Plain of Reeds. The in-situ monitoring system is equipped with twenty-one water level probes and seven water quality monitoring stations. They all have a robust design, autonomous power supply, and the ability to gather reliable data over a long period of time with a high temporal resolution. The water quality parameters include suspended sediment concentration, pH, EC (electrical conductivity) and water temperature. Sediment traps were installed additionally and used in combination with recorded suspended sediment loads to investigate deposition and erosion in the floodplains. This in-situ data collection was complemented by high-resolution inundation maps derived from the TerraSAR-X satellite. Hence, the floodplain hydrology of the Delta could be described quantitatively for the first time. In detail, the present study investigates: (1) spatial and temporal floodplain inundation processes, (2) anthropogenic influence on floodplain hydrology, (3) the tidal influence on flow regime, (4) suspended sediment dynamics, and (5) the erosion and deposition processes during flood season. These processes were analysed quantitatively, providing insights into basic control parameters, dynamics of the processes and the quantity and timing of human interference. The practical contribution of this study is to fill the knowledge gaps in water resources management in order to foster a sustainable future development of the Delta. The scientific contributions are the new ideas in the in-situ monitoring system for floodplain inundation study. In particular, it provided insights into the sedimentation process and enabled an estimation of the key parameters for deposition and erosion as a basis for future model based quantitative estimations of floodplain sedimentation.

Kurzfassung

Das Mekong Delta gehört zu den größten und intensivst genutzten Ästuare der Welt. Die jährliche und weitverbreitete Überflutung stellt sowohl die Lebensgrundlage, als auch die Hauptgefährdung für mehr als 17 Millionen Menschen dar. In Folge der intensiven Landwirtschaft werden die ursprünglichen Überflutungsflächen im vietnamesischen Teil des Deltas heute von einem Kanalnetzwerk durchzogen und durch Deiche in Nutzflächen für Landwirtschaft und Aquakulturen geteilt. Sedimentdynamiken spielen eine wichtige Rolle beim Transport von Schadstoffen, Bakterien, Nährstoffen, Schwermetallen, Phytoplankton und Pestiziden. Sie sind eine wichtige Quelle für die biologische Produktivität auf den Überflutungsflächen und für ein nachhaltiges Agra-Ökosystem im Delta.

Betrachtet man Prozesse wie Erosion, Deposition und Suspension ist jedoch wenig bekannt über deren Dynamik in diesem komplexen System. Besonders quantitative Analysen fehlen aufgrund von nur spärlichen, bzw. gar nicht verfügbaren Daten zu Überflutungsprozessen auf den Überflutungsflächen des Deltas.

Aus diesem Grund wurde im Jahr 2008 ein umfassendes *in-situ* Monitoring System angelegt um die Überschwemmungen und die Sedimentdynamiken im Untersuchungsgebiet im Tam Nong Distrikt, Dong Thap Provinz, zu erfassen. Das Monitoring System besteht aus 21 Wasserstandssensoren und 7 Wasserqualitätsstationen. Diese baulich robusten Stationen mit autonomer Stromversorgung sind in der Lage hoch aufgelöste Daten über eine lange Zeitspanne zu liefern. Die Parameter zur Wasserqualität beinhalten suspendierte Sedimentfrachten, pH-Wert, elektrischen Leitfähigkeit (EC) und Wassertemperatur. Zusätzlich wurden Sedimentfallen in Kombination mit de Trübungssensoren verwendet um Deposition und Erosion auf den Überflutungsflächen zu untersuchen. Vervollständigt wurden diese Daten mit hoch aufgelösten Überflutungskarten aus TerraSAR-X Satellitendaten. Somit können erstmalig die relevanten hydrologischen Prozessee im Überschwemmungsgebiet quantifiziert werden. Im Detail untersucht diese Studie (1) die räumliche und zeitliche Dynamik der Überflutungsprozesse, (2) den anthropogenen Einfluss darauf und (3) den Einfluss des Gezeitenganges auf die Hydrologie der Überflutungsflächen, (4) die Dynamik der suspendierten Sedimente und, (5) die Erosions- und Depositionsprozesse während der Hochwassersaison auf den Überflutungsflächen.

Die quantitative Analyse ermöglicht die Bestimmung grundlegender Kontrollparameter und Quantifizierung dynamischer Prozesse, sowie die Identifikation des menschlichen Einflusses. Der angewandte Beitrag diese Arbeit schließt die systematische Lücke im Management von Wasserressourcen als Grundlage für eine nachhaltige Entwicklung des Mekong Deltas. Der wissenschaftliche Beitrag umfasst Konzepte zur messtechnischen Erfassung der Prozesse in Überflutungsflächen. Im Besonderen werden Einblicke in Sedimentationsprozesse gewährt

und somit die Schätzung von Schlüsselparametern ermöglicht, mit deren Hilfe eine flächenhafte Abschätzung der Erosion und Deposition im Delta erfolgen kann.

Das in-situ Monitoringsystem

Die in der Literatur beschriebenen praktischen Probleme bei der Untersuchung von Überschwemmungsgebieten lassen sich wie folgt zusammenfassen: (1) die Unregelmäßigkeit und die Unberechenbarkeit der Überschwemmung, (2) das Schadenspotential der Flut für die Instrumentierung. Das in-situ Monitoring System, das für diese Studie im Mekong Delta entwickelt wurde ist in dieser Hinsicht einzigartig. Das Monitoring System wurde 2008 installiert und registrierte seither Hochwasser und die Sedimentdynamik auf den Überschwemmungsflächen automatisch mit autonomer Stromversorgung. Bis zum jetzigen Zeitpunkt arbeitet das System zufriedenstellend zuverlässig. Die Zeitreihen für Wasserstand, Konzentration der suspendierten Sedimente, Wassertemperatur, elektrische Leitfähigkeit und pH-Wert sind einzigartig für das Mekong Delta. Dieser Datensatz des Monitoringsystems ist daher ein wichtiger Beitrag zur Füllung der Wissenslücken über die Sedimentdynamik im Kanalsystem und insbesondere auf den Überschwemmungsflächen des Deltas.

Charakterisierung der Prozesse auf den Überflutungsflächen

Während die großskaligen Hochwassercharakteristika gut bekannt sind, ist der Einfluss von Kontrollmaßnahmen auf die Prozesse auf den Überflutungsflächen noch nicht im Detail betrachtet worden. Die Hochwasserdynamik auf den Überflutungsflächen im Mekong Delta ist praktisch unbekannt. Diese Studie quantifiziert erstmalig die dominanten Mechanismen, exemplarisch für das Gebiet "Plain of Reeds" im nordöstlichen Teil des vietnamesischen Deltas.

a) Die Hochwassersaison kann in drei verschiedene Phasen mit eigenen hydraulischen Eigenschaften unterteilt werden: Eine „steigende Phase“, in der die Überflutung der Flächen durch die Höhe der Deiche und die Kontrolle von Deichschleusen reguliert wird, eine „hohe Phase“, in welcher die Überflutungsflächen und die Kanäle hydraulisch verbunden sind und Überflutungen von der natürlichen Fließcharakteristik bestimmt werden. Zuletzt eine „fallende Phase“, in der bei fallenden Wasserständen Wasser aus den Überflutungsflächen gepumpt wird und diese somit von den Kanälen getrennt werden.

b) Der anthropogene Einfluss durch den Einsatz von Deichschleusen und Pumpen auf die Überflutung konnte quantifiziert werden. Die hydraulische Anbindung zwischen Kanälen und verschiedenen Typen von Überflutungsflächen ist verschieden. Überflutungsflächen in hohen Deichringen zeigen eine schwächere hydraulische Verbindung mit den Kanälen, die durch die Kapazität und Steuerung der Deichschleusen bestimmt wird. Die Überflutungsflächen mit niedrigen Deichringen sind direkter mit den Kanälen verbunden. Aus diesem Grund zeigen die heutigen Überflutungen im Vergleich zu den einheitlichen

Mustern der Vergangenheit ein unstrukturiertes, lückenhaftes Bild. Hydraulische Modelle für das Mekong Delta vernachlässigen diese Komponente häufig. Bei der Implementierung oder Auswertung eines solchen Modells ist es also notwendig zu prüfen, ob der anthropogene Einfluss angemessen berücksichtigt wurde.

c) Fernerkundungsdaten werden heute ausgiebig bei Analyse von hydrologischen und hydraulischen Modellen genutzt. Im Mekong Delta sind hochauflösende und hoch genaue Daten notwendig da es sich bei dem Deich- und Kanalnetzwerk um sehr dünne, lineare Strukturen handelt. Trotzdem stellen diese Schlüsselfaktoren für den Überflutungsprozess dar. In dieser Arbeit wurden TerraSAR-X Daten verwendet, mit denen die Überflutungskarten mit hoher Genauigkeit und Auflösung (bis zu 3m) für das Untersuchungsgebiet erstellt wurden. Die Karten erwiesen sich als ausgesprochen wertvolle Quelle für die Erfassung der flächigen Überflutungsprozesse. Durch die kurze Wellenlänge des X-Bandes kann es allerdings zu Interferenzen und somit fehlerhaften Kartierungen bei hohen und dichten Altocumulus Wolken mit hohem Wassergehalt – also Wolken, die typisch für tropische konvektive Gewitterstürme sind - kommen.

Dynamik der suspendierten Sedimente

Die jährliche Fracht an suspendierten Sedimenten, die das Mekong Delta erreichen, beträgt ca. 160 Millionen Tonnen (Oanh et al., 2002; Walling, 2008). Davon werden 6 Million Tonnen in den Tonle Sap See abgeleitet und ca. 2 Millionen Tonnen kommen zurück in den Mekong, wenn sich die Fließrichtung umgekehrt (Kummu et al., 2008). Eine detaillierte Datenbasis für das Mekong Einzugsgebiet existiert allerdings nicht und aus diesem Grund gehört die Sedimentdynamik zu einer Fragestellung, die zu den größten Missverständnissen zwischen Managern und Wissenschaftlern führte (Campbell, 2007). Das Kanalnetzwerk im Mekong Delta spielt eine wichtige Rolle bei der Verteilung der Sedimentfracht vom Mekong auf die Überflutungsflächen. Basierend auf den Messungen von drei Hochwassersaisons können folgende wichtige Charakteristika zur Sedimentdynamik beschrieben werden:

a) Die Sedimentdynamik auf den Überflutungsflächen im Mekong Delta hängt von zwei Mechanismen ab: zum einem der Hochwasserwelle und zum anderen von den Gezeiten, die mit einer höheren Häufigkeit auftreten. Die Resultate aus drei Jahren Monitoring von suspendierten Sedimenten (SS) zeigen: (1) während des Niedrigwassers ist die Konzentration von SS ca. 50 mg/l und sinkt in Folge der Gezeiten bedingten Flut auf ca. 20 mg/l. (2) Zum jährlichen Hochwasser beträgt die maximale Konzentration ca. 200 mg/l.

b) Der anthropogene Einfluss auf die Konzentration der suspendierten Sedimente konnte in dieser Studie qualitativ erfasst werden. Dieser erhöht die Konzentration in zwei Perioden: während der Öffnung der Deichschleusen im August und während des Auspumpens des Wassers von den Reisfeldern im November und Dezember.

c) Eine Reduzierung der Sedimentfracht entlang des Kanals konnte beobachtet und quantifiziert werden. Die exponentielle Abnahme erfolgt auf den ersten 10 Kilometern vom Mekong, nach dieser Entfernung stabilisiert sich die Konzentration.

d) Weil die Flokkulation nur sehr schwach ist und die Partikel dadurch sehr fein, lagern sich Sedimente nicht vollständig auf den Reisfeldern ab. Die Grundkonzentration beträgt um die 20 mg/l.

e) Die ermittelten Prognosen zur Sedimentfracht aus Sediment-Abfluss-Beziehungen für das Mekong Delta sind sehr ungenau. Aufgrund der variablen Fracht des Mekongs flussaufwärts, der Reduktion der Fracht im Kanal mit steigendem Abstand zum Mekong und des Einflusses der Gezeiten konnten Sediment-Abfluss-Beziehungen nicht abgeleitet werden. All diese Faktoren variieren in Zeit und Raum und erschweren daher die Schätzung des Sedimenttransportes durch einen solchen vereinfachten Ansatz erheblich.

f) Die Deichschleusen und Pumpstationen stellen Aus- und Eintrittspunkte der Sedimentfracht in die geschlossenen Überflutungsbereiche dar und sind zudem ein Schlüsselfaktor der Regulierung von Wasserstand und Sedimentkonzentration im Reisfeld.

g) Um die Düngung der Böden auf den Reisfeldern durch Sedimentablagerungen zu maximieren sollten folgende Punkte beachtet werden: (1) die Konzentration der suspendierten Sedimente im Kanal (Größenordnung und Zeitpunkt), (2) Wasserstand im Kanal in Relation zur Topographie der Reisfelder und (3) Deichschleusen in größerer Distanz zum Mekong sollten eher geöffnet werden, um eine einheitlicher Verteilung der Sedimente auf den Überflutungsflächen zu unterstützen.

Deposition und Erosion von Sedimenten auf den Überflutungsflächen

Deposition und Erosion agieren als gegensätzliche Aspekte und tragen eine Schlüsselrolle bei der Ablagerung der jährlichen Sedimente auf den Überflutungsflächen des Mekong Delta. Über Deposition und Erosion im Mekong Delta ist nur sehr wenig bekannt und es fehlen sogar Informationen über grundlegende Sedimenteigenschaften. Das Delta in Vietnam wird landwirtschaftlich intensiv genutzt und ist dem jährlichen Hochwasser ausgesetzt. Die natürlichen Überflutungsflächen werden durch das Kanalnetzwerk in viele verschiedene Reisfelder und Aquakulturen geteilt, zu denen keine quantitativen Angaben in Bezug auf ihre Sedimentaufnahme vorhanden sind. Aus diesem Grund beabsichtigt diese Studie die Fragestellung zu Deposition und Erosion basierend auf den suspendierten Sedimentdaten der Jahre 2008, 2009 und 2010 zu untersuchen. Zwei bestehende, aber gegensätzliche Paradigmen zu den Prozessen von Deposition und Erosion von kohäsiven Sedimenten werden betrachtet. Weiterhin wird eine Methode zur Schätzung der Schlüsselparameter, die Deposition und Erosion kontrollieren beschrieben (Schwellenwerte für Deposition und Erosion). Zusätzlich werden die grundlegenden Sediment- und Wassereigenschaften diskutiert. Die Unterschiede

bzgl. der Depositionsraten und deren variierende räumliche Verteilung zwischen den Teilgebieten mit hohen oder niedrigen Deichringen wird für das Jahr 2010 analysiert. Zuletzt wird das Gesamtvolumen der abgelagerten Sedimente im Untersuchungsgebiet mit verschiedenen Methoden geschätzt.

Die Quantifizierung von Deposition und Erosion von kohäsiven Sedimenten ist noch immer eine Herausforderung und die Debatte um das zu Grunde liegende Paradigma ebenso offen. Basierend auf unseren Messungen kann das "mutually exclusive" Paradigma angewendet werden. Bei Betrachtung der Daten wird folgendes deutlich: die kritische Sohlenschubspannung der Deposition liegt im Bereich T_d = [0,021-0,029] N/m^2, die kritische Sohlenschubspannung der Erosion im Bereich T_e = [0,028-0,044] N/m^2 und die Oberflächenerosionskonstante beträgt M_{SE} = [5,13 bis 88]*10^{-6} kg/m^2/s. Der Median der dispergierten Sedimentpartikel (D_{50}) aus den Überflutungsflächen beträgt 10-15 µm mit einer Tonfraktion (< 2 µm) von 50 bis 70 Prozent. Die Korngröße der flokkulierten Partikel wurde indirekt auf bis zu drei bis vier mal größer als der Median der dispergierten Sedimentpartikel geschätzt. Für dieses Untersuchungsgebiet empfehlen wir die Verwendung eines der 83 gleichwertigen Parametersätze im Appendix und einen Durchmesser von 35 µm für flokkulierte Partikel um die Sedimentationsbilanz zu errechnen. In den Reisfelder erfolgt die Deposition hauptsächlich am Anfang und Ende und die Erosion zum Höhepunkt der Hochwassersaison. Unter Anwendung der Methoden von Krone (1962) und Partheniades (1965) ist es möglich Deposition und Erosion unter Berücksichtigung der hydraulischen Gegebenheiten für einzelne Überflutungsflächen zu quantifizieren, sofern zeitreihen über Wasserstand, Wassertemperatur und suspendierte Sedimente vorliegen.

Die potentiellen Depositionsraten im Untersuchungsgebiet liegen zwischen 0.3 und 20 kg/m^2*Jahr und die durchschnittliche Rate basierend auf den drei Jahren Monitoring bei 6.83 kg/m^2*Jahr. Aufgrund der Verringerung der Konzentration der suspendierten Sedimente entlang des Kanals variiert die tatsächliche Menge in Abhängigkeit der Lage und der entsprechenden Entfernung vom Mekong. Die Gesamtdeposition im Untersuchungsgebiet liegt zwischen 1.0 und 1.3 Tonnen/Jahr.

Es ist wichtig zu erwähnen, dass die Höhe der Deiche die Depositionsraten und deren räumliche Verteilung beeinflusst. Während der Hochwasssersaison im Jahr 2010 fielen beispielsweise die Depositionsraten in hohen Deichringen im Vergleich zu niedrigen Deichringen um 17% niedriger aus. Des Weiteren wurde beobachtet, dass die Depositionsraten in niedrigen Deichringen räumlich homogener verteilt sind als in den hohen Deichringen.

Vorschläge für weitere Arbeiten

Trotz den gefundenen Ergebnissen dieser Arbeit bestehen noch immer viele anspruchsvolle offene Fragen. Zu diesen zählen unter anderen: Wie lässt sich die Dynamik kohäsiver Sedimente in Beziehung zu pH-Wert und elektrischer Leitfähigkeit setzen? Wie wird das Sediment an Kanalkreuzungen umverteilt? Wie viele Nährstoffe, Schwermetalle oder Schadstoffe sind in den suspendierten Sedimenten enthalten? Diese Studie trägt einen kleinen Beitrag zu den Arbeiten bei, die sich mit der Betrachtung von komplexen Kanal-Deich Systemen beschäftigen. Es gibt einige Punkte, die in zukünftigen Arbeiten betrachtet werden sollten:

a) Mit der Kombination von *in-situ* Monitoringstationen und Fernerkundungsdaten wird es möglich sein, die Ergebnisse diese Arbeit zu erweitern und auf größere Gebiete im Mekong Delta zu übertragen.

b) Eine weiterführende Analyse der auf dem in-situ Monitoringsystem basierenden Datengrundlage ist notwendig, um die Interaktion zwischen pH-Wert, elektrischer Leitfähigkeit und Sedimentdynamik zu verstehen. Dadurch könnte das Verständnis zu Fragestellungen der Wasserqualität auf den Überflutungsflächen verbessert und der Einfluss der Bodenazidität auf den Sedimenthaushalt eventuell quantifiziert werden.

c) Aufgrund vielfacher Einflussfaktoren auf den Sedimenttransport ist es nicht möglich einfache Sediment-Abflusskurven, die eine Beziehung zwischen Abfluss und der Konzentration der suspendierten Sediment herstellen, im Mekong Delta anzuwenden. Sollten solche Eichkurven erstellt werden, ist es notwendig, die Sedimentfracht in Relation zu Abfluss, Wassertemperatur, Abstand vom Mekong und mögliche anthropogene Einflüsse zu betrachten. Aufgrund der heterogenen Prozesse im Mekong Einzugsgebiet muss damit gerechnet werden, dass die Eichkurven nur für eine Hochwassersaison gelten.

d) Es ist sinnvoll, weitere Sediment-Fallen im Mekong Delta aufzustellen um so die Bilanz, Verteilung und Eigenschaften (Nährstoffe, Schadstoffe, Schwermetalle) von Sedimenten zu untersuchen. Diese sollten an strategisch wichtigen Punkten, also in hohen und niedrigen Deichringen, oder in verschiedenen Entfernungen zum Mekong installiert werden.

e) Kanäle, Deichringe, Deichschleusen und Pumpstationen werden als hydraulische Strukturen zu Unterstützung der Landwirtschaft betrachtet. Gemeinsam formen sie die hydrologischen Bedingungen auf den Überflutungsflächen im Mekong Delta. Aus diesem Grund, ist ein geeignetes Konzept zur Entwicklung und Operation dieser Strukturen erforderlich. Um die Nährstoffversorgung der Böden durch die Ablagerung von Sedimenten zu maximieren, sollten zwei wichtige Punkte beachtet werden. (1) Konzentration der suspendierten Sedimente im Kanal (Größenordnung und Zeitpunkt), (2)

Wasserstand im Kanal in Relation zur Topographie des Reisfeldes. Es ist ratsam, weiter vom Mekong entfernte Deichschleusen eher zu öffnen als Schleusen näher am Mekong. Weiterhin sollte die Höhe der Deichringe und die Größe der Deichschleusen an eine optimale Sedimentaufnahme für die Reisfelder angepasst werden. Im Detail bedeutet das, dass größere Deichschleusen eine bessere hydraulische Verbindung zwischen dem Kanal und der Zelle gewährleisten und somit den Sedimenttransport erhöhen. Während der Spitzenabflüsse des Hochwassers sollte die Deichschleuse allerdings geschlossen bleiben um der Erosion vorzubeugen. In diesem Sinne kann ein Kompromiss zwischen der Hochwassergefährdung und den Vorteilen des Hochwassers erzielt werden.

Tóm tắt

Đồng Bằng Sông Cửu Long (ĐBSCL) là một trong những vùng đồng bằng châu thổ lớn và giàu tiềm năng trên thế giới. Lũ lụt hàng năm vừa là thiên tai nhưng cũng là nguồn sống cho khoảng 17 triệu người thuộc vùng Nam Bộ của nước ta. Kể từ khi ĐBSCL phát triển nông ngư nghiệp mạnh mẽ, bãi ngập lũ nguyên thủy đã phải nhường chỗ cho hệ thống ruộng lúa, đê bao, bờ bao, kênh rạch, các ao nuôi trồng thủy sản. Vận chuyển phù sa trên các hệ thống này đóng vai trò hết sức quan trọng trong việc lan truyền chất ô nhiễm, vi khuẩn, dinh dưỡng, khóang chất, thực vật phù du, thuốc trừ sâu, v.v. Thế nhưng hiểu biết của chúng ta về quá trình vận chuyển phù sa, bồi lắng, xói lở vẫn còn rất nhiều hạn chế. Do thiếu tài liệu đo đạc, những phân tích có tính định lượng về các hiện tượng này hầu như chưa có, hoặc có cũng chỉ dừng lại ở mức độ định tính.

Chính vì vậy, vào năm 2008 nghiên cứu này thiết lập một hệ thống quan trắc tài liệu hiện đại ở huyện Tam Nông, Đồng Tháp, nhằm phục vụ cho việc nghiên cứu chi tiết về hiện tượng ngập lũ và vận chuyển bùn cát. Hệ thống quan trắc này bao gồm 21 máy đọc mực nước và 7 trạm đo chất lượng nước tự động. Tất cả đều được thiết kế với độ bền cao, kết quả đo có độ chính xác đáng tin cậy, có khả năng sử dụng nguồn năng lượng mặt trời và dung lượng bộ nhớ lớn để đo đạc liên tục trong khoảng thời gian dài. Các tài liệu chất lượng nước bao gồm: mực nước, nồng độ phù sa, pH, độ dẫn điện (EC), nhiệt độ nước, với bước thời gian quan trắc 15-30phút/1 số liệu đo và đo liên tục trong vòng 3 năm (2008, 2009, 2010). Đặc biệt là sự việc kết hợp giữa máy đo phù sa tự động và "bẫy" bùn cát (sediment trap) cho phép chúng ta nghiên cứu chi tiết về cơ chế bồi xói trên bãi ngập lũ. Mặt khác, bộ cơ sở dữ liệu được phân tích kết hợp với kết quả quan trắc từ ảnh viễn thám có độ phân giải cao (ảnh vệ tinh TerraSAR-X, độ phân giải nhỏ hơn 3m), cho phép chúng ta phân tích định lượng quá trình ngập lũ ở ĐBSCL. Cụ thể hơn, nghiên cứu này đã đi sâu phân tích vào các vấn đề: (1) Quá trình ngập lũ theo không gian và thời gian, (2) sự tác động của con người lên chế độ thủy văn bãi ngập lũ, (3) sự ảnh hưởng của thủy triều biển Đông, (4) quá trình vận chuyển của phù sa, (5) cơ chế bồi lắng và xói lở trên bãi ngập lũ.

Đóng góp thực tiễn của luận án là những hiểu biết có tính hệ thống về quá trình ngập lũ và vận chuyển phù sa, từ đó góp phần nâng cao năng lực quản lý nguồn nước ở ĐBSCL, tiến tới hoàn thiện và hiện đại hóa nông nghiệp. Đồng thời sự kết hợp giữa máy đo độ đục và bẫy bùn cát (sediment traps) để đánh giá cơ chế bồi lắng, xói lở, trên bãi ngập lũ là đóng góp mới cho tính tóan xói bồi bùn cát trên bãi ngập lũ. Qua đó các chỉ ra các tham số thực nghiệm, phương pháp để tính toán và khả năng áp dụng mô hình tóan để tính vận chuyển phù sa cho ĐBSCL được làm sáng tỏ.

Acknowledgement

My sincere acknowledgements go to the WISDOM project for their financial support. Many warmest thanks go to Section 5.4 Hydrology Engineering of German Research Centre for Geosciences (GFZ) in Potsdam, where I was educated in a beautiful scientific atmosphere with nice colleagues. Many thanks to my home institute, Southern Institute of Water Resource Research (SIWRR), for their allowing me the time to fulfil this study. I also acknowledge the International Doctoral Program Environment Water (ENWAT) for their accepting me into the PhD program at Stuttgart University. My sincere thanks go to Department of Agriculture and Rural Development (DARD) of Dong Thap, Navigation Board 15, and An Long Navigated Station for their support during my field work.

I wish to express my gratitude to Prof. Dr. Bruno Merz for his daily supervision and invaluable advice. My deep appreciation goes to Prof. Dr. András Bárdossy for his guidance and support. I also acknowledge Jun.-Prof. Oliver Röhrle for his chairmanship. I am grateful for the essential discussions with Jun.-Prof Wolfgang Nowak. Many thanks go to Dr. Gabriele Hartmann for her supports. I would like to thank Prof. Ted Chid Yang for his guidance and Prof. Hans Middelkoop for his priceless advice.

From a floating life in the Delta to the hill of science at GFZ in Potsdam, Dr. Heiko Apel and Heiko Thoss, Jose Delgado, Viet Dung were always beside to me with their willingness to help, daily scientific discussions, guidance, advice about problems with equipment. I would like to give my best thanks to all of them; without their help, this work would had never been accomplished.

My sincere thanks to my colleagues: Ass.Prof. Le Manh Hung, Ass.Prof. Tang Duc Thang, Ass.Prof. Dr. Vo Khac Tri, Dr. Trinh Thi Long, and many friends in an interdisplinary group of WISDOM for their encouragement in fulfilling this work. Special thanks go to Prof. Krystian Pilarzyck, and Prof. Luong Phuong Hau, as they motivated me to explore this line of study.

Last, but certainly not least, this work is dedicated to my family. I have so many thanks to give to my family members, including my parents, my lovely wife for her great efforts when I absent from home, and to my little lovely daughter Khanh Linh.

Potsdam, 08.09.2011

Nguyen Nghia Hung

Table of Contents

List of Figures

List of Tables

List of Symbols

A	the inundation area	(m^2)
a, b and p	are empirical parameters use in sediment rating curve	(-)
C	suspended concentration at height z above the river bed	(mg/l)
C_a	reference concentration at height (z = a) above the bed;	(mg/l)
C_b	near bed suspended sediment concentration	(mg/l)
C_o	the suspended concentration at river and channel conjunction	(mg/l)
D	deposition rate	($kg/m^2/s$)
g	acceleration of gravity, g=9.81	(m/s^2)
h	water depth	(m)
κ	Von Karman constant, $_K$=0.4	(-)
L	the distance from a location in secondary channel to the river	(km)
M_{se}	surface erosion rate constant	($kg/m^2/s$)
p	Rouse parameter	(-)
Q	water discharge	(m^3/s)
R^2	the coefficient of determination	(-)
SSC	Suspended sediment concentration	(mg/l)
SiO_2	the silicate reading from optical turbidity sensors	(mg/l)
S_{cal},	the calculated volume of sediment deposition	(kg/m^2)
S_{mea}	the measured volume of sediment deposition	(kg/m^2)
SS_{err}	the sum of squared residuals	(-)
s	Specific gravity of sediment particles (s=2.65, for quartz-rich sediment)	(-)
T	water temperature measured from sensor	(^oC)
T_d	critical bed shear stress for deposition	(N/m^2)
T_e	critical bed shear stress for erosion	(N/m^2)
T_1	the time of setting up the trap	(-)
T_2	the time of collecting the trap	(-)
τ_b	bed shear stress	(N/m2)
ΔT	duration of inundation period, determine from the Seba probe ($\Delta T=T_2-T_1$)	(s)
u_*	bed –shear velocity	(m/s)
V_d	the volume of sediment deposition	(kg)
υ	kinematic viscosity coefficient	(m^2/s)
w_s	particle settling velocity	(m/s)
β	constant of proportionality relate to the eddy diffusivity to eddy viscosity (β=1 for low concentration and β=1.35 for high concentration)	(-)

1 INTRODUCTION

1.1 Motivation

The largest part of the Mekong Delta is located in Southern Vietnam, where the Mekong River drains its water into the East Sea (Figure 1.1). The region encompasses an area of 39,000 km^2 and is home to about 17 million inhabitants. The climate is influenced by both South-West Indian monsoon and the North-West Pacific monsoon. There are two different seasons: the dry season starts in December and ends in April while the flood season lasts from May to November. The annual floods originating in the lower Mekong Basin during the flood season and the mixed semi-diurnal tide from the sea cause large inundations of about 19,000 km^2 in an average year (approximately 50% of the total area).

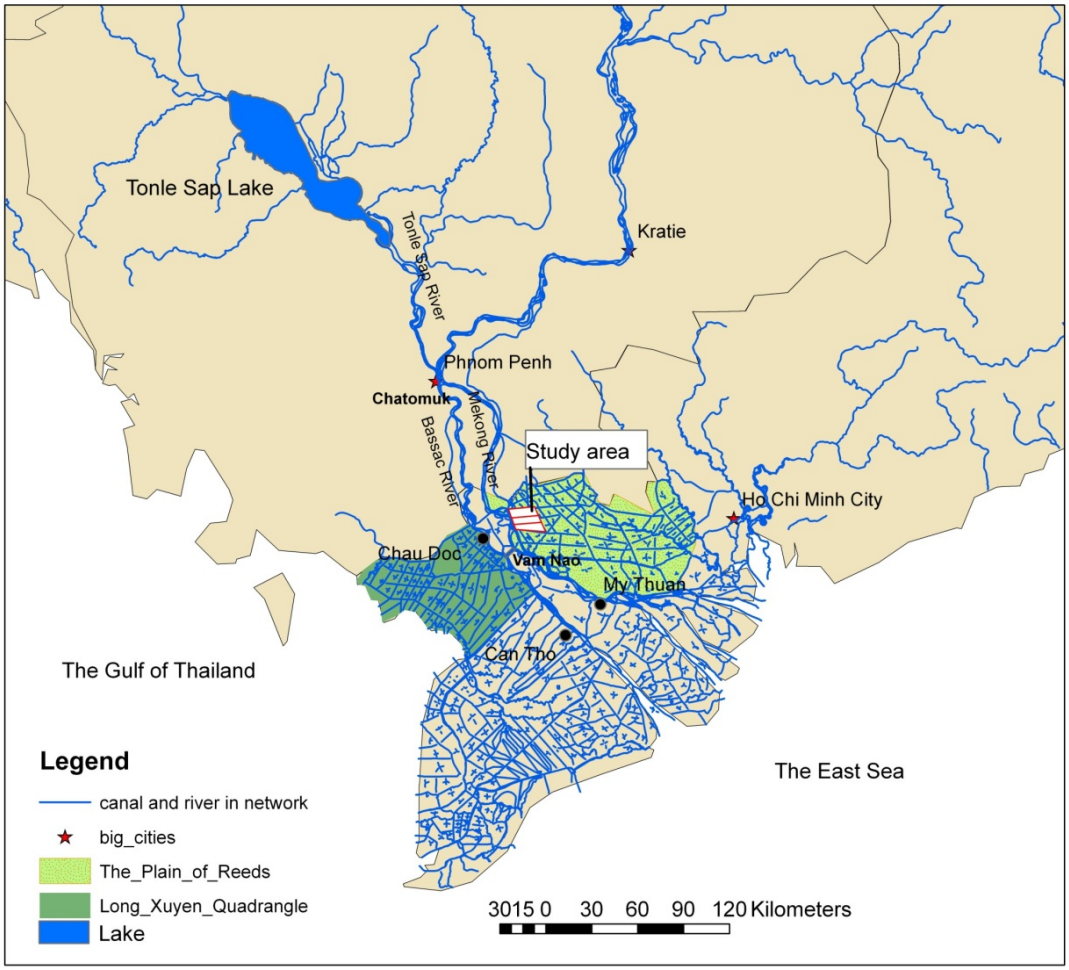

Figure 1.1 The Mekong Delta, including the major rivers and channels, the study area, and the two main inundation areas: Long Xuyen Quadrangle, and the Plain of Reeds

The man-made channel and dike system has greatly altered the natural hydrodynamic conditions in the Vietnamese part of the Delta. This man-made channel network had only two canals in 1819-1824 (Thoai Ha and Vinh Te), increased to 40 canals in 1934 (with a total length of about 1375km), and hundreds in 1980s with a rising trend still (Dieu, 1999; Yasuyuki, 2001). Today, the canal network covers thousands of channels with a total length of over 50,000 km, and it is under continuous development (Huy et al., 2010). Along with the development of the canal network the construction of high level flood protection dikes has been enforced in the last decades, especially after the devastating flood in 2000, cutting off more and more floodplains from the channel network and thus natural inundation. In wide areas in the Delta the floodplain inundation is controlled by sluice gates which are managed by the associated communities. In the areas completely enclosed by flood protection dikes, a trend towards growing three crops per year and blocking the natural inundation is observed. Beside the presence of social and economic benefits the adverse impacts manifest in water quality problems (MRC, 2007), riverbank erosion (Hung, 2004), and salt intrusion (Sam, 2004; Nguyen and Savenije, 2006). Furthermore, climate change and/or climate variability impacts, like increasing flood variability (Delgado et al., 2010), constructing dams in upstream river stretches (Lu and Siew, 2006; Kummu and Varis, 2007; Walling, 2008; Xue et al., 2010), and a prospected sea level rise (Doyle et al., 2010) are expected to change the hydrological condition in the Delta.

The floodplains play an important role in the sustainability of the agro-ecosystem as well as the socio-economy of the Mekong Delta. In particular, they provide natural flood retention, regulating flood and tide levels during the wet season. This natural flood retention has been strongly altered by flood mitigation structures and the development of agriculture, especially the popular cultivation of fruits and paddy rice. Traditionally, the rice cultivation controls the in- and outflow of water during the rising and falling stage of the flood period, i.e. in July and December. This is required in order to allow for two rice crops per year and is achieved by simple low dikes retaining the water from the floodplains until the rice is harvested in July and pumping the surplus water out of the floodplain in December. The low dikes also ensure that substantial amounts of sediment and thus nutrients are deposited in the floodplain. These sediments are the thriving source of the very productive agricultural system in the Delta. Complete flood protection (high dike) cuts this annual natural support of nutrients and is thus

object of controversial debates from the communal to national level in Vietnam. However, no quantitative data exit to support either position in this debate.

In our knowledge today, it is well-known about the role of suspended sediment in carrying contaminant, bacteria, nutrient, heavy metal, phytoplankton, and pesticide, etc (Wolan, 1977; Vannote et al., 1980; Junk et al., 1989; Droppo, 2001; Poole, 2002; Walling, 2005b). Fine sediment particles with attachment of those matters travel from the river to the channel network, from channels to the paddy fields. They are the primary source for the productivity of biota in floodplains as well as sustainable agro-ecosystem of the Delta. However, little is known about the dynamics of these suspended sediment including the multi-processes erosion, deposition, and suspension in this complex channel network in the Delta.

1.2 Problem identification

The sediment dynamics of the flood season play an important role in the agro-ecosystem of the Delta by providing nutrient input for the subsequent farming season. However, the actual inputs and dynamics have never been studied in detail, hence any quantitative information about the net input as well as the temporal dynamics are lacking. These gaps have generated a controversial discussion on the benefits of flood defense structures in light of their contribution to reduced nutrient input in the Delta. For this reason, sediment is one of water related issues that has generated most misunderstandings among managers and scientists, as reported by Campbell (2007).

1.3 Research objectives

The objective is to monitor, understand and quantify the sediment dynamics during the flood season in the floodplains of the Mekong Delta. This includes an intensive measuring campaign of time series of water depths, sediment transport and sedimentation in a selected investigation area in the Plain of Reeds. The data is used for interpreting in depth hydrodynamics condition of floodplain and the sediment transport, erosion, deposition in the channel network and floodplain compartment. In particular, the present study also gives the basic sediment properties and key parameters, e.g. critical shear stress for erosion and deposition, for the application of mathematical models of the transport processes.

1.4 Research concepts

To start this study in a data scarce region in regards to inundation and sediment processes, we had to implement an intensive *in-situ* monitoring system. The database from this monitoring system enables us to understand and quantify the inundation process in depth, as well as to find out key problems and parameters that control the sediment dynamics in the floodplain of the selected investigation area. Twenty-one pressure probes for water level monitoring were deployed to strategic locations in the investigation area. The probes could be submerged completely and record autonomously for several months. Additionally, seven water-quality stations were designed for long-term operation and deployed to channels and floodplains. The water-quality stations operate autonomously by solar power supply and are equipped with various sensors. The sediment traps were set up at the beginning of the flood seasons and collected for laboratory analysis at the end of each season. The data of the sediment traps were analysed and interpreted in combination with the readings of the turbidity sensors in the bottom layer of the floodplains. This combination enabled an identification and quantification of the major floodplain sedimentation, resp. erosion processes. Since floodplain inundation is usually irregular and unpredictable, monitoring of floodplain processes is difficult. The Mekong Delta offers an outstanding possibility for monitoring floodplain processes due to the regularity of its annual floods. Hence, the *in-situ* floodplain observatory implemented in this study is unique all over the world today.

This study aims to understand and quantify typical floodplain processes in the Vietnamese Mekong Delta. In particular, it investigates:

- the spatial and temporal characteristics of the floodplain inundation processes,
- the influence of the operation of water resources infrastructure (sluice gates, water pumping) on the inundation of floodplain compartments,
- the effect of the tidal influence,
- the hydraulic linkage between channel network and floodplain compartments,
- the basic sediment parameters and the suspended sediment dynamics in secondary channel and in floodplain compartments,
- the applicability of the sediment rating curve in the Delta,
- the erosion and deposition processes during flood season, including high dike ring and low dike ring deposition rates and the potential deposition in different places in the Delta.

In particular, the parameters which control erosion and deposition in the floodplain are investigated.

1.5 Outline of the thesis

Chapter II introduces the *in-situ* monitoring system which is considered as the centre part of this study. The existing technologies in monitoring suspended sediment as well as in monitoring floodplain sedimentation are reviewed. The *in-situ* monitoring scheme that has been designed and implemented for the Mekong Delta is described.

Chapter III introduces the hydraulics and hydrology of the floodplains in the Mekong Delta. This chapter was published in a modified version in Hydrological Processes by Hung et al. (2011). The *in-situ* measurements are used in combination with high resolution remote sensing images to analyse the spatial and temporal inundation process. This chapter sets up a basic understanding of the floodplain hydrology, including a quantitative description of the anthropogenic influence in the floodplains.

Chapter IV presents the results on the suspended sediment transport in the channel network. The seasonal dynamics of suspended sediment in secondary channels is analysed based on a continuous measurement in three flood seasons (2008, 2009, and 2010) in the Delta. The anthropogenic influence on the dynamics of suspended sediment in the channel network is investigated by comparing the suspended sediment dynamics in different locations. Moreover, in this chapter, the applicability of the sediment rating curve is analysed.

Chapter V is devoted to the understanding of deposition and erosion processes in the Delta. The two existing, yet conflicting, paradigms in the study of deposition and erosion of cohesive sediment are reviewed. This chapter shows the results from the combination of the sediment trap and the turbidity sensor for interpreting key parameters according to the method of Krone (1962) and Partheniades (1965). Moreover, differences in the deposition rate and its varying spatial distribution between low and high dike ring compartments are investigated.

Finally, conclusions and recommendations are given in chapter 6.

1.6 The study area

The study area encompasses five municipalities in the Tam Nong district, in the Plains of Reeds, Vietnam (Figure 1.1). About 30,000 people live along the channel and dike network and in a few scattered clusters. The area encompasses a number of man-made channels and thirty-nine ring dikes in floodplains which are mainly used for growing paddy rice and for aquaculture (fish and shrimp farms). The dike system is comprised of low and high dikes for crop and flood protection, respectively, an intervention which is very common in the Mekong Delta of Vietnam.

In general, the channel and dike rings system can easily be found in the Delta, and they are characterized by several levels of channels and two types of dike rings. By Vietnamese standards, these channels are categorized based on their size and location: level I – channel (so-called I-channel, kênh trục, kênh cấp I) connects to the main river with about 70-100m in width and 3-5m in depth; level II-channel (kênh cấp II) connects between two I - channels and is about 30-50m in width, and 2-3m in depth; III-channel (kênh cấp III) connects between two II-channels and is about 15-25m in width, and 1-2m in depth. Dike rings are classified into two types, depending on topography and the flood hydraulics. Low dike rings (Đê bao lửng) protect the rice crops in the early flood peak and high dike rings (Đê bao triệt để) protect the rice crop completely. The paddy fields are surrounded by a channel and a dike ring (see Figure 1.3 a,b).

Annual flooding causes two main inundation areas in the Delta: the Long Xuyen Quadrangle (Tứ Giác Long Xuyên) and the Plains of Reeds (Đồng Tháp Mười) including the study area (Figure 1.1). The study area in Tam Nong was selected, because it has deep inundation depths. Further, its characteristics are typical for the Mekong Delta. The total area is about 16,500 ha, of which 4.5% is used for shrimp farming, 0.5% for fish farming, and 95.0% for paddy and vegetable cultivating. The channel density of 11.6 m/ha is somewhat below the average density in the whole Delta (14 m/ha, including river and natural channel network). 67% of the dikes are low dikes with average crest levels of about 2.5 m.a.s.l, and 33% are high dikes for flood protection with average crest levels of about 4.5 m.a.s.l. These fractions are representative for the whole Plain of Reeds.

Different land use leads to different water demand and control schemes. The requirements for water for agriculture are different to those for aquaculture in terms of quantity, quality and regulation scheme. In the case of floodplain compartments fully protected by high dike rings, the water flow is entirely controlled, enabling three crops per year. Consequently, the water management in these areas differs considerably from the areas under the natural inundation regime.

The combination of

- annual floods inundating the area directly from the Mekong River,
- flooding due to overland flow from the Cambodian-Vietnamese border (Dung et al., 2011),
- the bi-modal tidal influence,
- the low topography and hydraulic gradients,
- the diverse man-made channel system with its numerous control structures

creates a highly complex hydraulic scheme. The resulting inundation levels in the floodplains range from one to three meters depending on topography, flood magnitude, tidal amplitude and control of sluice gates and pumps. In the case of completely controlled floodplain compartments, the control of the system may cause different water levels in adjacent compartments (Figure 1.2 bottom).

In the Mekong Delta in general and in the study area in particular, there are two more important hydraulic systems, which people use to control flood levels for their crop; the sluice gate system and the pumping stations (Figure 1.3c, d). The sluice gates vary in shape and size, the maximum width of the sluice gates is about 1.5m and the most common use is a small culvert with a dimension of about 30 cm located underneath the dike system in the paddy field (Figure 1.3d). There are two types of pumping stations, the movable and the fixed- electricity-pumping and both of them have capacity less than 1500 (m^3/h). In our study area, both pump types are used temporarily in the period toward the end of the flood season.

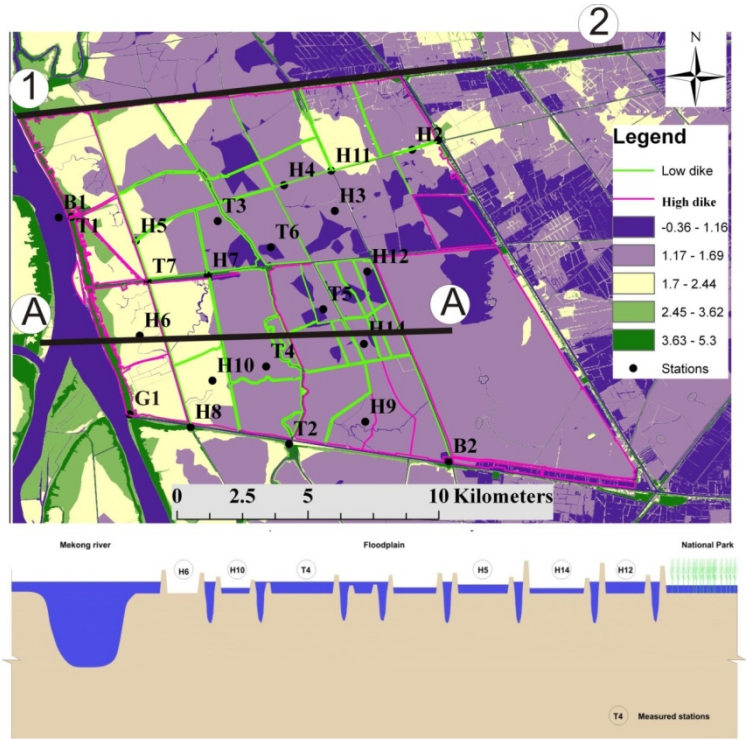

Figure 1.2 The upper map indicates the study area and its topography and dike systems, the lower cross-section A-A shows different compartments with different water levels.

Figure 1.3 Hydraulic features in study area: a) low dike and channel conjunction; b) high dike ring; c) movable pumping station; d) pre-casting culverts

In conclusion, this is a representative study area because it provides many possibilities to study typical hydrodynamic and sediment transport processes within floodplains in-depth. The topography, the water demand and control scheme show evidence of a strongly anthropogenic influence.

2 *IN-SITU* MONITORING SYSTEM

2.1 Purpose and objectives

Due to the singular nature of flood events in general and the complex canal system in the Mekong Delta in particular, monitoring of flood events in both channels and floodplains is an extremely difficult task. In recent years the use of remote sensing products for flood mapping has received a large boost from new techniques and platforms (LiDAR, SAR, optical system, both satellite and airborn) and has proved to be a significant step forward in floodplain inundation studies, as well. Despite this, remote sensing is not the encompassing answer to the chronic lack of floodplain inundation data. Due to restrictions in sensor availability, revisit cycle frequencies of satellite, unfavorable atmospheric conditions and difficulties in signal interpretation, remote sensing products usually provide only a short but spatially extensive view on the inundation process. Therefore ground based methods have to be applied in order to collect data on hydraulic parameters *in situ*. A special focus is on the collection of continuous time series of water depths and suspended sediment load in the floodplains, where data are usually missing for flood events. This serious lack of flood data poses considerable problems for the basic understanding of sediment dynamics in the Delta as well as for mathematical model development.

The *in-situ* monitoring system is equipped with twenty-one water level probes and seven water quality stations. The water level probes were submerged in water during flood season. These probes record water depth according to the pressure principle. Seven water quality stations were installed for a long term operation. The water quality parameters are turbidity, pH, EC (electrical conductivity) and water temperature. The sampling interval of water level is fifteen minutes and for the water quality it is thirty minutes. The sediment traps were also used to investigate the deposition and erosion in the floodplains of the Delta.

In summary, the objective of using an *in-situ* monitoring system was to accumulate an extensive database which yields the basic understanding of floodplain hydrology and sediment dynamics in the floodplains of the Delta.

2.2 Technology of suspended sediment monitoring

Suspended sediment is the sediment that is suspended in water and transported under the flow condition (WMO, 2003). In sediment transport studies, the suspended sediment load is normally divided into two components the so-called "wash load" and "bed material load" (van Rijn, 1993). The term "load" refers to the sediment that is being transported. The wash load consists of very fine sediment particles (<62µm) which are transported through the complete cross-section (Woo et al., 1986). The bed material load refers to a load of particles that are transported, e.g. by saltating (jumping), eroded and deposited near the bed. There are some parameters that should be collected in order to get a basic sediment dataset: (1) sediment concentration of suspended sediment, (2) grain size distribution of suspended sediment, (3) velocity or discharge, (4) water depth, (5) hydraulic gradient, and (6) water temperature (WMO, 2003).

In 1937, Rouse introduced the most famous equation for the suspended sediment distribution in a vertical profile, which is still widely applied today. Rouse's equation to compute the suspended sediment profile for steady uniform flow:

$$\frac{C}{C_a} = \left(\frac{h-z}{z}\frac{a}{h-a}\right)^P \tag{2.1}$$

Where C = suspended concentration at height z above the river bed (mg/l);

C_a = reference concentration at height (z = a) above the bed;

h = water depth (m);

p = Rouse parameter;

$$p = \frac{w_s}{\beta \kappa u_*} \tag{2.2}$$

w_s = particle settling velocity (m/s);

K = Von Karman constant (0.4);

u_* = bed –shear velocity (m/s);

β = ratio of sediment and fluid mixing coefficient (β=1 for low concentration and β=1.35 for high concentration).

According to Rouse (1937), the suspended sediment concentration (SSC) is highest at the point closest to the river bed and lowest at the point nearest to the water surface.

Since the beginning of 20th century, technology for measuring suspended sediment has been developing. The initial idea was to monitor suspended sediment for the understanding of river morphology or geology. The science of making suspended data measurement more accurate have been attracted many scientists for decades, though it is still an intensively developing topic.

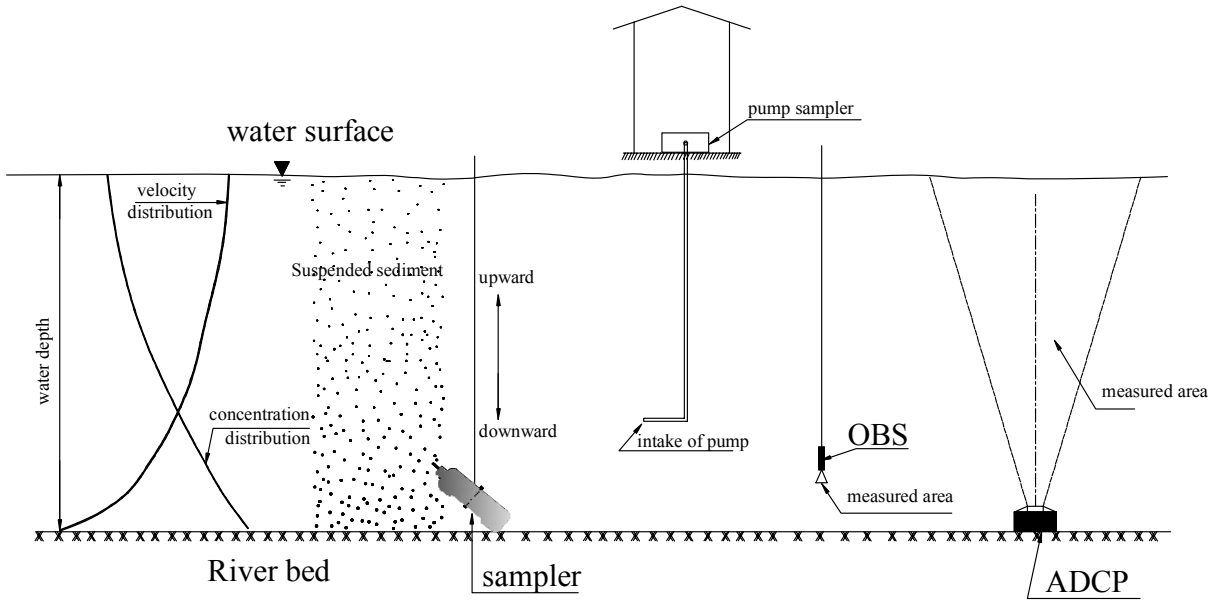

Figure 2.1. Manual sampler, acoustic equipment (ADCP), optical backscatter sensor (OBS)

Figure 2.1 shows the manual sampler (left) and high-tech equipment (right) to measure suspended sediment in water. The manual sampler retrieves samples in an upward or downward direction to make a representative profile. The sampling method could be either point integration or depth integration. In practices, the field condition is not always allowing to access to use manual sampler for sample collection. This can happen, for instance, in a flash flood event. Therefore, the automatic pump is investigated, they could pump water samples automatically. Later on, there are numerous surrogate technologies to measure fluvial suspended sediment indirectly via its indicator (e.g turbidity). These technologies have made a major change in the data collection of sediment in recent years. It allows scientist to get the real-time suspended sediment concentration and to do the data transfer could be done from remote distance. The most common use of these technologies at a reliable cost are optical

backscatter (e.g OBS) and acoustic backscatter (e.g ADCP). This equipment could be fixed to measure stationary data or be made movable within the cross-section.

In the traditional technique, measurement of suspended sediment concentration is often implemented at several representative profiles within a cross-section. Each profile is the boundary of a small area in each section. Sediment discharge passing through the cross-section is computed based on the accumulated sediment discharge of these small fragments in the cross-section (see Figure 2.2). Depending on the actual circumstance (hydraulic condition, sediment properties, geometry), the number of representative profiles could be 1, 3, 5 or more. The sampling method could be point-integration or depth-integration. The sampler is designed to take a representative sample in an upward direction from the river bed or downwards from the water surface. The Point-integration takes samples at several points of measurement (many samples in a profile, 0H (surface), 0.2H, 0.6H, 0.8H, 1H (near bed)) and in the Depth-integration method the sampler is moved continuously in vertical direction within a depth (one sample in one profile).

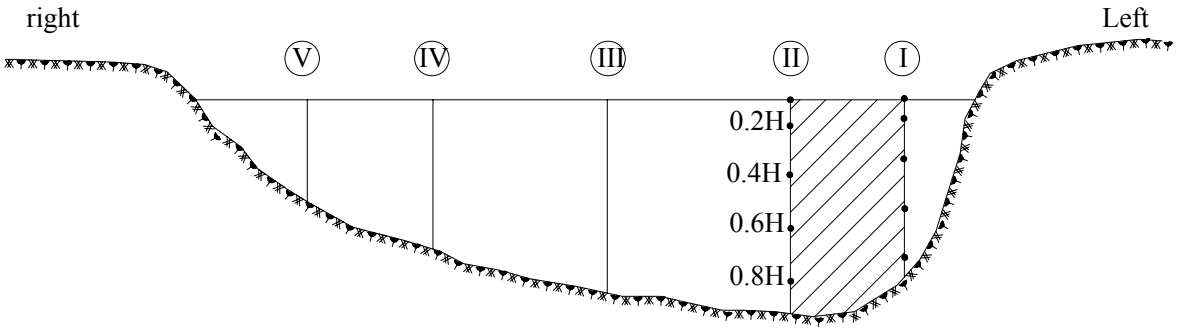

Figure 2.2. Example of the representative measured profile, measured point, and segment of computing suspended sediment concentration, H is water depth at the profile

Turbidity can be measured as the surrogate of suspended sediment concentration relying on high-tech equipment. The equipment can be fixed or movable within a cross-section (e.g. Figure 2.1). In order to calibrate and validate the turbidity measurements, a number of water samples are needed, taken at the same time as the turbidity measurement. From these data, the relation between true suspended sediment concentration, derived from the samples, and turbidity is established. This relationship has been found to be linear or exponential (Minella et al., 2008). The technologies used in monitoring turbidity are, among others, laser, optical

backscatter, acoustic backscatter, ultrasonic, or nuclear (Wren et al., 2000; Gray and Gartner, 2009). These technologies will be introduced in next section. In comparison, the traditional technique has to take a water sample directly (or indirectly) from the measured point and analyse this sample in a laboratory to determine the suspended concentration. Since the traditional technique is cumbersome and requires much labor, it cannot produce a continuous data series. Modern technology yields a continuous data series *in-situ* with less laboratory work.

Overall, it is possible to trace back the technology used in suspended sediment monitoring into three main types: **manual sampler**, **pump sampler**, **and surrogate technology.**

2.2.1 Manual sampler development

In the early stage of suspended sediment investigation, each investigator or agency developed their own sampling technique. For instance, early samplers were the Nansen Bottle (in 1910) and the sampler developed by Shale Niskin (in 1966). Delft Hydraulic Institute developed the Delft Bottle, and FISP (Federal Inter-Agency Sedimentation Project, USA) developed a series of depth integrating samplers (DH) and point integrating samplers (P) since the 1940s. Today, manual samplers are of optimal design and developed to operate with different principles of sampling methods; either water-trapping or flow-through. The manual sampler has been applied in countries all over the world. It can be classified into three types of samplers: (1) instantaneous sampler, (2) time integration sampler, (3) accumulation sampler (WMO, 2003). The instantaneous sampler applies the water trapping principle. A popular example is the Niskin bottle or Delft-trap bottle. The time integration and accumulation sampler are based on the flow-through principle. The sediment sample is taken in a period of time, therefore, this method can reduce the fluctuation of suspended sediment concentration. In a time integration sampler, the water sample has to be taken isokinetically via its nozzle in order to yield representative samples. This means that the velocity entering the container of the sampler should be equal to the water velocity around the nozzle. Edwards and Glysson (1999) elaborates this requirement indicated in Figure 2.3. The representative sample is the one that has isokinetic sampling (A), when the average velocity of stream is equal to the sampler nozzle velocity.

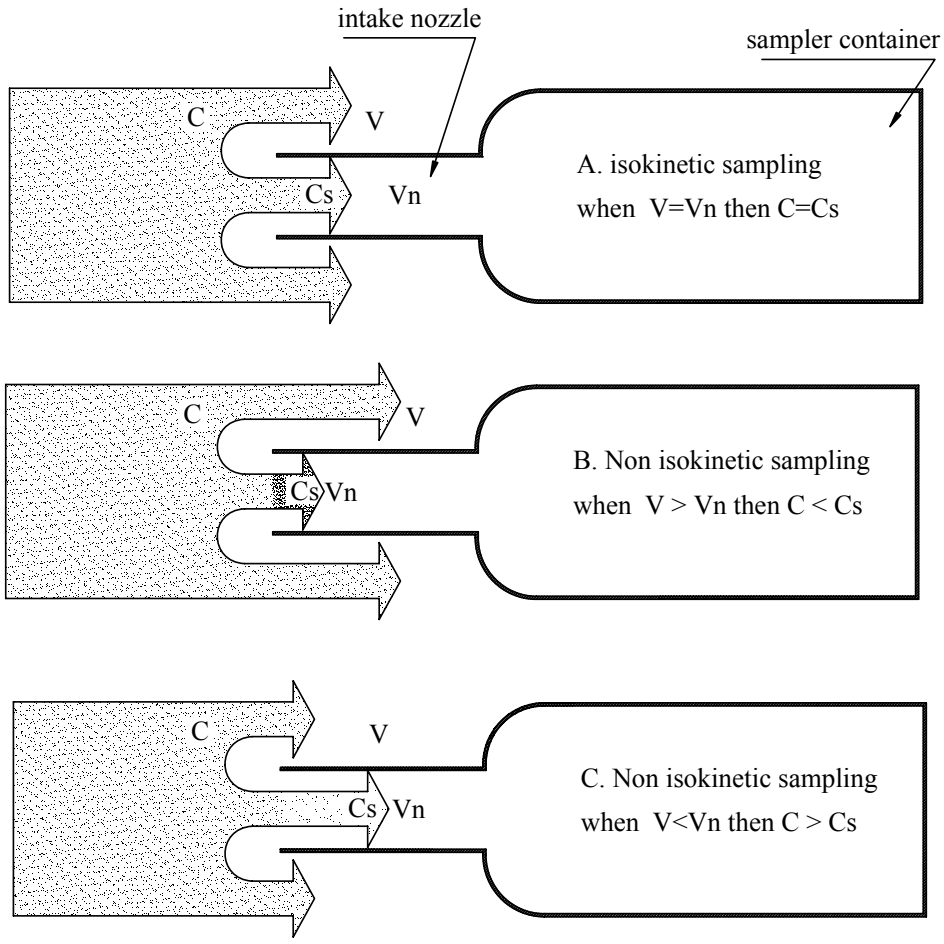

Figure 2.3.The important isokinematic sampling modified from Edwards and Glysson (1999), V = average flow velocity, V_n = velocity in the sampler nozzle, C = mean sediment concentration of water, C_s= sample sediment concentration

Since the 1940s, there was a series of suspended sediment samplers designed by FISP. However, to select a proper sampler, the sampling method has to be based on the actual circumstances. For instance, depending on depth and velocity, the sampler is selected (David, 2005; WMO, 2003). Normally, there is more than one type of sampler found in a gaging station, because of the variability of flow conditions over time. It is also wise to compare different types of samplers for evaluating the most appropriate method.

An ideal manual sampler has to fit four basic requirements (WMO, 2003): (1) equal intake velocity of the nozzle, (2) ability to collect the sample close to the bed, (3) enough weight for stabilization in the water, and (4) a sufficient sampling volume. In a case where the flow velocity is less than 0.5m/s and the sediment properties are mostly silt and clay, the suspended

sediment concentration is relatively uniform from surface to bed (Edwards and Glysson, 1999). Hence, it is not necessary to keep the isokinetic velocity at the nozzle of sampler.

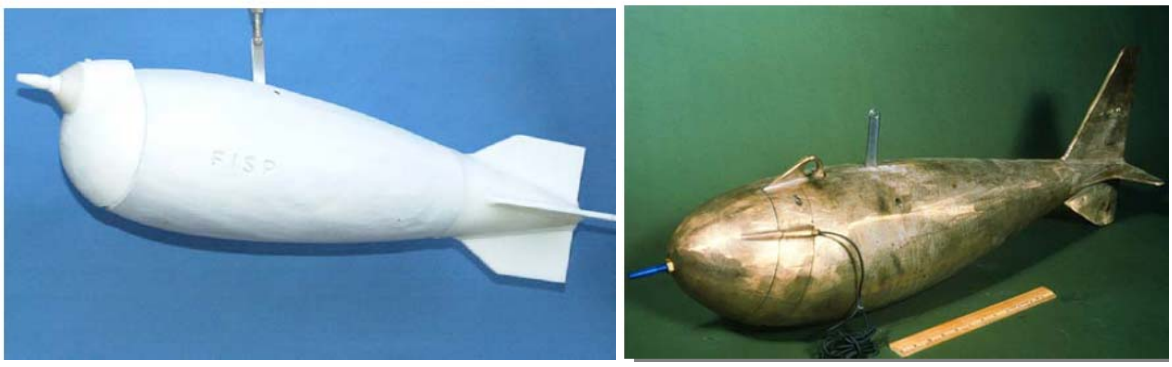

Figure 2.4. Example of manual sampler (left: Model US-DH-99 and right US-P63), source WMO (2003), regarding to the sampler name: US indicates country name, D= depth integration, P= point integration, H= Hand line, 99 or 63 is year of invention.

In summary, the advantage of manual samplers is that they are simple to handle with high accuracy of fluvial sediment data. However, the disadvantages are discontinuous data and a huge requirement of field and laboratory work. It is highly recommend that to use manual sampler for calibrating or evaluating the high-tech equipment.

2.2.2 Pump sampler development

If we use a manual sampler for taking samples frequently at the same place, it consumes costs and labor. In some cases, the sediment samples need to be taken more regularly at a gauging station or when the water stage is rapidly rising and the field condition does not allowing to access for a manual sampler (e.g flash flood). To overcome this difficulty, the pumping sampler was invented in the 1960s. The general idea is to install a pumping station located close to the measured cross-section. This pump can be triggered to take a sample either by electricity, stage of water, or timing (Walling and Teer, 1971; Turton and Wigington, 1984).

In order to design a proper automatic pump sampler station, there are at least seventeen optimum criteria to take into consideration (Edwards and Glysson, 1999). These requirements should be investigated for reducing costs but increasing the quality of data:

1. Location of the automatic pump sampler must be recorded for understanding of sediment budget of catchment or stream flow. The pump sampler should be located at a safe place to guard against the riverbank erosion or morphology change. The intake

is always submerged and resistant to trash floating or ice blocking in water. The limitation of the automatic pump is that water sample can only be taken at several points in a profile. Therefore, the suspended sediment concentration at the intake must be comparable to the average concentration of the cross-section. For that reason, the relationship between one point or one profile to the overall suspended sediment transport of the cross-section has to be established and validated regularly by manual sampler application.

2. Similar to the manual sampler, the water sample has to be pumped isokinetically at the intake of pump sampler. This requires compensation between the pump capacity and the flow velocity in the measured cross-section. The suspended concentration and grain size distribution of the stream and of pump samples have to be equal. The automatic sampler should have enough capacity to collect the highest suspended concentration at its station in significant flood events.
3. The volume of a sample bottle should be at least 350ml in order to get a proper representative sample. The sample container should be designed as removal unit to facilitate the retrieval of samples for laboratory analysis.
4. Again, in comparison with the manual sampler, the automatic pump sampler only saves labor and the cost of field work to collect the samples. However, there still remains quite a bit of work in the laboratory. Nevertheless, the automatic pump sampler is very useful when we use it for monitoring suspended sediment in a rapidly rising water stage or during times when access is impossible for manual sampler monitoring.

Today, the fixed automatic pump sampler is rarely applied in many countries because of high operation and maintenance costs. Conversely, the portable pump sampler is very commonly used because it is less of an investment, adaptable to field conditions, and easy to handle in intensive field campaigns. In using the portable automatic pump sampler, one can gather the exact sample volume and collecting time of sample needed for calibration turbidity probes.

Figure 2.5 shows an example of a portable automatic pump sampler by RD Instrument (ISCO 3700) used to collect samples at the quality stations during the field campaign in the Mekong Delta. The samples from this automatic sampler were analyzed independently and used to support the calibration function in estimating suspended sediment concentration from turbidity monitoring. The samples container includes about 25 sample bottles with 500ml per

bottle. The control table could be used to set up time steps for sampling and velocity of pump, depending on the flow velocity.

Figure 2.5. Portable automatic pump ISCO 3700

2.2.3 Surrogate technologies

It is about 173 years since the first suspended sediment sample was taken by Captain Andrew Talcott in the Mississippi River (Gray and Gartner, 2009), and there have been numerous efforts around the world to overcome the difficulties of retrieving sediment data. Due to the fact that the concentration of suspended sediment is related to the motion of particles in water, this is a random process. Therefore, reliable sediment data has been a critical issue for centuries. Ideally, engineers would like to know all the suspended sediment concentrations at all points in a cross section at all times, past and present. However, this is impossible in a practical point of view. The second best is to know the concentrations of suspended sediment at several points in several profiles of a cross-section at all times. The problem then comes up because of the limited of number of measured points and the timing of sampling in the field and work in laboratory. This requirement could be done neither by manual sampler nor by automatic sampler. Therefore, different a method must be investigated for sediment monitoring technology.

In Florida in 1998, there was a workshop called “Sediment Technology for the 21st Century,” which first drew attention to state-of-the-art of the sediment technology and future trend development (Proceedings of the Federal Interagency Workshop, 1998). However, the surrogate technology to measure suspended sediment became more reliable in the workshop in Reno 2002 (Proceedings of the Federal Interagency Workshop, 2002).

Up until now, there were about ten technologies (listed below in no particular order) to measure the turbidity as a surrogate of suspended sediment concentration. Most of these technologies were either acoustic technique or light backscatter, or laser or nuclear, depending on the presence of particle size and concentration in water. In addition, many of them relied on the Beer-Lambert's law and Doppler Effect principle. Figure 2.6 shows the principle of surrogate technology. A source of acoustic, optic, or laser energy is emitted directly to the water sample, and the particles present reflect a portion of this source's so-called backscatter signal to a detector. The strength of this back scatter signal is used to convert into the suspended sediment concentration.

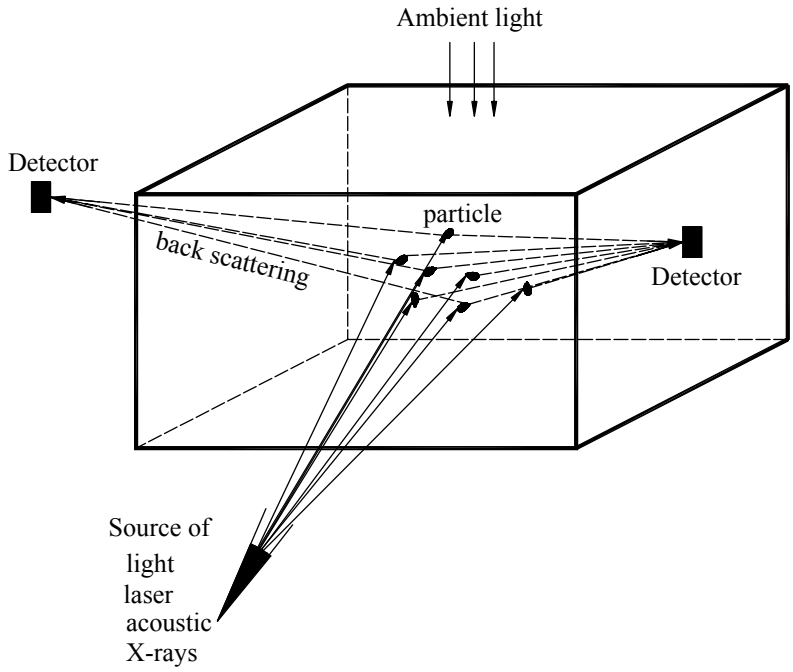

Figure 2.6. The principle of back scattering used in surrogate technology

1. Optical backscatter (OBS): A ray of light (infrared or visible) is directly emitted into the water sample, the presence of particles in suspension leads a portion of this light backscatter. The strength of the backscatter is the basic information for calculating the water turbidity. An empirical relationship has to be made in order to convert this backscatter light into suspended sediment concentration. Depending on the wave length of the light (200 to 600nm), the particle size range can be detected. This varies from 10μm to 400μm, with the suspended sediment concentration up to 100g/l (Black and Resenberg,

1994; Zeigler, 2002; Anderson, 2005). There are several issues that should be taken into account when applying this technology, as they might affect to the measured result:

- The biological fouling, that is the organic matter that grows in water and reduces the capacity of the emitter.
- The particle color would also impact the strength of back scatter (Sutherland et al., 2000).
- Ambient light from other sources, such the sun if the water is relatively shallow, will influence to the backscatter (Zeigler, 2002).
- Air bubbles could also influence measurement results because of their presence in water (Anderson, 2005).

The devices author used for his field measurement is Visolid700IQ were designed base on this technology. They are of robust design, including an automatic ultrasonic cleaning system, which could reduce very much biological fouling (WTW, 2006).

2. Optical transmission: Using the source of light as optical backscatter technology, however, the emitter and receiver are designed and fixed differently. The ray of light is focused toward the water sample, and the particle in suspension will scatter or absorb a portion of this light. The opposite detector measures the attenuation of the strength of the light. The strength of the light at the detector can covert the light energy to water turbidity (Clifford et al., 1995; Wren et al., 2000; Anderson, 2005). The disadvantage of this technology depends on the presence of sediment particles in the water sample, if the particle is too small, it is likely silt, clay, or an organism. If its concentration is small, the bias of measurement could be relatively large. Moreover, it is an optical backscatter modifier, so the limitations described above, such as biological fouling, particle color, air bubbles, and ambient light could also happen.
3. Focused beam reflectance: This is another optical backscatter modifier. A rotational beam directs the laser into the water samples with a very small spot ($<2\mu m^2$). The beam is rotated very quickly (many times per second). While it is rotating, the laser collides with a particle that reflects a portion of laser. This reflection allows us to calculate the suspended sediment in water sample. The advantages of this technique are (1) less dependency on the particles in the water sample, (2) the size of the particle could be measured from very small to large (1-1000μm), as well as (3) the suspended sediment concentration from 0.010-50 g/l (Phillips and Walling, 1995; Wren et al., 2000). However, in order to apply this

technology to the field condition, the robust design is needed and the cost of this instrument is very expensive (Wren et al., 2000). Inasmuch as the limitation of sample volume (several centimeters squared), the measurement can be implemented at one point only.

4. Laser diffraction: Although this technology was invented in the 1970's, it has had strong development in the way of particle size distribution. The technology is now used for particle size analysis in cement, coffee, chocolate, sediment particle size distribution, etc. In other words, it is used wherever the size distribution needs to be measured (Agrawal and Pottsmith, 2004). In measuring suspended sediment, a laser beam is used directly toward the sample volume, where particles in suspension absorb, scatter, and reflect the beam. The laser scattering is received by a detector that allows the measurement of the beam's scattering angle. From this information, the size distribution and the concentration of suspended sediment can be produced. The laser path length is between 2.5-5cm, the particle size range is 1.25-500 μm, and the maximum concentration is up to 5g/l (Agrawal and Pottsmith, 1994; Wren and Kuhnle, 2002). The most famous device of this technology is LISST family (e.g LISST-25, LISST-100). They are remain at a reliable price on the market and have a robust design, which has wide application. LISST-100 can classify up to 32 particle size classes (Agrawal et al., 2008). The disadvantage of this technology is that it is intrusive into the water sample and has only one point measurement.
5. Acoustic: In the four previous technologies, all used a source of light (infrared, visible, or laser), whereas this one uses acoustic technology, which relies on Doppler Effect principle. In general, a sound with high frequency (600-5000 kHz) is transmitted directly toward the water sample, and the sediment particle in suspension scatters a portion of this sound back to the transducer. The information from acoustic backscatter is used to define the suspended sediment concentration. The strength of acoustic backscatter depends on the particle size, concentration, and sound frequency. The measurement range of a particle is from 62 to 2000 μm and the concentration is up to 30g/l. The greatest advantage of this technology is the ability to measure the profile of suspended concentration, water velocity, and topography at the same time. In comparison with previous optical technology, this technology is more reliable for future trends (Wren et al., 2000; Thorn and Hanes, 2002; Sung et al., 2007). The most common use of this technology on the present market is

ADCP from RD instruments (Rio Grande) containing 4 transducers with the sound frequencies from 600 to 1200 kHz.

6. Nuclear: When the X, or Gamma, ray is directed at the water sample, this radiation will be backscattered and attenuated by suspension particles in water. By doing this, we establish the empirical relationship between backscatter of radiation and suspended sediment concentration. The range measurement of nuclear technology has a relatively high the concentration from 0.5 to 12 g/l (McHenry et al., 1967, Papadopoulos and Ziegler, 1967). Nowadays, this technology is rarely in use. Perhaps other surrogate technology tends to dominate on market because of its reliable data accuracy and lower cost.
7. Spectral reflectance: This technology can be applied for a wider spatial area, such as a coastal area, inundation area, and lakes. The technology relies on remote sensing analysis from satellite images, airplanes, etc, and the suspended sediment concentration in the water. The reflection of radiation particles in the water is the basic information to compute the suspended sediment concentration. In addition, the spectral reflectance can also be use via spectral reflectance meter in the laboratory (Chen et al., 1991). It is therefore an advantage that measured area could cover an area from meters to kilometers squared but only apply for water surface. Along with development of satellite or airborne technology, the applications are still developing, and there are currently many applications (e.g Curran and Novo, 1988; Nanu and Robertson, 1990; Doxara et al., 2002; Liew et al., 2009). The ground trust data must be collected at the same time of the visit of satellite or airplane. The limitations of this technology are also the limitations of satellite or airplane, for example, the frequency of the satellite's return, the weather conditions, the resolution, as well as the color and sediment properties of water.
8. Photo optic Imaging data: The movement of particles in water can be captured from digital-optical camera. This technology was invented in the 1980’s in the medical industry to determine red blood cell concentration. The presence of particles in motion allows us to compute the concentration and particle size via a series of images. The USGS have applied this technology in the field in Vancouver, Washington (Gray et al., 2003).This is still a new technique and not very developed in comparison with backscattering technology. It has potential to develop in future trends in laboratory studies (Gooding, 2001). The advantage of this technology is that it does not need calibration with the probe. However, the difficulty of this technology is image processing when it is influenced by air bubbles.

9. Vibrating tube: The technology was invented in the 1980s and is based on the relationship between water density, suspended sediment, and frequency of vibration. The water is diverted into a vibrating tube located near the measurement cross-section. Two relationships have to be investigated: density versus suspended concentration, and density versus vibrating frequency. Today, this technology is limited because of accuracy and the applicability of field conditions. According to the author's knowledge, there are many factors that influence the result of measurement such as water and air temperature, water velocity, and debris that could block the tube. It is best to apply this technology only where there is a very high suspended sediment concentration (Szalona, 1986).
10. Differential pressure: In principle, this technology is used to make a pressure measurement. Many pressured sensors are installed in a vertical distribution, and the different pressure from these sensors is recorded. Bernoulli's theorem is applied to compute the difference of water mixture and sediment density. From this sediment density, we find the suspended sediment concentration. The initial idea of this technology is from the early 1960's (Inter-Agency Committee on Water Resource, 1961). Today, the field application has been investigated by USGS on the lower Rio Caguitas in Puerto Rico (Larsen et al., 2001), and in Japan (Sumi et al., 2002). There are two pieces of equipment called Double Bubbler Pressure Differential Instrument (Gray et al., 2009) and SMDP (Sumi et al., 2002). The previous investigators recommend that this technology should be applied for a high concentration suspended sediment. Because this equipment is not available on the market, the application can only be done after development the equipment on one's own (Lewis and Rasmussen, 1996; Gray et al., 2009).

2.2.4 Summary

In summary, we presented the continuing development of technology in suspended sediment monitoring. There is no "one size fits all" solution. Manual samplers can estimate the suspended sediment concentration with high accuracy. However, the cumbersome field and laboratory work involved limits the possibilities for establishing high-resolution time series. The automatic pump sampler can, in some cases, reduce the cost of labor in sample collection, but the cost of investment in installation and operation is relatively high. In addition, it also limits high-resolution time series.

The surrogate technologies can give reasonable estimates of suspended sediment concentration. They overcome the obstacles associated with the spatial and temporal resolution. Moreover, they are modest in terms of field costs and labor, in particular reducing laboratory work. There are two principles that dominate the technology of monitoring suspended sediment: Optical scattering and acoustic scattering. These technologies rely on the Beer-Lambert's Law and the Doppler Effect, respectively, and they use one or two empirical equations between the true suspended sediment data and the surrogate - either turbidity or acoustic. These empirical equations can change in relation to the hydraulic conditions, sediment properties, as well as aquatic life. Therefore, probe calibration and validation are needed. Table 2.1 shows the advantages and disadvantages of each of the technologies.

Table 2.1. Summary of the advantages and disadvantages of the different technologies used in suspended sediment monitoring

Nº	**Name or description of technology**	**Advantage and disadvantage**
1	Manual sampler instantaneous sampler, point and depth integrated sampler	- Easy to handle - Requires isokinetic nozzle - High accuracy, discontinuous time series
2	Automatic sampler portable automatic sampler, fixed automatic sampler	- Easy to handle - Require isokinetic nozzle - Save labor in sample collection, discontinuous time series - During rapid rising flood stage, a remote access by automatic trigger pump.
3	Optical backscatter	- Relatively cheap compared with other surrogate technology - Robust design - High spatial and temporal resolution - Require calibration
4	Optical transmission	- Relatively cheap compared with other surrogate technology - Require calibration - High spatial and temporal resolution
5	Focused beam reflectance	- High spatial and temporal resolution - Grain size 1 to 1000 μm - Concentration 0.01- 50g/l - Require calibration

Table 2.1 Summary of the advantages and disadvantages of technology used in suspended sediment monitoring (continue)

6	Laser Diffraction	- High spatial and temporal resolution - High accuracy - grain size distribution up to 32 classes (from silt to sand) - grain size 1 to 1000 μm, concentration up to 5g/l - Require calibration
7	Acoustic backscatter	- High spatial and temporal resolution - Profile (or cross-section) measurement - Grain size 62 to 2000 μm and concentration is up to 30g/l - Require calibration
8	Nuclear	- Large range of measured concentration, 0.01 to 12g/l
9	Spectral reflectance	- Large measurement area (m^2 to km^2) - Low cost for field campaign - Require ground trust data
10	Photo optic Imaging data	- No need for calibration - High temporal and spatial resolution - Difficulty of image processing, e.g air bubble influences
11	Vibrating tube	- Adequate for high concentration river - Grain size distribution measurement - Relatively inexpensive investment - Less accuracy
12	Differential pressure	- Adequate for high concentration river - Depends on sensitivity of pressure sensors

2.3 Technology of floodplain sedimentation monitoring

The floodplain is a common feature of a river, where flood water is either stored or passing through during the overbank flow. Due to the hydrological cycle, the floodplain might be inundated one or several times in a year (Wolman and Leopold, 1957). The flood pulse is a primary driving force for the existence, productivity and the biota in the river floodplain (Junk et al., 1989). The fine sediment caused by erosion, deposition, and transport within the floodplain plays an important role in carrying nutrients, biota, contaminants, pesticides, as well as other organism matter (Vannote et al., 1980; Junk et al., 1989; Poole, 2002; Walling, 2005). Therefore, the quantification of the patterns, properties, and characteristics of sedimentation within floodplains has received much scientific attention (e.g. Wolman and Leopold, 1957; Walling and He, 1998; Asselman and Middelkoop, 1995; Thoms et al., 2000; Baborowski et al., 2007).

While the floodplain is quite well-known in public media, the spatial and temporal deposition of floodplain has only been documented since the 1950's. Wolman and Leopold (1957) made what is considered to be the first accurate description related to this topic. From them, we understand that the practical difficulties in floodplain sedimentation study are (1) the irregularly and unpredictably of inundation of the area of the interest for planning a survey, (2) the potential of flood damage faced by the equipment and fieldwork. (3) Furthermore, the complexity of a multi-water body environment as well as the diversity of topography leads to many difficulties for understanding deposition and erosion processes.

Until now, researchers have used many technologies to monitor the patterns and characteristics of sedimentation in the floodplain. These characteristics include the deposition rate, organic and inorganic contents, contaminant contents, particle distribution, and heavy metal contents. One should select the adequate technology to use depending on the geological timescale of interest. For example, to study floodplain sedimentation in a long term study (100-1000yrs), one should use boreholes (e.g Oanh et al., 2002), or radionuclide dating (^{90}Sr, ^{134}Cs and ^{137}Cs, ^{239}Pu and ^{240}Pu, ^{241}Np, ^{241}Pu and ^{241}Am, and ^{14}Cbomb) (Roux and Marshall, 2010). In a medium term study (10-100yrs), tracers, topographical surveys, and historical markers (Walling and He, 1993; Asselman and Middelkoop, 1995) would be more helpful. In a short term study (1-5yrs), it is advisable to use topographical surveys, historical markers, erosion pins, and sediment traps (Steiger et al., 2003; Asselman and Middelkoop, 1995). The present study will focus on the technologies investigating sedimentation in the short-term.

2.3.1 Historical mark, topographical survey, remote sensing data

In order to map the sediment deposition or erosion rate in the floodplain, techniques such as historical markers or topographical surveys were selected. These techniques reconstruct sedimentation after the fact. The artificial markers are spread throughout the study area, and they are measured and collected either after each flood event or after one or several years (Steiger et al., 2003; Middelkoop, 2005). The position of the marker and the difference of the soil surface before and after a flood inundation event are measured for mapping the deposition and erosion of the floodplain.

Alternatively, the topographical survey could be implemented repeatedly to map the elevation. These elevation maps are constructed by laying one over the next to interpret the deposition and erosion area and their thicknesses. This technology is more accurate than the artificial mark although it is very expensive due to the amount of fieldwork and labor. Nowadays, the electronic theodolite, or GPS remote sensing, improves the topographical survey with a higher accuracy and wider measured area. On the other hand, remote sensing, such as a Digital Elevation Map derived from the satellite image, could also be used as a similar technique in floodplain sedimentation study.

Both of the above technologies rely on the density of a measure point: either an historical marker or an elevation map. Depending on the actual circumstance (hydraulic gradient, sediment properties, etc.) the density of the measured point can be decided in order to gather the proper information. In principle, the higher the density of measured point, the higher the accuracy of the map, though this is often question of time and money.

The limitation of these technologies is that they provide information for the mass or volume analysis at one event, but they do not provide the analysis of sediment properties such as organic and inorganic matter, contaminant, nutrient, etc. That extra information has to be determined from collected samples from the study site. In the low hydraulic gradient floodplain and flat topography as the Mekong Delta, the topographical survey should be implemented with many measured points spatially distributed with high accuracy. This might give possibility to acquire the differences deposition rate between each flood event.

2.3.2 Erosion pins

The erosion pin is an innovative technology first used in river bank erosion studies (Lawler, 1992). The Photo-Electronic Erosion Pin sensor (PEEP) could monitor the temporal variation

of surface soil based on the light detector principle. The principle idea is to set up a long tube (up to 66cm) containing an array of photosensitive material along its body (Figure 2.7). This tube is inserted into the soil from its surface to its sub-layers. The erosion or deposition will be detected by comparing voltage output from the reference photosensitive material and the exposed photosensitive material. As the soil is removed due to the erosion process, more photosensitive material is exposed to the light. Conversely, in the case of the deposition process, more photosensitive material is concealed from the light. The length of the exposed tube can be computed based on the photo voltaic ratio between the reference and the exposed photosensitive material. The tube has a cable and transfers information to a data logger for continuous recording (Lawer, 1992).

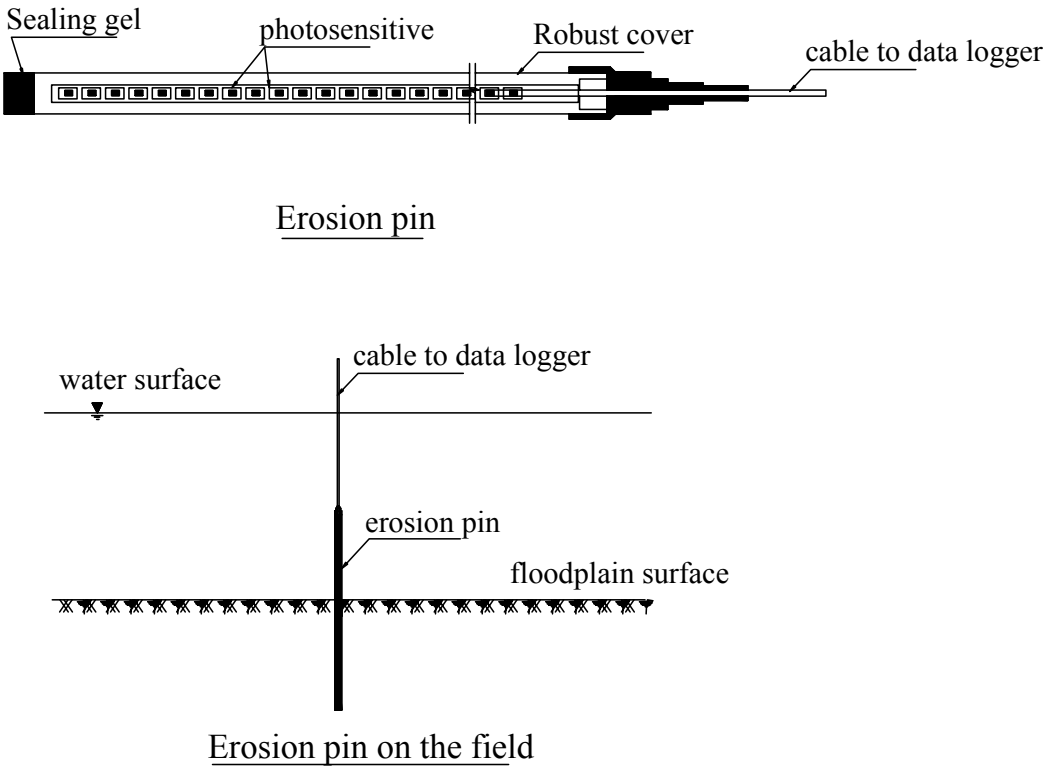

Figure 2.7. The erosion pin (design and fixed on the field)

The limitations of this technology include: (1) in lower light or at night, the deposition and erosion cannot be detected, (2) after being submerged in biological fouling for several days, the organic matter could blind the photosensitive material, (3) although the diameter of the tube is several centimeters, it could be influenced by hydrodynamic conditions, (4) in the case of high current, the stabilization of the tube is a problem, (5) the soil moisture affects the photosensitive signal, (6) it does not provide the sample properties, such as organic or

inorganic, contaminant, etc. Up until now, the latest version is PEEP 3T, equipped with more thermistor and artificial light, which could eliminate the soil moisture and natural light effects. This technology is still being used and tested, but if it can be applied properly, the obstacle in understanding of deposition and erosion process could be improved (Lawer, 2008).

2.3.3 Load-cell sensor

Alternatively, the load cell sensor could also be employed to monitor floodplain sedimentation. The principle of this technology is a sensitive balance (like a plate balance) placed on the floodplain surface. This balance detects any change in load including sediment and water, as well as the deposition and erosion of matter above it. The accumulative weight will be accompanied by a pore pressure conductor. The difference between the two weights is the weight of the sediment erosion or deposition (Carpenter, USGS). Though little information related to this new technology exists, it is in development by USGS, with the field study implemented in Green River, USA.

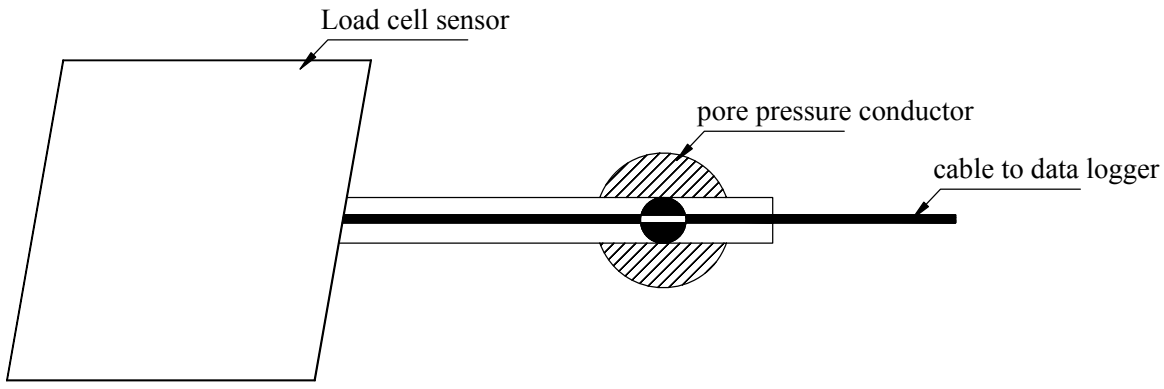

Figure 2.8. The load- cell sensor (according to Carpenter)

2.3.4 Sediment traps

Since the 1950s, cylindrical or bottle-shaped sediment traps have been used in limnology and coastal studies (Bloesch and Burns, 1980). The idea of the sediment trap is to trap sediment particles while they are settling in water. There are many types of sediment traps. They are in flat or vessel shape, or in cylinder or bottle shape. The flat trap is, for example, a rectangular plate and is installed at the water bed to collect the sediment deposition. The cylinder and bottle are fixed near the bed or at some point in water column. Steiger et al (2003) summarized many types of traps according to their sampling positions: (1) bottom sediment

traps, (2) sediment vessel near the sediment surface, (3) sediment vessel in the water column; (4) buoy-carried sediment traps, (5) moored sediment traps, and (6) free-drifting sediment traps. They are all applicable for the limnology, but the floodplains often have a higher hydraulic gradient than in lakes. Therefore, the flat traps may be more effective (Steiger et al., 2003).

Until now, the flat trap was made from wood, steel, or plastic, and the results from the different types of traps were not much different (Steiger et al., 2003). To date, the plastic trap with artificial turf is preferable (e.g Lambert and Walling, 1987; Asselman and Middelkoop, 1995; Steiger et al., 2003). It looks like the artificial grass used for a tennis or football field. The dimensions of the trap are about 50x50cm or 35x40cm, depending on the local circumstance. The reason why this type of sediment trap is preferred: (i) they are robust and re-usable; (ii) they are light and easily manipulated in a field with many traps (iii) their surface roughness is comparable to grass in the floodplain, so sediment is not removed by rainfall; (iv) they are very flexible, allowing them to be measured at different floodplain surfaces; (v) they can be fixed to the ground with metal sticks or pins.

The sediment traps are placed before and retrieved after a flood event. The trapped sediment is washed by a high pressure cleaner in a bucket, and then this sediment is analyzed in the laboratory. The information possible to derive from the sediment and the trap includes the volume of sediment deposition (kg/m^2), the organic or inorganic contents, the metal or contaminant contents, the grain size distribution, the dry and wet bulk density of the sediment for a single trap, and, if we install many traps, the spatial distribution could also be estimated.

Since the settling process of suspended sediment on flood plain not only depends on the flow and particle size (Stokes's Law) but also on the chemistry process. The trap or a cluster of traps, therefore, should be installed in a representative place. For example, the traps were distributed in a popular grid and in a cross-section parallel and perpendicular to the flow stream (Asselman and Middelkoop, 1995). In order to quantify spatial deposition distribution, the traps should be properly distributed, using the spatial interpolation methods such as kriging (Asselman and Middelkoop, 1995).

In addition, to select a sampling method and the sediment trap type, one should rely on the local conditions. In the Mekong Delta there is a strongly anthropogenic influence from cultivating paddy rice. The time to install and retrieve the sediment traps, therefore, is of high priority. Figure 2.9 depicts the sediment traps at four stations in the floodplain of the 2008

season. It shows that the deposition rate is very much different from one location to another. The T4 stations are located at a deep area, whereas the T3 and T6 located very near the sluice gates.

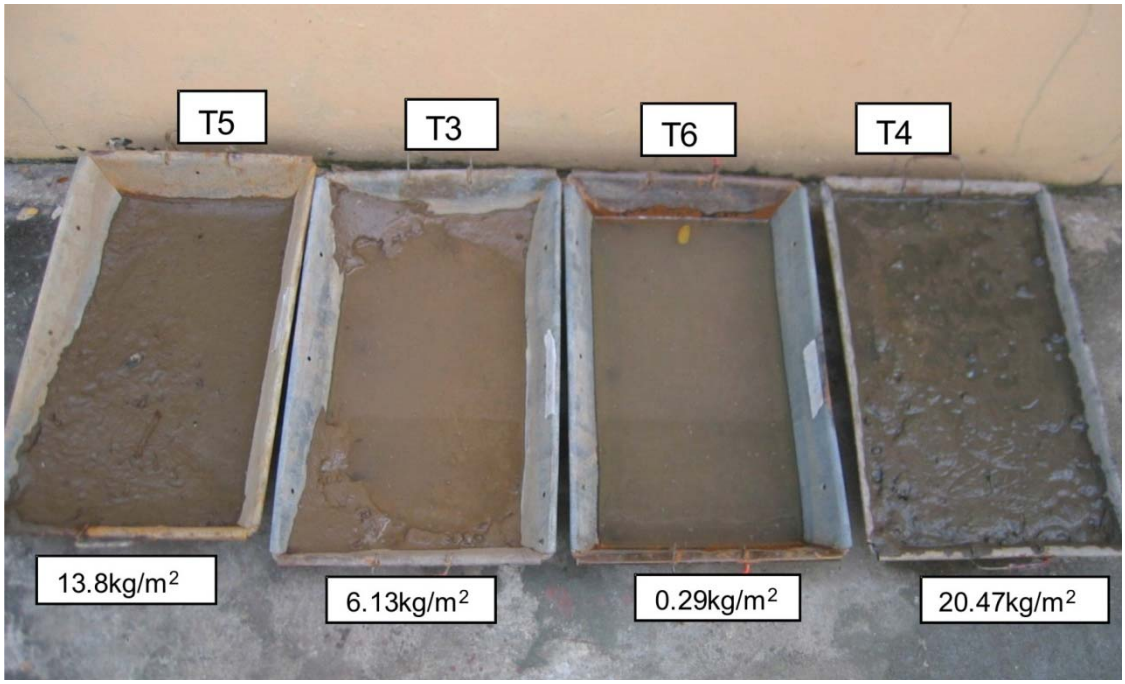

Figure 2.9. The vessel steel trap in flood season 2008. The trap was fixed on the ground for collecting sediment

2.4 Monitoring scheme

The monitoring scheme plays a very important role in archiving the research objectives. Relying on the circumstance of the study area as introduced in section 1.6, the concepts of monitoring scheme will be discussed in this part.

2.4.1 Ideas and action plans

Although the general flood characteristics of the Mekong Delta are well known, there is little information on the inundation processes in the floodplains. The general information, such as the initial time of flooding (likely in July), the harvest time of paddy crops (likely at beginning of August), the elevation of the dike, and the width of the channel, are useful for beginning the measurement. The author paid more attention to the compartments with low and high dike rings, channels, sluice gates, pumping stations, as well as the flood pulse from the river to the flood plain. In fact, they are all interrelated, making an hydraulic situation in the floodplain of the Mekong Delta.

From these crucial points, the requirements of the *in-situ* monitoring system are listed below:

- Spatial distribution must be high enough for allowing a quantitative analysis of floodplain inundation;
- Temporary resolution should be chosen such that the tidal influence and the anthropogenic influence are captured. This is of particular importance for the calibration and validation of the mathematical model later on;
- When using the turbidity sensor and sediment trap, one should apply the methods for calculation of deposition and erosion, and key experimental parameters could also be investigated;

Figure 2.10 depicts the concept of the *in-situ* monitoring system in combination with remote sensing from the satellite. The satellite observes the inundation process for a large spatial area, but with low temporal resolution of eleven days (TerraSAR-X Satellite). On the other hand, the submerged sensors produce a very fine temporal resolution (every fifteen minutes), but they deliver point information for strategic locations (Figure 2.13). Both the remote sensing data and the *in-situ* data are combined for the three flood seasons 2008, 2009, and 2010, in order to understand the inundation processes for the study area. In that sense, the findings in the study area could also be representative of the whole Delta.

During the flood season, there were also many short field campaigns to investigate the suspended sediment along the channel system, the discharge and water velocity, and to take water samples periodically to calibrate the optical turbidity sensors. Travelling with a boat along the channel network, we carried ADCP for measuring the water velocity, discharge, and turbidity distribution in a cross-section. The portable turbidity sensor was also included in this trip to monitor suspended sediment along the channel network. Finally, we investigated the calibration function for converting turbidity to suspended sediment concentration.

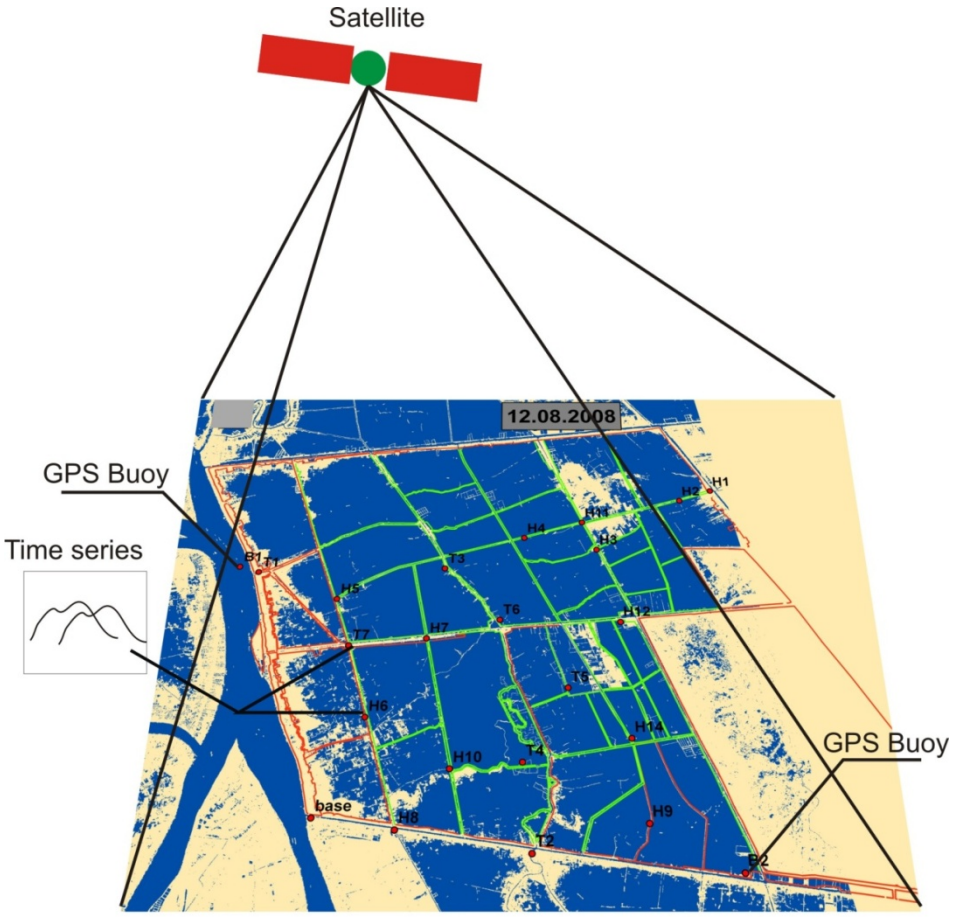

Figure 2.10. The concept of the monitoring scheme; shown is the inundation on 12nd August, 2008; the satellite (TerraSAR-X) scanned the study area while submerged sensors recorded the time series during flood season. (Blue – water, gray – ground, green - low dike ring, red - high dike ring, T- water quality stations, H - water depth stations, B - GPS buoy stations)

2.4.2 Equipment and technologies used

Twenty-one pressure probes for water level monitoring (H-stations) were deployed to selected locations. We used absolute pressure probes, facilitating deployment at any location without needing to record atmospheric pressure. Thus, the probes could be submerged completely, and they recorded autonomously for several months. The pressure readings were corrected offline for atmospheric pressure after retrieval. Figure 2.11 (top right) shows a typical floodplain station with its protective steel box and warning sign for fishermen.

Figure 2.11. Top left: water quality stations in channels; Top right: water level stations in floodplains; Bottom: quality stations in floodplains (dry and flood season).

Additionally, seven water quality stations were designed for long-term operation and deployed to channels and floodplains. The water quality stations (T-stations) operate autonomously from solar power and are equipped with various sensors. Because the power supply and data loggers cannot be inundated, the T-stations contain a weather- and lightning-proof steel box hosting the solar panels, battery, and data loggers. The box is mounted either on a bridge or, for floodplain deployment, on a pylon 4 m high (Figure 2.11, top left and bottom).

The technology used in suspended sediment monitoring is optical backscatter from WTW Company. It is robust in design and able to link with the same data logger as other sensors such as pH and electrical conductivity (Figure 2.14 right). The main advantage of this equipment is its ultrasonic cleaning system, which dramatically reduces biological fouling. Optical backscatter is a point measurement. Therefore we have to secure that the point

measurement is representative for a cross-section. To evaluate the representativeness, ADCP (acoustic technology) which can measure the suspended sediment across a cross-section, and the automatic sampler for collecting water samples in a profile independently were used. Figure 2.12 left (data from ADCP) shows that the suspended sediment was well distributed from the water surface to the channel bed. Figure 2.12 right shows one of the suspended sediment concentration profiles (acoustic backscatter). The measurements show a uniform distribution of suspended sediment concentration within the cross-section.

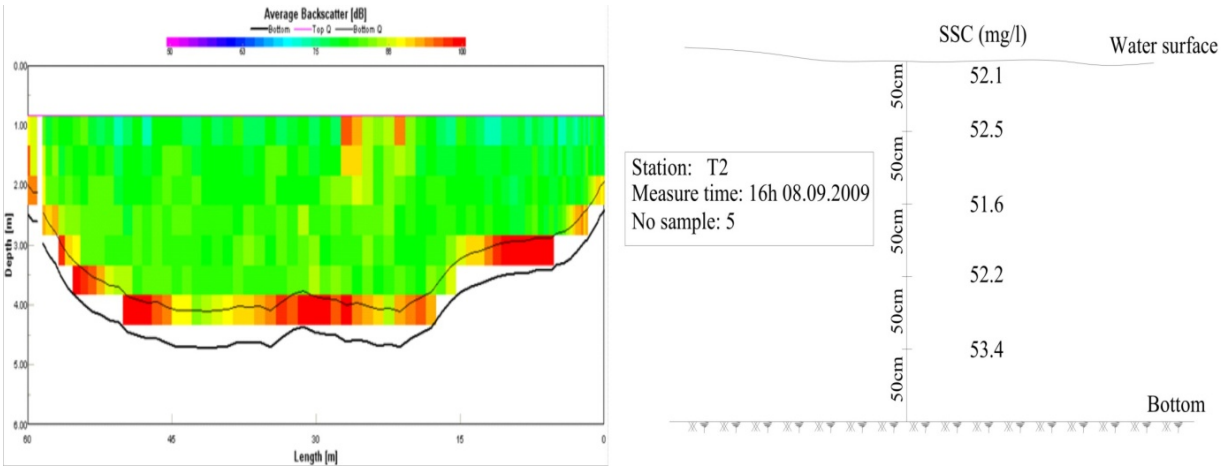

Figure 2.12. The backscatter distribution across a cross-section from ADCP (left) and the suspended sediment concentration profile from automatic sampler (right).

The point measurement time series of the turbidity were converted to the suspended sediment concentration by a calibration function (eq. 2.3). In order to remove short-term fluctuations from the original data, the time series were filtered with a Butterworth.

$$SSC=0.088SiO2+6.4475 \qquad R^2=0.93 \qquad (2.3)$$

where SSC, suspended sediment concentration (mg/l)

SiO2, the silicate reading from optical turbidity sensors (mg/l)

Table 2.2 shows the summary of the instruments and their technical description which were used for the *in-situ* monitoring system.

Table 2.2. The main instruments and their technical description

Nº	Parameters	Instruments	Technical descriptions
1	Water depth	Seba, OTT-mini	Pressure (water – air)
2	Turbidity	Visolid ®700IQ	Optical back scatter, ultrasonic cleaning
3	pH, Water Temperature	SensoLyt®700IQ	Pre-calibrated
4	Conductivity, Water Temperature	TetraCon®700IQ	Automatic temperature compensation
5	Sedimentation	Pan trap	Accumulative collector
6	Fine resolution of water level, flow direction	GPS Bouy	New development, floating GPS bouy
7	Water sample	RD Instrument ISCO 3700	Automatic sampler which calibrates and validates the turbidity sensor
8	Water discharge and velocity, suspended sediment distribution	ADCP	The acoustic technology for measuring velocity, water discharge, and backscatter
9	portable turbidity sensor	PTM	The portable turbidity sensor is used to investigate the reduction of suspended sediment along the channel

We also deployed GPS-buoys, a new technology for precise water level monitoring. The buoys were developed specifically for deployment in large rivers, differing them from ocean buoys. By using high precision receivers on both buoy and the reference stations, water level records could be derived with comparable accuracy to pressure gauges. Additionally the position records of the buoys can be used to detect flow direction changes. However, the data and results are not reported in this work. For details refer to Apel et al. (2011).

2.4.3 Distributed and installed stations

To capture the important inundation processes, the stations were strategically distributed in the investigation area (Figure 2.10). By placing the probes in the channel, on low dikes, and in the floodplains, we intended to quantify the different inundation controlling processes (dike overflow, sluice gate and pump operation) (Figure 2.13).

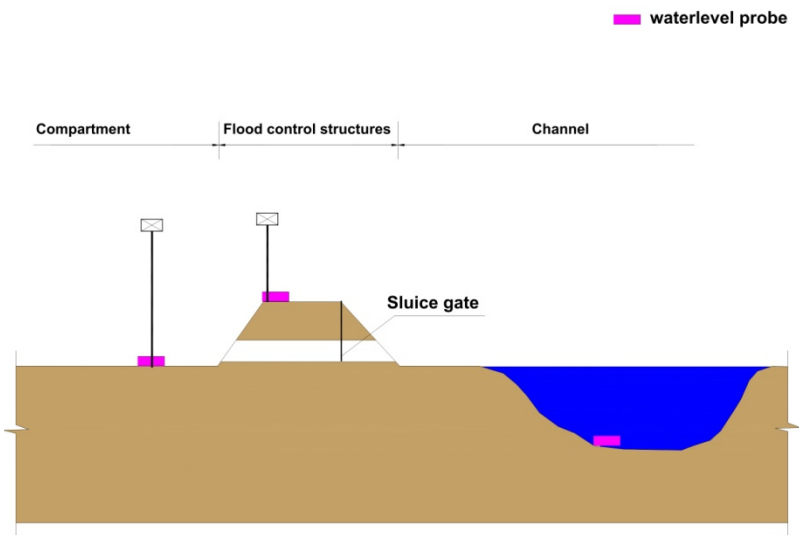

Figure 2.13. Distributed water probes for quantifying inundation processes

Out of the seven T-stations, four were placed in the floodplains, while three were deployed in the channels. Besides the water level, the T-stations record turbidity, conductivity, water temperature, and pH. All these stations were designed to run autonomously for a period of six months and gather sampling data at short intervals. The T-stations in the channel network were distributed from close to the Mekong River (T1) to the boundary of the study area (Figure 2.10). Station T1 recorded the suspended sediment near the Mekong River, while two other stations (T2 and T7) recorded the suspended sediment inside the study area. This arrangement was chosen to investigate the difference between the sediment supply from the Mekong and the anthropogenic influence inside the study area.

In addition, underneath the turbidity sensor in the floodplains, the sediment trap was installed for collecting deposition (Figure 2.14 left). This scheme allowed, according to Krone's equation (1962), to calculate the deposition rate, and to quantify the processes of deposition and erosion. Key parameters, such as the threshold for deposition and erosion, could be derived (further described in chapter 5). Hence, the combination of turbidity sensor and sediment trap can be regarded as a new field monitoring approach and provides new possibilities for quantifying floodplain processes.

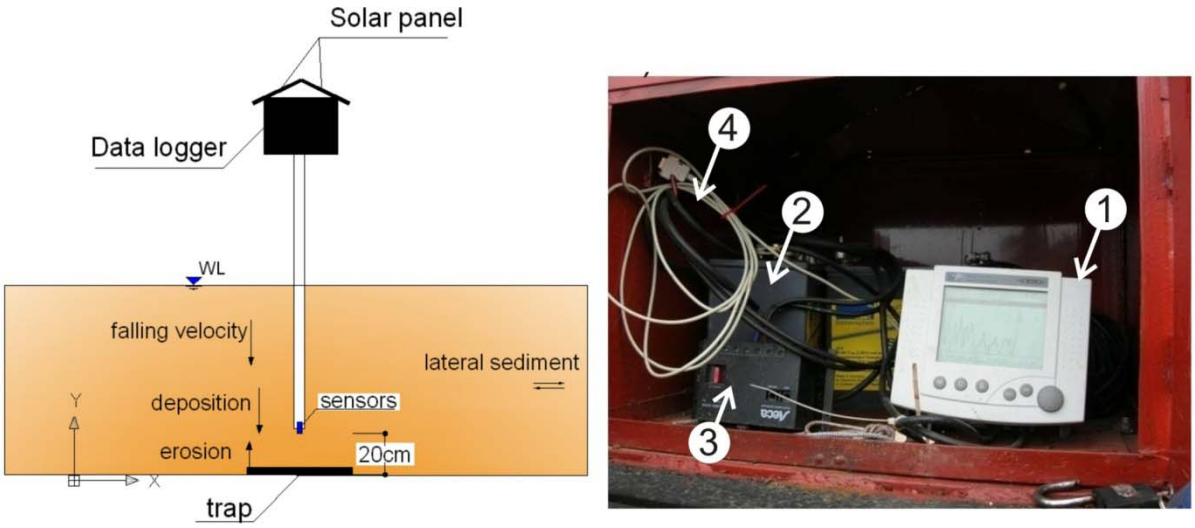

Figure 2.14. Scheme of turbidity sensor and sediment trap at T-stations in the floodplain (left), inside the data logger (right): (1) data logger, (2) battery, (3) solar control, (4) data cable.

2.4.4 Summary

The *in-situ* monitoring system has been implemented in 2008 and has monitored floodplain inundation and suspended sediment for three years (2008, 2009, and 2010). Until now, the system has proven to work very consistently with reliable data collection. The time series of water level, suspended sediment concentration, water temperature, electrical conductivity, and pH are unique for the Mekong Delta. The system has provides the most reliable and comprehensive data set for the Mekong Delta, into which we will seek more insight in the next chapters.

3 FLOODPLAIN HYDROLOGY OF THE MEKONG DELTA

3.1 General flood characteristics in the Mekong Delta

The annual flood volume of the Mekong River is about 475,000 million cubic metres. In a global comparison of large rivers, the Mekong River has the largest runoff per unit area, whereas it seems to be one of the large rivers with comparatively little anthropogenic interference (Adamson et al., 2009). However, this situation is likely to change in the future due to a number of dam projects along major tributaries and along the main river in Laos and Cambodia (Lu and Siew, 2006; Walling, 2008; Västilä et al., 2010; Xue et al., 2010).

The inundations in the Mekong Delta are dominated by three factors: (1) the flood hydrograph originating in the Mekong basin upstream of Kratie, (2) the buffering of the flood wave in the Tonle Sap lake system, and (3) the tides of the East Sea and the Gulf of Thailand (Figure 1.1). The Tonle Sap plays the most important role with regard to the duration of the flood in the Delta. At the beginning of the flood season, the flow is divided into two parts: flow to the Tonle Sap Lake and water flowing into the Delta. The water in the Tonle Sap Lake is reversed back to the Mekong River when the water level in the Mekong River is lower than the lake water level. This natural system buffers the floods reaching the Delta, resulting in less severe but prolonged floods compared to the floods at Kratie. The flow into the Tonle Sap starts around middle of June, while the return flow to the Mekong River normally initiates in the beginning of October. The annual average inflow and outflow volume of the Tonle Sap Lake is about 79.0 km^3 and 78.6 km^3, respectively (Kummu and Sarkkula, 2008).

The hydraulic gradient in the main river of the Mekong Delta is relatively small, about 2 to 5 cm/km. Data from 1978 to 2009 show that the travel time from Tan Chau to My Thuan (Figure 1.1) is about 7 to 22 days, corresponding to 5 km/day to 17 km/day. The flood hydrograph in the Mekong Delta has often two peaks, whereas the early peak arrives from mid-July to mid-August and the second peak from September to October. The second peak is associated with the landfall of typhoons from the East Sea.

3.2 Floodplain hydrology and hydraulics

Figure 3.1 shows water level time series for two stations, representative for the main river (T1) and for a secondary channel in the floodplains (H11). It can be seen that the hydrograph characteristics in the channel and the floodplain are generally identical, except with regard to

the tidal influence. The tidal influence is dampened in the floodplains due to the low momentum of the large inundation area.

The inter-annual comparison shows that in 2008 the first flood peak was more pronounced and the typhoon season increased the flood magnitude only slightly. In 2008 there was no major typhoon landfall in southern or middle Vietnam. In 2009, in contrast, there was a more distinct flood peak at the end of October indicating a more violent typhoon activity. On September 29th and 30th 2009 Typhoon Ketsana hit Central Vietnam, leading to heavy rainfall in the mountainous area along the border between Laos and Vietnam and to rapidly rising water levels in Laos between Pakse and Stung Treng. The resulting flood wave arrived in the investigation area around October 12th.

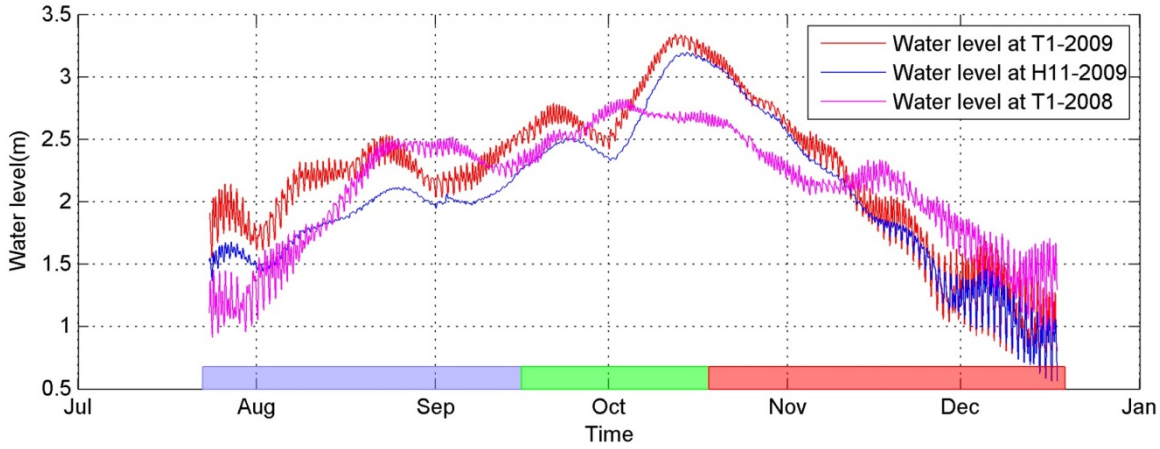

Figure 3.1. Water elevation at station T1 (2008, 2009) and H11 (2009). The coloured boxes in the lower panel indicate the stage of the flood (blue = rising, green = high, red = falling)

In order to discuss the inundation dynamics in a more structured way, the typical flood hydrograph in the Mekong Delta is divided in three periods: “rising stage”, “high stage”, and “falling stage”.

a) “Rising stage”: In this stage the flood regime is controlled by the inflow into the Tonle Sap and by the tidal influence. Flood control in the Vietnamese part of the Delta serves mainly for the purpose of crop protection. The second rice crop is usually harvested in August and the low dikes protect the paddy fields from inundation until they are harvested. As shown in Figure 3.1, the tide plays an important role during this period. Tides may cause short-term floodplain inundation in the case of coincidence of spring tides and early small flood peaks coming from upstream. The higher the flood level, the more attenuated is the tidal effect. This is shown in the comparison of the hydrographs of 2008 and 2009 at station T1. The tidal

influence is dampened with distance from the main river, as shown in Figure 3.3. H11 is located in a secondary channel at about 11 km distance from the Mekong River, resp. station T1.

b) "High stage": With rising water levels, the hydrodynamic processes change. Floodplain inundation is initiated by overbank flow or sluice gate operation in case of closed dike rings. The influence of the tides on the inundated progression is diminishing. At the upstream boundary, the Tonle Sap Lake releases water back into the Mekong River, while in the Plain of Reeds in the Delta the flood peaks from the Mekong and the overland flow from the Cambodian border coincide. Additionally, the hydraulic head created by the overland from North-East changes the stage-discharge relationship in the secondary channels: at the same river water level less water flows from the Mekong River into the channels (Figure 3.2, green marked data). During this period, typhoons may hit the southern part of the Lower Mekong basin. Typhoon induced floods superimpose the normal flood hydrograph caused by the South-West monsoon which may cause high flood peaks.

c) "Falling stage": From mid-October the water levels fall gradually, and there are no further flood peaks caused by tropical typhoons. Water levels are characterized by rising tidal influence and widespread human activities to regulate the remaining inundation waters in the floodplains. Traditionally, water is pumped out from the floodplains when the water level in the channels falls below the elevation of the low dikes. This facilitates the timely planting of the first paddy crop of the new cropping season. A particular feature at the beginning of this stage, i.e. between mid-October and mid-November, are stagnant and even reversal flow conditions, mainly in East-West channels. This is caused by a phase shift between the second flood wave coming overland from the Cambodian -Vietnamese border and the flood wave in the Mekong River. This feature is visible in the stage-discharge plot in Figure 3.2 (red marked data).

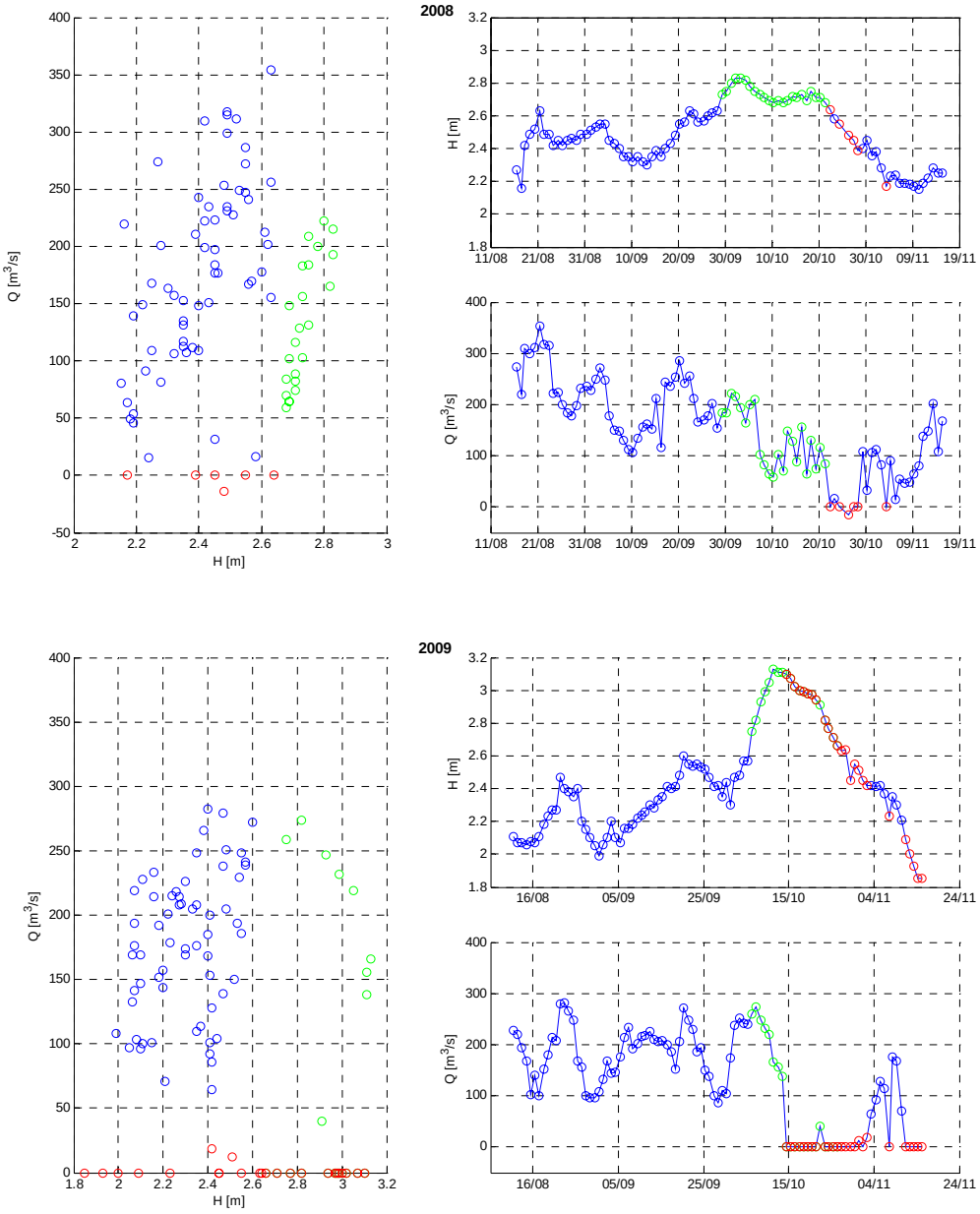

Figure 3.2. Stage-discharge relationships at station G1 (cf. Fig. 13) for the flood seasons 2008 and 2009. The colours indicate the stage of the flood 1) blue = rising, 2) green= high and 3) red= falling.

In Figure 3.2, the blue marked data represent the “normal” relationship during low flow and the rising stage of the flood, which is dominated by the flood wave of the Mekong River. The scatter in the data has to be attributed to the tidal influence. The green data indicate the high stage of the flood, where the flood wave of the Mekong River and the overland flood from North-East coincide. The red data indicate stagnant or even reverse flow conditions in the first phase of the falling flood stage, where the hydraulic head of the Mekong is falling below or

equal to that of the overland flood wave. Slightly rising water levels in the Mekong River by minor flood peaks alleviate this situation which is observable in 2009.

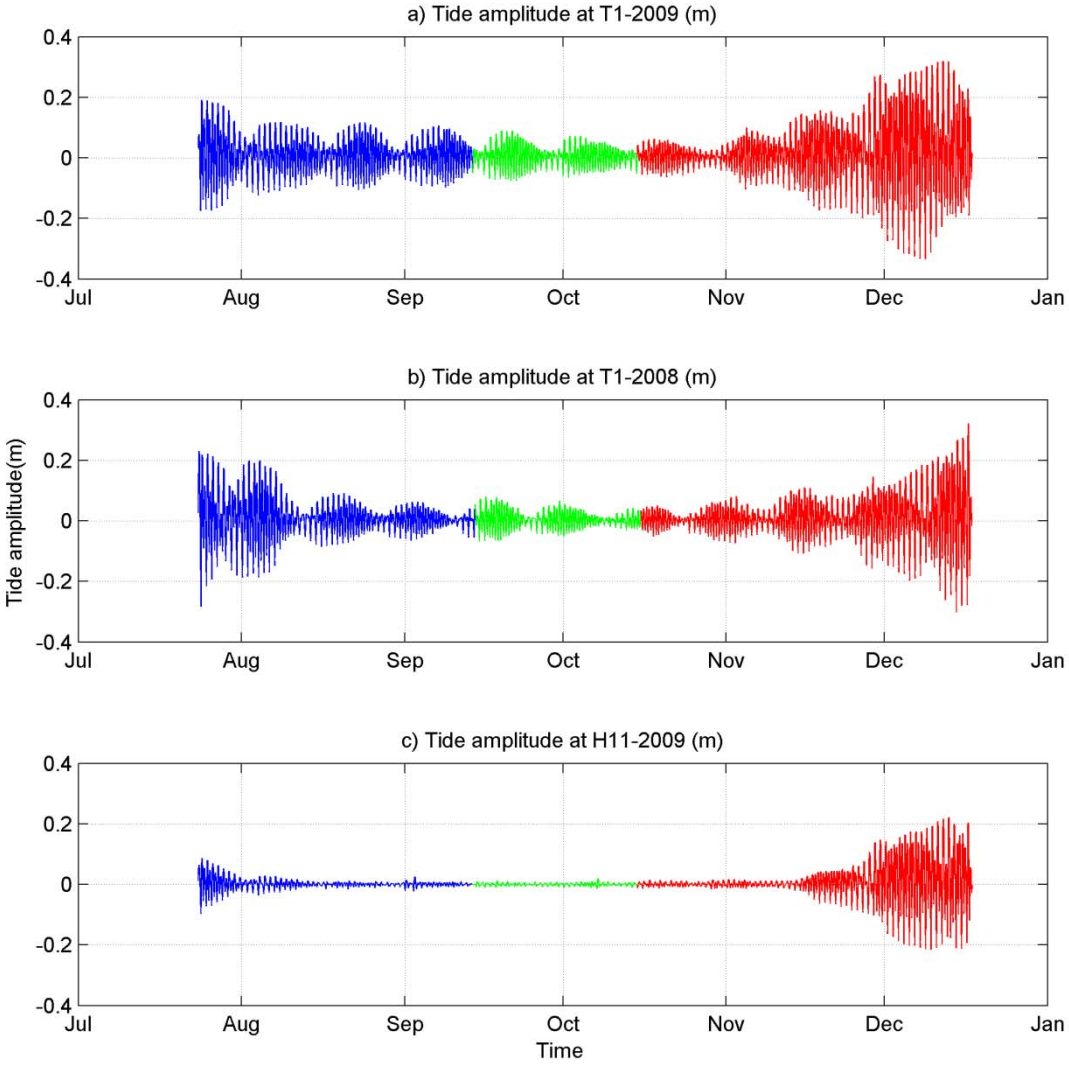

Figure 3.3. The tide signal of the water elevation, extracted by a Butterworth band-pass digital frequency filter with a band pass period of [low, high]=[6, 24] hours. The colour indicates different flood stages (blue = rising, green = high, red = falling).

In order to separate the tidal influence from the flood hydrograph, the tide signal was extracted by a Butterworth band-pass digital frequency filter with a band pass period of [6, 24] hours. In Figure 3.3, three distinct features become obvious:

1. The tidal influence is generally dampened during high flows, resp. high water levels: The amplitude during low flow is in the range of 1 m in the channels, while it is reduced to below 15 cm during high flow.

2. The tidal amplitude is dampened with distance to the Mekong River (compare H11 to T1), especially during high flows: T1 close to the main river still shows an amplitude of 20 cm, whereas H11 at 11 km orthogonal distance from the Mekong exhibits hardly any tidal influence during high flows (< 3 cm). This is due to travel time in the channel, but also due to the additional hydraulic head imposed by the overland flood from the Vietnamese-Cambodian border.
3. The tidal amplitudes in secondary channels and floodplains are generally lower than in the main river.

This means that the tidal influence is small during high flows in our study area. However, this is different in other parts of the Delta, especially those closer to the coastal line where high tides can trigger short-term inundations.

3.3 Floodplain inundation – spatial dynamics

Using a series of inundation maps derived from TerraSAR-X for the years 2008 and 2009, the impact of the dike systems and human control on the floodplain inundation could be assessed. Figure 3.4 shows inundation maps for the three flood stages “rising”, “high” and “falling” for comparable dates of both flood seasons 2008 and 2009 (blue = water, light yellow = no water, green = low dike, red = high dike). Figure 3.4a shows the “rising” stage, where the influence of flood control structures can be inferred comparing 2008 and 2009 in the surrounding area of station H6 and east of H11 and H3, and 3.4 b depicts the “high” stage features complete inundation of the area with flow over low dikes, and 3.4 c) shows in the “falling” stage the effect of the water pumping is visible, again most pronounced in the enclosed dike ring of station T6. The red circle indicates high convective alto-cumulous clouds with high water contents which are typical for tropical thunderstorms. These clouds cannot be penetrated by the X-band radar and the diffuse scattering from the clouds is interpreted as dry surface area.

Figure 3.4. Inundation maps of the study area derived from TerraSAR-X satellite images during the flood seasons 2008 and 2009

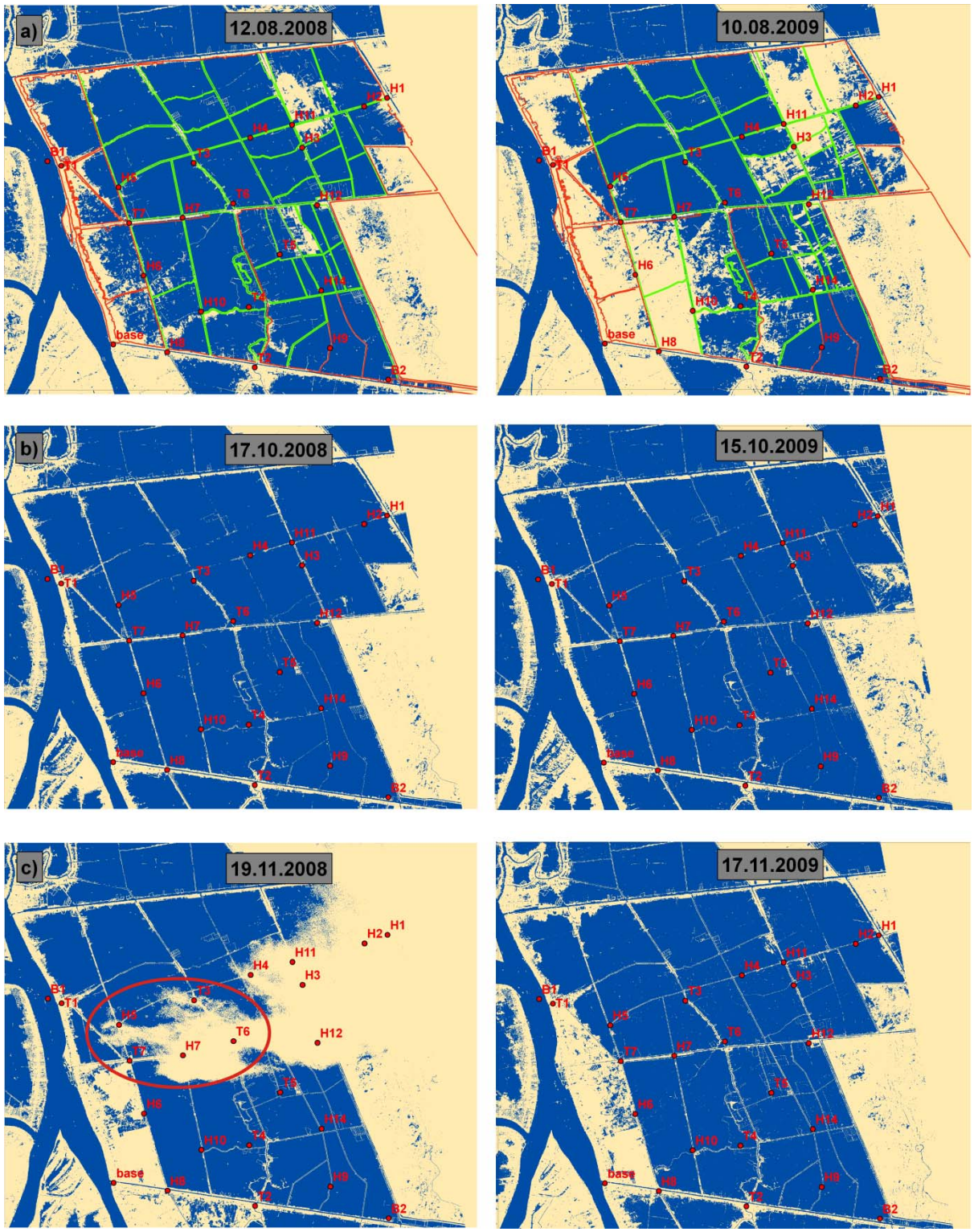

a) "Rising stage": Figure 3.4a shows that some floodplain compartments were flooded while others were not. Most of the dikes and channels are still continuously visible. This indicates that there was no or little overbank flow and that most of the floodplain inundation was

triggered by sluice gates operation. Especially floodplains that are completely enclosed by dike rings, e.g. the compartment in which station H6 is located, show a decoupling from the expected natural inundation dynamics triggered by overflow of low dikes. This is illustrated by the comparison of the water level at T1 and the inundation maps of 2008 and 2009. The water levels at T1 in the flood years 2008/2009 are 1.8/2.1m for Figure 3.4a, 2.7/3.3m for Figure 3.4b, and 2.2/2.0m for Figure 3.4c, respectively. In 2009, the water level was higher than that in 2008 at the time of image acquisition, but the compartment was not flooded which indicates a later opening of the sluice gates.

b) "High stage": During the high stage in mid-October a number of smaller channels and dikes are no longer visible. That indicates dike overtopping and, consequently, a hydraulic connection between channels and floodplains as well as between individual floodplain compartments. At this stage the inundation is uncontrollable by sluice gates in low dike systems. The sluice gates of the high dike ring systems are opened for agricultural benefits (e.g. input of sediments and nutrients).

c) "Falling stage": In this stage human interferences start again by pumping water out of the compartments with dike ring. In Figure 3.4c the compartment around H6 is already dry and the new cropping period is prepared. In compartments with low dikes the pumping cannot work before the water levels in the floodplains are below the dike levels. Inspection of the water masks in Figure 3.4b and 3.4c allows identifying the compartments fully protected by dike rings.

3.4 Floodplain inundation – temporal dynamics

The particular features of the channel-floodplain interaction identified by the satellite images, i.e. hydraulic linkage and anthropogenic interference, can be quantified in terms of their timing and capacity by the *in-situ* monitoring system described in chapter 2. Figure 3.5 shows the hydrographs for 2009 of gauging stations in neighbouring channels and floodplains for a dike ring with high dike levels in Figure 3.5a, and for a floodplain with low dike levels in Figure 3.5b. In case of compartments with high dikes, the floodplain inundation is completely controlled by sluice gates operation. This can be seen from the comparison of the hydrographs of station T7 in the channel and H6 in the floodplain along with the ground and dike levels of the floodplain compartments. The flood level is below the dike levels indicating the flood protection character of the dike ring. The first minor flood peak does not inundate the floodplain due to closed sluice gates. The opening of the sluice gates is recorded by H6. After

the opening, the inundation in the floodplain follows the channel water level with a slight delay. This delay is partly attributed to the distance between the stations, but also to the limited discharge capacity of the sluice gates. This limits the reaction of the floodplain to water level changes in the channels, causing a weaker hydraulic connection compared to low dike compartments. This weak hydraulic connection is also responsible for the low tidal influence on the floodplain hydrograph compared to the channel. At the end of the flood season the closing of the sluice gates and the operation of the pumps are detectable by the divergence of the time series in the floodplains and the channels. The water level in the floodplain drops linearly without any visible tide influence, indicating the pumping operation and pumping capacity.

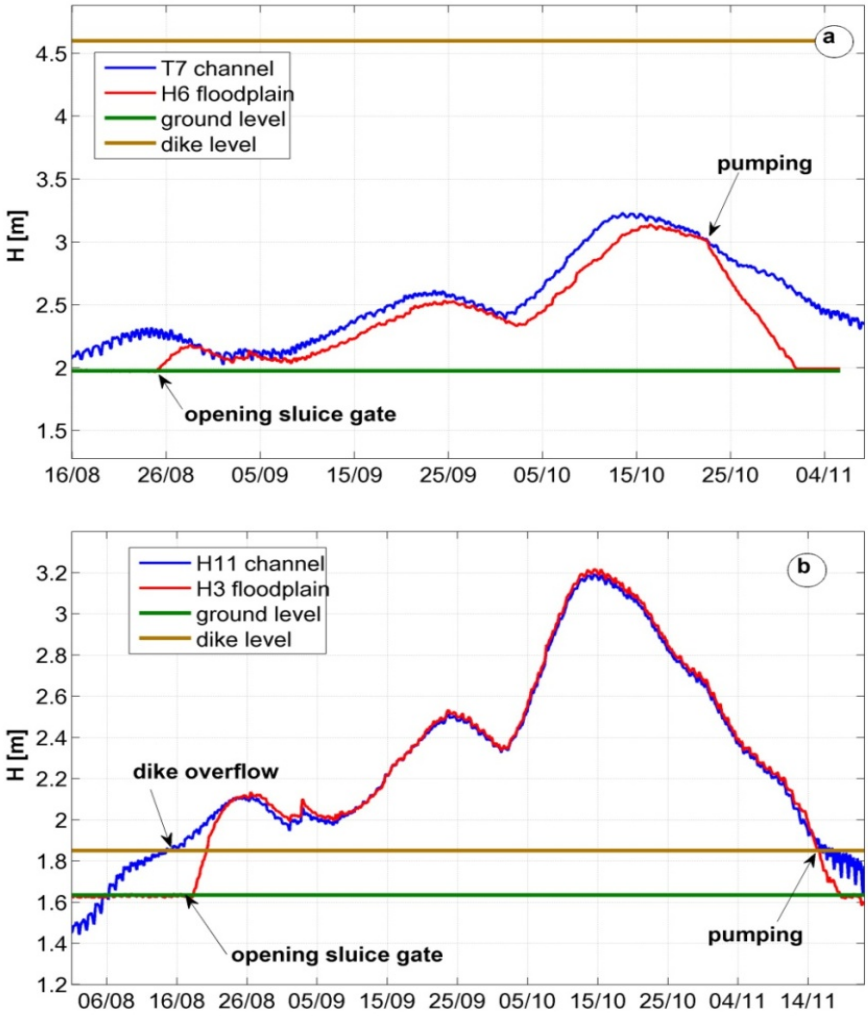

Figure 3.5. Comparison of channel and floodplain hydrographs in a dike ring with high flood protection dikes (a) and a floodplain compartment with low dikes (b) for the flood season 2009.

In contrast, the inundation of floodplain compartments with low dike levels is controlled by dike overflow. This is shown in Figure 3.5b by the comparison of the hydrographs of H11 in the channel and H3 in the floodplain. The onset of the floodplain inundation is clearly related to the lowest dike levels in the vicinity of H3. As soon as this level is exceeded, the floodplain inundation starts and quickly balances with the water level in the channel. The hydraulic connection between channel and floodplain is established over the entire length of low dikes and is thus more direct compared to dike rings with high dike levels. Figure 3.5b illustrates the close match between floodplain and channel hydrographs including the tidal influence. The pumping in these compartments cannot start before the water level drops below the dike level. Figure 3.5b also shows this effect: The divergence of the floodplain and channel water levels starts as soon as the dike level is reached. Then, the floodplain water level decreases linearly, indicating the pumping operation.

Using the recorded time series and topographical information, the capacity of the sluice gates and the pumps could be quantified. Table 3.1 lists the maximum volume of different compartments and the time required to fill up the compartment until equilibrium level. From these values the average discharge of all sluice gates of the specific compartment or the combination of sluice gate discharge and dike overflow can be calculated. It can be seen that the sluice gates in the high dike ring of H6 have the lowest capacity which explains the weak hydraulic connection discussed above. This hydraulic link has direct implications for the sediment budget in the floodplains.

Table 3.1. Sluice gate control and discharge, calculated from the recorded floodplain water level time series (T_1 is the initial time of flooding in the compartment, T_2 is the time when the water level inside the compartment equals the outside water level, $Q=V/\Delta T$, V is fill volume, $\Delta T=T_2-T_1$); at H3 the fill discharge is a combination of sluice gate and over-dike flow.

Station	Sluice opening time (T_1)	Levelled time (T_2)	Fill volume V [m^3]	Fill discharge Q [m^3/s]	Notes
H6	23/08/2009 22:15	26/08/2009 14:00	678,243	**2.95**	High dike
H12	14/08/2009 18:15	23/08/2009 12:30	2,997,487	**3.96**	Low dike
H14	13/08/2009 08:45	17/08/2009 22:15	1,890,895	**4.80**	Low dike
H3	17/08/2009 06:15	22/08/2009 08:30	3,325,825	**7.56**	Low dike

Similarly, the capacity of the pumps operated in the different floodplain compartments could also be estimated from the water level records. Table 3.2 shows that the high dike ring at H6 has a higher pump discharge and a higher volume. Since high dike rings are intended to grow three crops per year, they are provided with higher pumping capacities compared to low dike rings. This shows that if more high dike ring compartments are constructed, more water will be pumped out at the falling-flood stage, possibly leading to higher flood hazard downstream.

Table 3.2. Floodplain pump volume and discharge, calculated from recorded floodplain water level time series (T_1 is start of pumping, T_2 is end of pumping, $Q=V/\Delta T$, V is pump volume, $\Delta T=T_2-T_1$)

Station	Start pumping time (T_1)	End pumping time (T_2)	Pump volume V[m^3]	Pump discharge Q [m^3/s]	Notes
H6	21/10/2009 10:30	30/10/2009 23:00	6,182,167	**7.5**	High dike
H12	10/11/2009 13:45	20/11/2009 13:00	3,164,104	**4.1**	Low dike
H14	10/11/2009 14:30	19/11/2009 24:00	2,513,140	**3.1**	Low dike
H3	11/11/2009 08:45	20/11/2009 23:15	3,336,112	**4.0**	Low dike
T3	16/11/2009 10:15	21/11/2009 05:45	1,465,617	**3.5**	Low dike

The analysis shows that human activities influence the floodplain inundation in two ways. First, the construction of dikes for different purposes and, hence, protection levels influence the flood propagation. Second, the floodplain inundation and the associated sediment budget are heavily influenced by the operation of sluice gates in the rising stage and pumps in the falling stage. Hence, the size of the sluice gates and the operation schemes are key factors in the hydraulic linkage between channel (high concentration of sediment) and dike ring compartment (low concentration of sediment). The development of new dike ring compartments in the next decades has to take into account both aspects, the sediment trapping and the water pumping induced flood hazard to downstream areas.

3.5 Conclusions

While the large-scale flood characteristics are quite well known, the influence of control measures on the local floodplain inundation has not been studied in detail. The dynamics of floodplain inundation in the Mekong Delta is practically unknown. This study quantified, for

the first time, the dominant mechanisms, exemplarily for a typical area in the Plain of Reeds in the North-Eastern part of the Vietnamese Delta. The main findings are:

- The flood season can be distinguished into three different phases with their own specific hydraulic features: A rising stage where the inundation start in the floodplains is controlled by dike elevation and control of sluice gates, a high stage where floodplains and channels are hydraulically linked and the inundation dynamics are governed by the natural flood regime, and finally a falling stage where human control of inundation levels is resumed by pumping water out of the floodplains which prematurely disconnects the floodplains from the channels.
- The human impact on floodplain inundation through sluice gate operation and pumping could be quantitatively described. The hydraulic linkage between channels and floodplains differs between different types of floodplains. Floodplains in high dike rings have a weaker hydraulic linkage; this link is governed by the capacity of the sluice gates. Other floodplains are more directly linked to the channels. Today's inundation patterns are therefore patchy, compared to more continuous patterns which would result from pristine floodplain processes. Hydraulic models of floodplain processes often neglect these human controls. When implementing a hydraulic model, it is necessary to check if these human controls must be considered.
- Today, remote sensing data are extensively used for analysing hydrological and hydraulic systems. For the Mekong Delta, high resolution and high accuracy data are necessary, since the dike lines and channel network are very thin line object. However, they are key factors for flood inundation processes. The study used TerraSAR-X which is has the advantages of high accuracy and very high resolution (up to 3 m). This data set proved to be a very valuable information source for the study. However, a problem of the X-band radar is that the short wave length cannot penetrate high and dense alto-cumulus clouds with high water contents which are typical for tropical convective thunderstorm in the Delta.

In summary, this chapter gave quantitative insights into the complex interaction caused by the natural flood regime and the human interference of channel-floodplain inundation in the Vietnamese Mekong Delta. The information gained serves as a basis for land development and flood management planning. In addition, the unique time series of floodplain inundation dynamics will serve as a valuable set for in-depth hydraulic model calibration, calculation of suspended sediment dynamics in floodplain as well as the deposition and erosion processes.

4 SUSPENDED SEDIMENT DYNAMICS

4.1 Introduction

On a basin scale, the annual suspended sediment load into the Mekong Delta is about 160 million tons/year (Oanh et al., 2002; Walling, 2008) of which about 6 million tons are diverted into the Tonle Sap Lake and 2 million tons return to the river when the flow is reversed (Kummu et al., 2008). However, a sediment database is critically lacking in the Mekong basin. For this reason, sediment is one of the water-related issues that has generated the most misunderstanding among managers and scientists, as reported by Campbell (2007). Walling (2005) attempted to analyze and evaluate the sediment data for five key hydrological stations in the lower Mekong River, but none of those stations was located in the Delta. In 1998, the sediment monitoring program started at several hydrological stations: Tan Chau, Chau Doc, Vam Nao, My Thuan and Can Tho (Figure 1.1). With only one grab surface sample per day during the flood season, errors can easily occur, like overestimating or underestimating in total suspended sediment budget. These uncertainties arise not only due to the coarse temporal resolution but also due to the representation of a cross section 0.6km ÷ 2km wide and 15÷30 m deep by a single sampling point. Consequently, in a regional workshop held by Mekong River Commission in 2008 (MRC, 2008) it was decided to set up permanent sediment monitoring stations in the main rivers of the Mekong in the Vietnamese Mekong Delta starting in 2008. The stations were installed at Tan Chau, Chau Doc, Vam Nao, My Thuan, and Can Tho. At these stations the suspended sediment concentration is measured daily in a single vertical profile of the cross section.

There are a few studies containing information on sediment properties in the Delta. These are based on several field measurements in the Delta, such as floodplain sedimentation (MRCS/WUP-FIN, 2007), and riverbank erosion along main rivers by Hung et al. (2004) or Luu et al. (2004) for the Tan Chau river bend. In particular, Wolanski et al. (1996, 1998) studied the fine sediment dynamics in high and low flow conditions in the Bassac estuaries (from Can Tho City to the coast). They learned that the fraction of silt and clay is about 15 to 20%, flocculation occurs in fresh water regions, and tides play a very important role in fine sediment dynamics as well as in the erosion and deposition process. Concerning floodplains, there were two important technical reports by Thuyen et al. (2000) for the Long Xuyen Quadrangle and Kim et al. (2007) for the Plain of Reeds. Based on several field measurements

in three flood years (1997, 1998, 1999), Thuyen et al. (2000) reported that, through greater sediment trapping by developing a channel network, the nutrients from the Mekong River make a stronger contribution to the paddy fields. Kim et al. (2007) also indicated the high and low suspended concentration areas in the Plain of Reeds, based on their measurements of suspended sediment in 2000. These contributions were important for the initial exploration of sediment dynamics in the Delta. However, due to the very limited measurements and field campaigns, the information gained was very limited.

4.2 Seasonal dynamics of sediment in secondary channels

The secondary channel system distributes the water from the Mekong River into the floodplains, playing an important role in the sediment dynamics in the floodplain of the Mekong Delta. It navigates the sediments from the river to the fields and distributes them into floodplain compartments. These artificial channels are almost straight lines, and, although helical flow is negligible, the distribution of suspended sediment concentration across the cross sections is almost uniform, as shown in Figure 2.12. However, at the conjunction of channels, the suspended sediment concentration of both channels mixes very complexity.

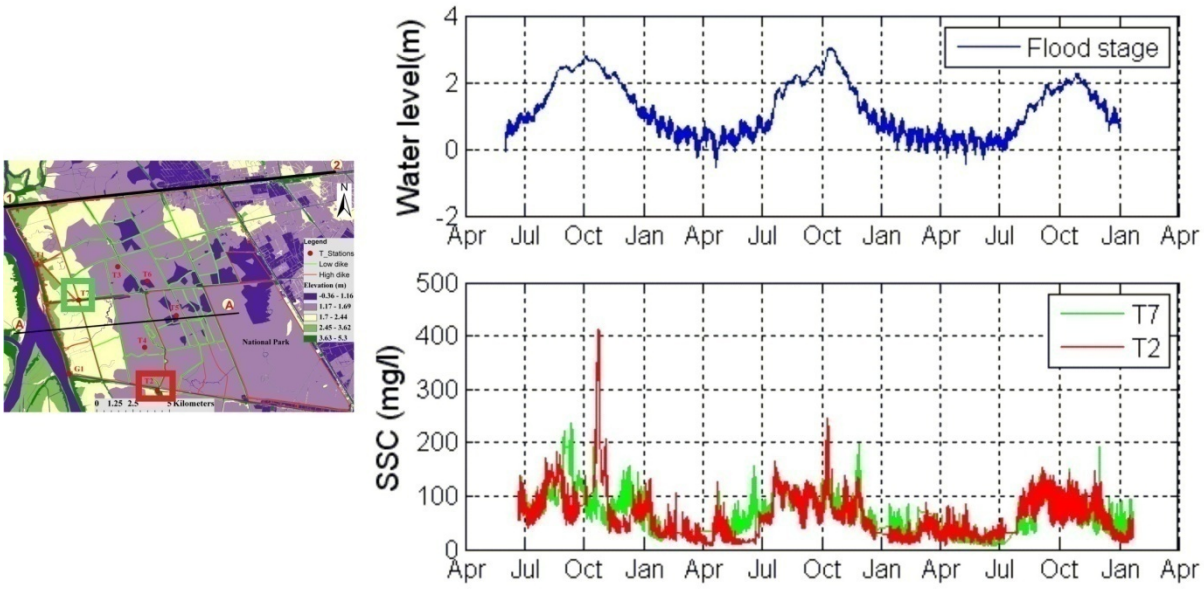

Figure 4.1 SSC at stations T2 and T7 in three flood seasons 2008, 2009, and 2010, on the left: red and green rectangle are location of T2 and T7, respectively, and at the top-right is water level at T2, at the bottom right shows time series of suspended sediment concentration.

Figure 4.1 depicts the variation of suspended sediment in the channel at the T2 and T7 stations. The following aspects can be derived:

- During the low flow season (January to July), SSC is relatively low: about 50mg/l on average in the channel network. The tide amplitude is about 1 m (Figure 3.3), and it dominates the variation of SSC during this period;
- During the high flow season (July to December), SSC rises at the beginning of July and reaches its maximum between September and October in 2008, 2009, and 2010;
- During the flood of 2008, there was a maximum SSC of about 400 mg/l at station T2 in October. However, at the same time, SSC at T7 was much lower. We do not have an explanation for this stark difference; it might indicate the influence of local activities that influence SSC at T2;
- During 2010, a very small flood year, the maximum of SSC was lower than 200mg/l, while in the other years (2008 and 2009) this value was significantly higher. In addition, tides dominate significantly the variation of SSC in the entire flood season of 2010.

It is clear that the suspended sediment is affected by two mechanisms: the flood wave and the tidal waves, with much higher frequency. Although the tide in the low flow period is stronger than in the high flow period, the suspended sediment concentration in the low flow period is relatively small, lower than 100mg/l. However, there is a small variation of SSC with tide variation. In that sense, the suspended sediment that the flood brings to the Delta from upstream plays a very important role in the annual sediment budget of the whole Delta.

The results from three years of monitoring show: (1) during low flow, the SSC is approximately 50mg/l, and the variation due to tide is about 20mg/l on average, (2) during high flow, the maximum SSC is about 200mg/l (exception 400mg/l with a question mark), (3) tides dominate the variation of suspended sediment in the comparatively low flood season 2010; the variation of SSC due to tides is about 50mg/l.

4.3 Anthropogenic influence on SSC dynamics

The manifold activities in the floodplains of the Delta affect the suspended sediment concentration. To investigate this influence, the author selected station T1 as reference station. T1 is close to the Mekong River and is less anthropogenically affected. T1 is compared to other strongly influenced stations. The channel geometry at the three stations T1, T2 and T7 is comparable since there is little difference in the water discharge between these cross sections. The variation of SSC due to the tide influence was removed by a Butterworth filter. Thus, the

high frequency variation of SSC as seen in Figure 4.1 is removed, the results are shown in Figure 4.2.

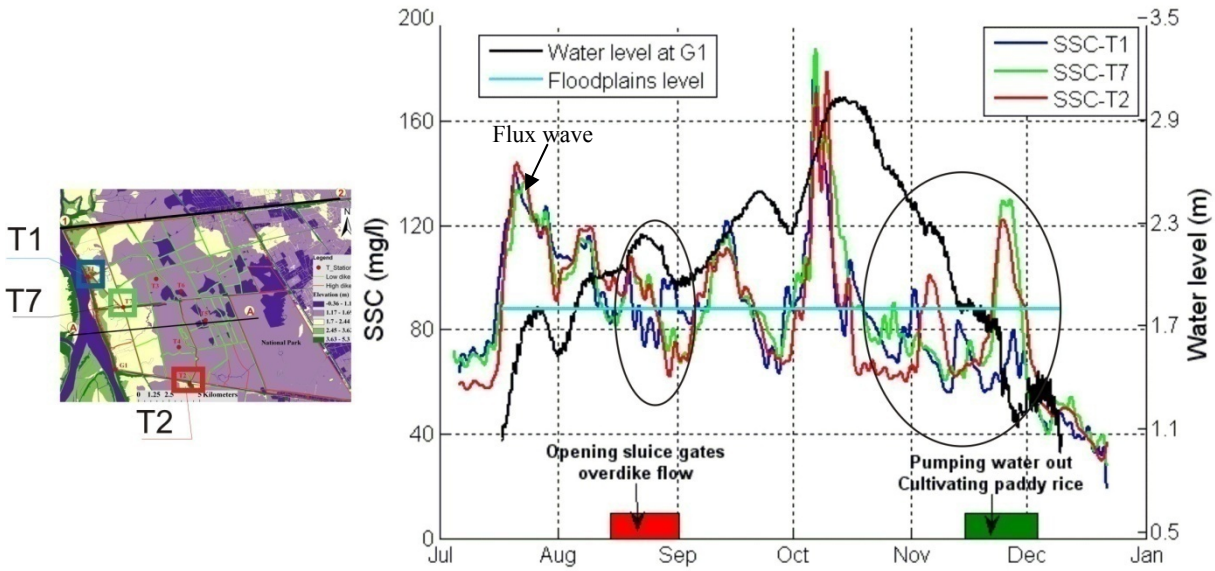

Figure 4.2. Time series of water levels and SSC in comparison to the anthropogenic influences sluice gates operation and pumping in flood 2009

Figure 4.2 on the right is the SSC after removing the short-term variations by a Butterworth band-pass digital high frequency filter with a band pass period of [0.5, 24] hours. The red, green, and blue lines show the suspended sediment concentration at the T2, T7, and T1 stations with the corresponding color on the left for their location. The comparison of the different time series shows:

- At the beginning of the flood season (July and August), the SSC in the secondary channels at different places (T1, T2, T7) is more or less identical. However, SSC begins to diversify when the flood stage reaches the floodplain level (about 1.8m a.m.s.l). In addition, at this time, the operating of sluice gates and overbank flow is initiated (Hung et al., 2011);
- From the beginning of September to middle of October, the difference in SSC in the different channels is small;
- The SSC values start to vary again with the stagnant stage of overland flow from Cambodia in mid-October. Additionally, pumping water out of the floodplains and starting the new crops in mid-November to December (section 3.4) increases the SSC inside the floodplain, but that does not influence station T1 because it is so near to the river.

Moreover, in Figure 4.2 on the right, we see a period with high sediment concentration (flux wave) close the end of July in 2009. At that time, however, the flood level was not equal to the paddy field level. Therefore, this sediment could not enter the paddy compartment. In order to maximize sediment trapping in the paddy field, we therefore, maybe lost this period of high sediment concentration.

In conclusion, by filtering the tide influence on the suspended sediment, the anthropogenic influence can be detected qualitatively. This influence increases the suspended concentration in two periods, namely during the opening of the sluice gate and the pumping of water out of the paddy field. Moreover, the data shows that, the early flood might carrying higher sediment concentration however this sediment would not enter the paddy field because the flood level is lower than the topography of the paddy field.

4.4 Reduction of suspended sediment concentration

In terms of (1) concentration, (2) deposition rate, and (3) particles size distribution, a reduction of suspended sediment in the floodplains and secondary channels has been found by many previous studies (e.g Pizzuto, 1987; Nicholas and Walling, 1997; Asselman, 1997; Middelkop, 1997). The present study measured the reduction of suspended sediment concentration quantitatively in the flood seasons 2008 and 2009. The first field measurement campaign was performed in mid-October 2008. We used a boat along with a manual sampler and portable turbidity sensor (PTM) to make a travel-measurement along the Hong Ngu channel – the Northern channel of the study area (Figure 4.3a). The portable turbidity meter was fixed one meter under the water's surface, and grab samples were taken during this travel measurement. The measurement lasted approximately from 8:30 to 10:00 on September 14th, 2008. The turbidity reading interval of the portable turbidity sensor was thirty seconds. There was no reversed flow from Cambodia, and water flow was directional from the Mekong River to the floodplain. The second measurement campaign was performed in the 2009 flood season at G1 (at the channel and river connection, see Figure 4.3a) and T2 (in the secondary channel). A Secchi disk (diameter = 30cm) measured turbidity at G1 every day at noon. At T2, a fixed optical backscatter sensor measured turbidity.

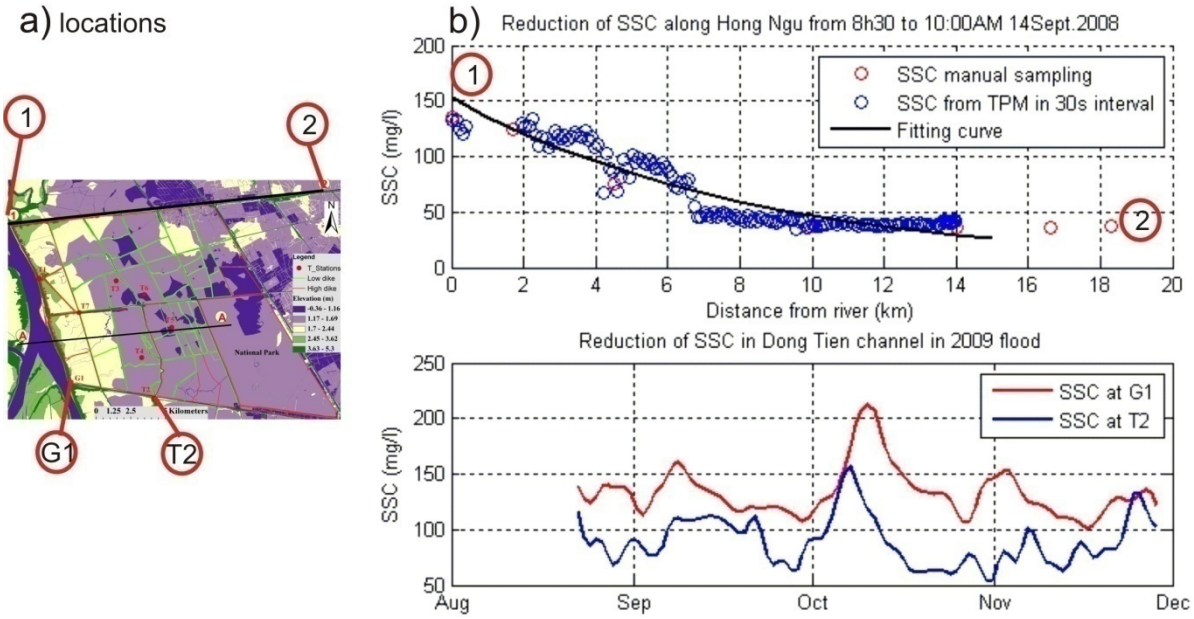

Figure 4.3. a) locations of stations monitoring the reduction of SSC; b) top, reduction of suspended sediment concentration along the Hong Ngu channel in 2008 from 8:30 to 10:30 on Sep. 14th. b) bottom, suspended sediment concentration at G1 (An Long) and station T2 in 2009 (distance between G1 and T2 = 6.4km).

Figure 4.3 shows the results of these measurement campaigns on the reduction of the suspended sediment concentration in the secondary channels. The distance between point (1) to point (2) is about 18.2km, and the distance from G1 to T2 is about 6.4km. In Figure 4.3b, the top depicts an exponential decrease of SSC along the Hong Ngu channel, where SSC was reduced from 140mg/l to only 50mg/l within a distance of 8km. Afterwards, SSC tends to stabilize. By monitoring with a very fine temporal resolution from the portable turbidity meter, one could also detect the drop in suspended concentration when the boat passed the channel conjunction. At the bottom of Figure 4.3b, there is the daily measured suspended sediment concentration at the G1 station with the Secchi disk in 2009 (conjunction between river and channel) compared with the concentration at T2 station (at the lower boundary of the study area). The suspended sediment concentration at the G1 station is always higher than that at the T2 station. The suspended sediment concentration at T2 station reaches its highest peak a bit earlier compared to the G1 station. This effect can be explained by the coarse daily time step which is not able to resolve the SSC variations induced by the tide.

The data from PTM was used to build a relationship between suspended sediment concentration (SSC) and channel distance from the Mekong River. The SSC reduction was estimated as:

$$SSC=1.16*C_0*Exp(-0.118L) \qquad R^2=0.87 \qquad (4.1)$$

whereas SSC is suspended sediment concentration (mg/l), C_o, the suspended concentration at the beginning of channel, and L is the distance from the connection between the Mekong River and the channel (km). R^2 is the coefficient of determination.

In summary, the reduction of the suspended sediment concentration along the secondary channel was measured quantitatively in the study area. This reduction of SSC happened within a distance of ten kilometres from the Mekong River, and the SSC tends to stabilize in the secondary channel after that. It should be noted that this finding is very important in optimizing sluice gate system operation to maximize sediment trapping for paddy fields. In order to trap more sediment into the floodplain to fertilize the soil, sluice gates located further from the Mekong River should be opened earlier than the one close to the River.

4.5 Sediment rating curve

In theory, total suspended sediment load includes two components: bed material load and wash load. The term "load" refers to the sediment being transported. The wash load has no relation to the sediment transport capacity of the stream flow; it is very fine sediment (grain size <62µm) (Jansen et al., 1979; Woo et al., 1986). As it has no relation to the stream transport capacity, determining the wash load, therefore, has to be based on an empirical relationship, like sediment rating curves (Asselman, 2000).

Walling (2005) reported that the main fraction of the sediment particles is clay and silt in the lower Mekong River, and that the wash load might dominate the total suspended load. In Laos, Cambodia and Thailand, sediment rating curves have been used for estimating total suspended sediment load and the effects of dams (Walling, 2005; Lu and Siew, 2006; Kummu and Varis, 2007; Walling, 2008; Wang et al., 2009). The present study tested the sediment rating curve approach by Asselman (2000) and by a quadratic relation for the study area. Asselman (2000) reported that the suspended sediment concentration has a power relationship with the water discharge:

$$SSC= aQ^b +p \qquad (4.2)$$

where SSC is suspended sediment concentration (mg/l), Q is water discharge (m3/s), and a, b and p are empirical parameters.

The daily discharge was provided by the Southern Regional Hydro-Meteorological Centre for two flood seasons 2008, 2009 at station T1, and for 2009 at station T2. The discharge was measured from bridges using wing flow velocity meters. The measurement range is about 0.15 to 3.5m/s with an error of <1.5%. This data is used in combination with the SSC from turbidity sensor measurements to test sediment rating curves. For this purpose SSC and water discharge of station T1 in 2009 is used to estimate sediment rating curves based on two different equations:

Asselman (2000):

$$SSC = 5.5675 * Q^{0.5569} + 42.913 \qquad R^2 = 0.29 \qquad (4.3)$$

and quadratic equation

$$SSC = 0.0078 * Q^{2} - 0.17 * Q + 77 \qquad R^2 = 0.36 \qquad (4.4)$$

Where SSC is suspended sediment concentration (mg/l), Q is water discharge (m3/s);

Both equations (4.3) and (4.4) explain the relationship between SSC and water discharge only poorly, as expressed by the low R^2 values and the scatter of the measured data in Figure 4.4b. However, the quadratic relationship has a slightly higher coefficient of determination and will be used for test calculations of SSC for selected stations and years in order to test the spatial and temporal transferability of the estimated relation.

Figure 4.4a and c shows the comparison between the measurement and the prediction of sediment concentration at station T1 for different years (2008, 2009). Figure 4.4c and d shows the comparison between the measurement and the prediction of sediment concentration at different locations but in the same year 2009. One finds that using the established sediment rating curve for a given year works better estimating SSC for other locations in the same year than at the same location but for different years. But in any case the predictions using a sediment rating curve are of low quality. This had to be expected due different influences determining SSC, i.e. the general load from the upstream Mekong basin, the reduction of the sediment concentration with distance from the main river and the tidal influence. All these factors differ in time and space, making an estimation of a generally valid sediment rating curve very complicated. Thus, valid sediment rating curves for the Mekong Delta have to be established for every flood season and have to take the different influencing factors into

account. However, this is not within the scope of the presented work, and the tested simple sediment rating curves will not be used herein.

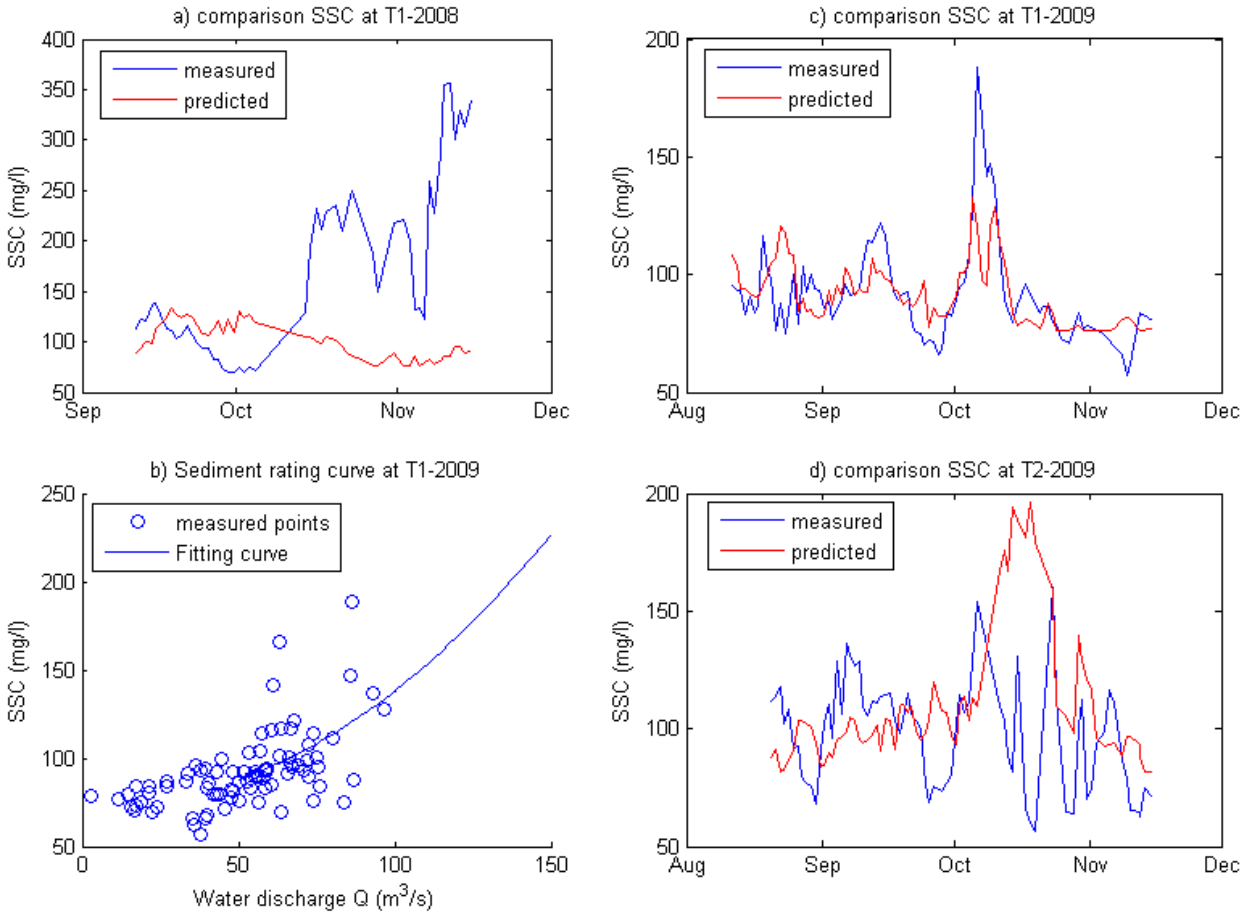

Figure 4.4. The applicability of sediment rating curve for predicting SSC in study area

4.6 Sources and sinks of sediment in the floodplains

The sediment is often captured into compartments via sluice gates or simultaneous overbank flow. This feature must be kept in mind during the data interpretation and mathematical modelling of sediment dynamics in the Mekong Delta. The sources and sinks play very important roles in any description of sediment dynamics:

- The source of sediment in the type I-channels (connection to the Mekong River) is the sediment at the conjunction of the channel and the Mekong river;
- The source of sediment in the type II-channels (connection between two I-channels) is the type I-channels, etc.
- The sources of sediment in compartments are sluice gates and dike overflow.

The paddy compartments work as sinks of suspended sediment while the channels work as sediment carrier. The channels and sluice gates navigate sediment entering the fields, a part of this sediment will be deposited in the compartments after a flood season. The capacity of the hydraulic linkage between compartment and channel is reported in table 3.1 in chapter 3. The maximum filling discharge of a low dike compartment is about 7.5m^3/s, and this discharge happens in a period of five days in mid - August (the filling discharge is that which fills the compartment from the empty state to the water level equal to the channel). Multiplying this discharge by the suspended concentration in the channel results in the suspended sediment flux from the channel to the paddy field at the initial stage. This is, however, a very rough estimation because the exchange of water between compartment and channel still occurs during flood season.

Figure 4.5a shows the different sediment concentrations of the channel and paddy field compartment. The suspended concentration inside the compartment is lower than in the channel, which is proven by the turbidity sensor data in Figure 4.5b. At the time of this picture, the channel water level nearly reaches the crest of the dike. If overflow happened, the suspended concentration in the channel and in the paddy field would have mixed.

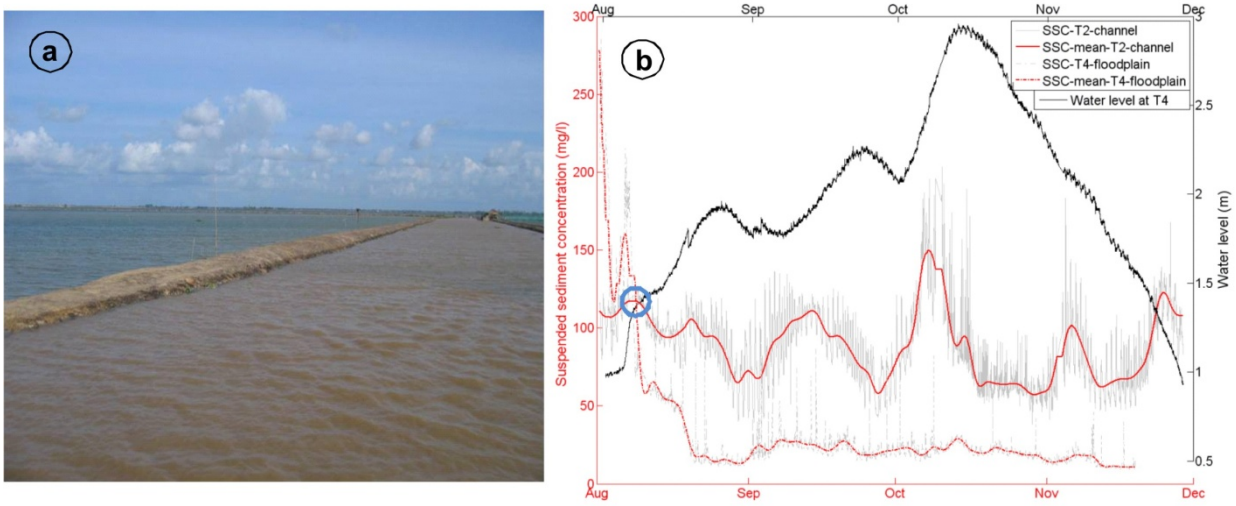

Figure 4.5. a) different sediment concentration in channel (right) and floodplain compartments (left), b) sediment concentration at T2 in channel and T4 in floodplain compartment, flood season 2009.

In addition, Figure 4.5b shows that the suspended sediment concentration in the floodplain compartment (T4) decreases with time, while the suspended sediment concentration in the channel (T2) has a very strong variation related to the flood flow regime. The suspended

concentration inside the compartment is less influenced by tidal effects than in the channel. Floodplain data shows that not all sediment will be deposited in the compartment, the concentration is about 20mg/l, which stabilizes with time.

Moreover, in Figure 4.5b, one sees that the initial SSC in the compartment is higher than in the channel. This is because some rice stubbles remain from the previous crop. When this material putrefies, it is considered organic matter in the water and is detected by our turbidity sensor. The blue circle points out the moment when the concentration of suspended sediment inside and outside of the floodplain compartment is equal. This again suggests that opening the sluice gates when the channel has high suspended sediment concentration it might bring more sediment into the paddy fields.

4.7 Conclusions

The results from the measurements allow us to conclude several main points:

- The suspended sediment dynamics in the floodplain of the Mekong Delta relies on two mechanisms: one being the flood wave, the other being the tidal waves that have a much higher frequency. The results from three years monitoring of suspended sediment in our study area show: (1) during low flow, the SSC is approximately 50mg/l and varies due to the tide at about 20mg/l, (2) during high flow, the maximum SSC is about 200mg/l.
- The anthropogenic influence on suspended sediment concentration can be qualitatively detected. This influence increases the suspended concentration during two periods: sluice gate opening in August and pumping water out of the paddy field between November to December.
- We observed and quantified the reduction of sediment along the channel. This exponential decrease happened within 10km from the Mekong River; beyond this distance, the concentration tends to stabilize.
- Not all suspended sediment entering the paddy fields is deposited. Because flocculation is weak, particles are very fine. Therefore, the background concentration of SSC in the floodplain was about 20mg/l.
- One finds that using the established sediment rating curve for a given year, the annual variability is stronger than the spatial variation. But in any case the predictions using a sediment rating curve are of low quality. This had to be expected due different

influences determining SSC, i.e. the general load from the upstream Mekong basin, the reduction of the sediment concentration with distance from the main river and the tidal influence. All these factors differ in time and space, making an estimation of a generally valid sediment rating curve very complicated.

- The sluice gates and pump stations are point sources of SSC entering or exiting the floodplain compartments. They are the key factor in terms of regulating flood water as well as sediment trapping in the paddy fields. However, a better design for operating the sluice gates and pumps is an urgent necessity.
- To maximize sediment trapping in order to fertilize the soil in the paddy fields, some important factors should be taken into account: (1) the suspended sediment concentration in the channel (magnitude and time of occurrence), (2) the channel flood stage in comparison to the paddy field topography levels, (3) sluices located further from the Mekong River should be opened earlier.

5 SEDIMENT DEPOSITION AND EROSION DYNAMICS

5.1 Introduction

Deposition and erosion are twin aspects in studying the river and coastal morphology and their reclamation. They play a key role in

- determining the sediment budget of a river basin, reservoir sediment trapping, floodplain sedimentation, transport and storage of contaminants, design of flood protection measures, stabilization of the riverbanks;
- estuary deposition and erosion, access channel deposition, port sedimentation;
- canal deposition, reduction of capacity of irrigation structures;
- ecological rehabilitation, etc.

As little is known about erosion and deposition in the Mekong Delta, even basic sediment properties are lacking. The Delta in Vietnam is intensively used for agriculture, and it is prone to annual widespread flooding. The natural floodplains have been cut off by channel networks and many different paddy fields and aquaculture ponds. Despite this, no quantitative information on their sediment trapping has been reported. This chapter, therefore, aims at clarifying the deposition/erosion issues based on a database of measurements in three flood years (2008, 2009, and 2010).

The chapter is devoted to the understanding of deposition and erosion processes in the Delta. The two existing, yet conflicting, paradigms in the study of deposition and erosion of cohesive sediment are reviewed. The method for estimating the key parameters that control the deposition and erosion is described (threshold for deposition and erosion). Moreover, the basic sediment and water properties are discussed. The differences in the deposition rate and its varying spatial distribution between low and high dike ring compartments are investigated in a low flood year 2010. Finally, the total volume of sediment deposition in the study area is estimated based on different methods.

5.2 State of the art

5.2.1 Floodplain sedimentation studies

Quantification of patterns, properties, and characteristics of sedimentation in floodplains around the world have received much scientific attention (e.g. Wolman and Leopold, 1957; Walling and He, 1998; Asselman and Middelkoop, 1995; Thoms et al., 2000; Baborowski et al., 2007). There are many field studies for quantifying the sedimentation rate using varying technologies: sediment traps, erosion pins, topographical surveys, radionuclide dating, tracer studies, historical marks, artificial markers (Walling 1999; Middelkoop, 2005; Seiger et al., 2003). Among these methods, the use of the sediment trap may be the most efficient and convenient approach due to its simplify and low cost in the field, and inexpensive laboratory work (Seiger et al., 2003). In general, sediment traps are installed in advance of a specific flood event and are retrieved for sediment analysis after that flood event. The information derived from those sediment traps includes deposition rates, spatial pattern of deposition, particle distribution, clay and silt fractions, organic and inorganic contents, etc. Clusters of sediment traps have been used to represent patterns of floodplain deposition (Middelkoop, 2005; Seiger et al., 2003). The limitations of sediment traps are the necessity of post-event-evaluation and missing linkage between sediment characteristics measured at the trap and hydraulic condition. Questions regarding the dynamics of erosion and deposition during floods are difficult to answer.

Since the 1980's, mathematical models have been applied in the study of floodplain sedimentation (Pizzuto, 1987; Nicolas and Walling, 1997; Asselman and Wijngaarden, 2002). Sediment transported in a floodplain has usually very fine grains containing mainly silt and clay, and showing cohesive sediment characteristics. Their interaction in water is quite complex (Metha et al., 1989; Droppo, 2001; Partheniades, 2007). To quantify cohesive sediment processes, we can use a hydraulic model coupled with deposition and/or erosion modules (Pizzuto, 1987; Nicolas and Walling, 1997, Middelkoop and Van der Berg, 1998). Other alternatives in mathematical studies of floodplain sedimentation are the method of sediment trapping efficiency (Narinesingh et al., 1999; Asselman and Wijngaarden, 2002) and the conveyance loss by Walling et al (1986).

In the study of deposition and erosion of cohesive sediment, a mathematical application has to determine some key parameters, such as the threshold for deposition and erosion. Until now, the threshold for erosion has been widely accepted, and there are numerous *in-situ*

instruments for measuring this threshold (e.g Houwing, 1999; Lawler, 2004). The threshold for erosion tends to be correlated with the dry or wet bulk density of the bed material (e.g. Hwang and Mehta, 1989; van Rijn, 1993). However, the existence of a threshold for deposition is still under discussion (Winterwerp, 2007, Ha and Maa, 2009). There are two conflicting paradigms which indicate the deposition rate and erosion rate differently: the exclusive paradigm and the simultaneous paradigm. The exclusive paradigm suggests that the erosion process and deposition process do not occur at the same time, while the simultaneous paradigm suggests they occur at the same time. Hence, the quantification of erosion rate and deposition rate are different for the two paradigms. Almost all studies related to these two paradigms have been based on laboratory experiments (Winterwerp, 2007, Ha and Maa, 2009). It is quite common in engineering applications to follow the exclusive paradigm by using the work of Krone (1962) for deposition, and the work of Partheniades (1965) for erosion.

This study investigates the erosion and deposition processes in floodplains of the Delta. The sediment traps were strategically distributed in the study area in order to collect the highest possible deposition rate for the floodplains. Moreover, the deposition rate in compartments with low and high dike rings is investigated. The combination of sediment traps and turbidity sensors allow us to understand the dynamic processes of deposition and erosion in the study area and to define key parameters for calculating deposition and erosion. The results offer a basic understanding of deposition and erosion in the floodplains of the Mekong Delta.

5.2.2 The two conflicting paradigms of cohesive sediment processes

The subject of sediment transport has been studied for centuries, and there have been many efforts to develop sediment transport functions or formulas around the world. There exit numerous empirical formulas, used for solving engineering and environmental problems. However, the results obtained from different formulas differ from each other and from the field measurement.

Non-cohesive and cohesive sediment has different transport mechanisms. While non-cohesive sediment has received attention earlier (1870s), cohesive sediment research has started in the 1960s. The classification of cohesive sediment and non-cohesive sediment is fuzzy. In general, the finer the sediment, the more cohesive the sediment is. Sediment with a particle size smaller than 2μm is considered as cohesive sediment, and larger than 62 μm is

considered as non-cohesive sediment. Between 2μm to 62 μm is silt which is in the transition zone between cohesive and non-cohesive sediment.

Until now, there have been several major contributions, and most of them have been derived from laboratory and field observations in cohesive sediment studies. Krone (1962) reported from his laboratory experiment of sediment of San Francisco Bay that the deposition occurred when the bed shear stress (or critical velocity) was below a certain threshold. Later on, Partheniades (1965) and Mehta et al (1973) repeated Krone's experiment. Their results agreed with what have been found by Krone (1962). Moreover, Partheniades (1965) indicated that erosion will occur while the bed shear stress is larger than a threshold for erosion. So, the shear stress threshold for deposition is lower than for erosion. These findings suggest that erosion and deposition do not occur at the same time - so called the mutually exclusive paradigm. In other words, there is a period of time while the bed shear stress is smaller than the threshold for erosion and larger than the threshold for deposition ($T_d < \tau_b < T_e$). During this period, neither erosion nor deposition occurs. Based on these concepts, Krone (1962) and Partheniades (1965) produced two equations for calculating deposition and erosion rate, depicted in Table 5.1. These equations have been used widely in limnology, coastal and river morphology. In general, non cohesive sediment has only a single threshold for both deposition and erosion, the deposition or erosion will occurs when the bed shear stress is lower or higher than this threshold. The presence of critical shear stress for deposition, therefore, make different between non cohesive and cohesive sediment transporting mechanism.

However, when Sanford and Halka (1993) analyzed a series of field measurements under tidal conditions, they found that their field measurements could not be simulated well with the mutually exclusive paradigm. According to Sanford and Halka (1993), deposition and erosion can occur at the same time, thus, generated a conflict amongst latter studies. Especially, Winterwerp (2007) re-analysed the experiment of Krone (1962) by a simple mass balance model and the shear stress described by a skewed probability density function. He concluded that the threshold for deposition does not exist.

Recently, Ha and Maa (2009) performed laboratory experiments for evaluating the two paradigms and concluded that the threshold for deposition does exit. The debate is still ongoing, and its shows that process understanding is weak and quantification of sedimentation processes is mainly based on empirical evidence.

Table 5.1. Summary the two conflicting paradigms

	Exclusive paradigm	Simultaneous paradigm
Definition	Deposition and Erosion do not occur at the same time	Deposition and Erosion occur at the same time
Bottom layer boundary condition	$\frac{\partial C}{\partial t} = E \; for \; \tau_b > T_e$ $\frac{\partial C}{\partial t} = D \; for \; \tau_b < T_d$	$\frac{\partial C}{\partial t} = E - D$
Existence of T_d	Yes	No
Existence of T_e	Yes	Yes
Deposition rate	$D = w_s C_b \left(1 - \frac{\tau_b}{T_d}\right)$ for $\tau_b < T_d$ D=0 for $\tau_b > T_d$	$D = w_s C_b$
Erosion rate	$E = M_{se}\left(\frac{\tau_b}{T_e} - 1\right)$ E = 0 for $\tau_b < T_e$	$E = M_{se}\left(\frac{\tau_b}{T_e} - 1\right)$ E = 0 for $\tau_b < T_e$

Where C is the depth average suspended sediment concentration; C_b, near bed suspended sediment concentration; E, erosion rate (kg/m^2/s); D, deposition rate (kg/m^2/s); τ_b, bed shear stress (N/m^2); w_s, particle settling velocity (m/s) Empirical parameters: T_e, critical bed shear stress for erosion; T_d, critical bed shear stress for deposition, M_{se}, constant erosion rate (kg/m^2/s).

5.3 Basic sediment and water parameters

5.3.1 Water temperature

Water temperature is a basic factor controlling the processes of fine particles in suspension as well as the water quality (Webb et al., 2008). However, it has received little attention in the hydrological monitoring program at the main stations in the Mekong Delta. In our monitoring system, water temperature was investigated at seven water quality stations (T-stations), representative of channel water temperatures, and floodplain temperatures.

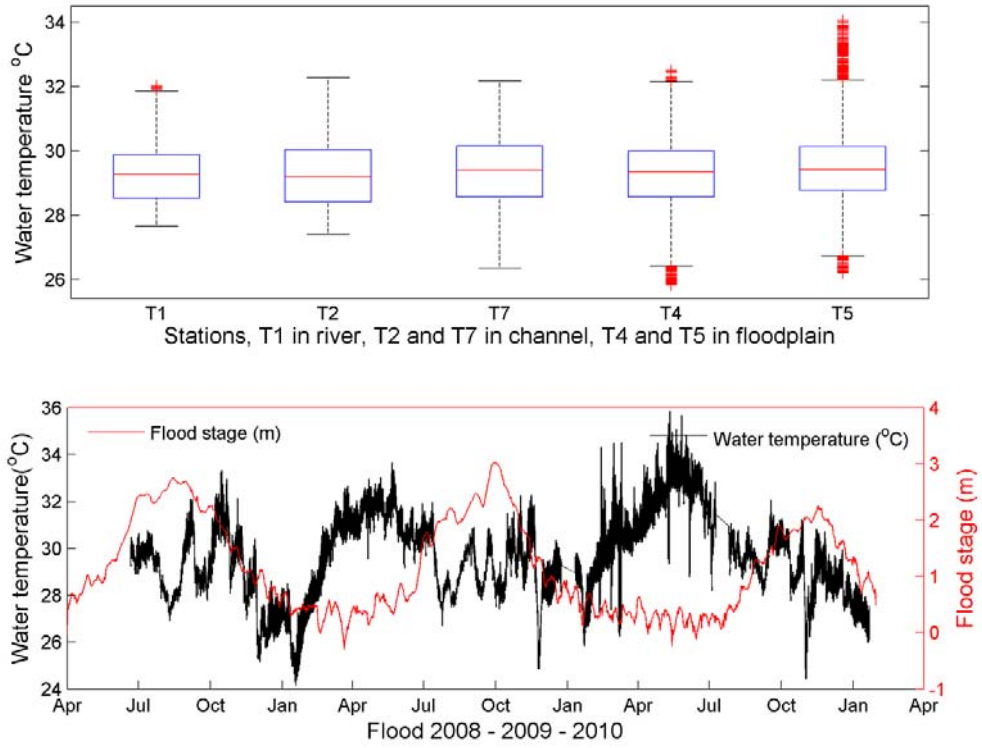

Figure 5.1 The variation of water temperature and flood stage: at the top is the variation of water temperature in the river, channel, and floodplain in the 2009 flood; at the bottom is the water variation in the three years of 2008, 2009, and 2010 at station T2.

The top of Figure 5.1 depicts the variation of water temperature during flooding in 2009 at different locations. It is interesting that the average water temperature is quite homogeneous across the stations (about 29^{o}C), while the daily variation is relatively large. The station T1 (near the river) shows a smaller variation of water temperature than the ones in the secondary channel and in the floodplain. The variation of water temperature in the river is around 5^{o}C while it is 8^{o}C to 10^{o}C in the secondary channel and floodplain, respectively. Figure 5.1 also includes red dots, especially in the floodplain stations (T4 and T5). They represent the water temperature at very low water depth in the compartment. When the water depth is very shallow (at the beginning or end of the flood season), the air and water temperature variation is quite similar. Moreover, station T1 also shows some red dots. Because this station is located on a high bridge, it requires a longer cable to submerge the sensor in the water. The cable, however, was not of sufficient length, so there were a few measurements when the sensor was not submerged in the water or was very close beneath the water's surface.

The bottom of Figure 5.1 shows the whole three year water temperature monitoring at station T2 in a secondary channel. The red line depicts the water level after removal of the tide

influence and the black line shows the daily variation of water temperature. During the low flow season (January to June) the water temperature is higher and stronger in variation. However, when the flood arrived the stream became colder (June to December). Overall, the variation of water temperature is in range of 24°C to 36°C.

Moreover, the diurnal temperature cycle seems to be linked a SSC cycle of equal period at the water quality station in the paddy fields. A wavelet approach was applied to estimate the different phase shifts in the temperature and SSC cycle at station T4 in the 2009 flood. This method estimates the strength of the phase coherence and the phase shift over time, by smoothing a time-frequency spectrum based on the Morlet wavelet (Torrence and Compo, 1998).

The phase shift between the two signals (temperature and SSC) was estimated as a lag time. Different lag times were found at different stages of the hydrographs, as shown in figure 5.2. Note that the localization of the different stages is only approximate, due to a necessary smoothing of the time-frequency spectrum. The lag times appear to follow water levels (or water depth). By reconstructing the frequencies on the daily range (between 18 and 30 hours) for time intervals of significant phase coherence, and by correcting their phase shift by the respective time lag, it was possible to find a clear relationship between temperature and SSC, as shown in the scatter plots of figure 5.2. Temperature is by no means the only influencing factor of SSC, but the dominating one on the daily scale, especially in stagnant water.

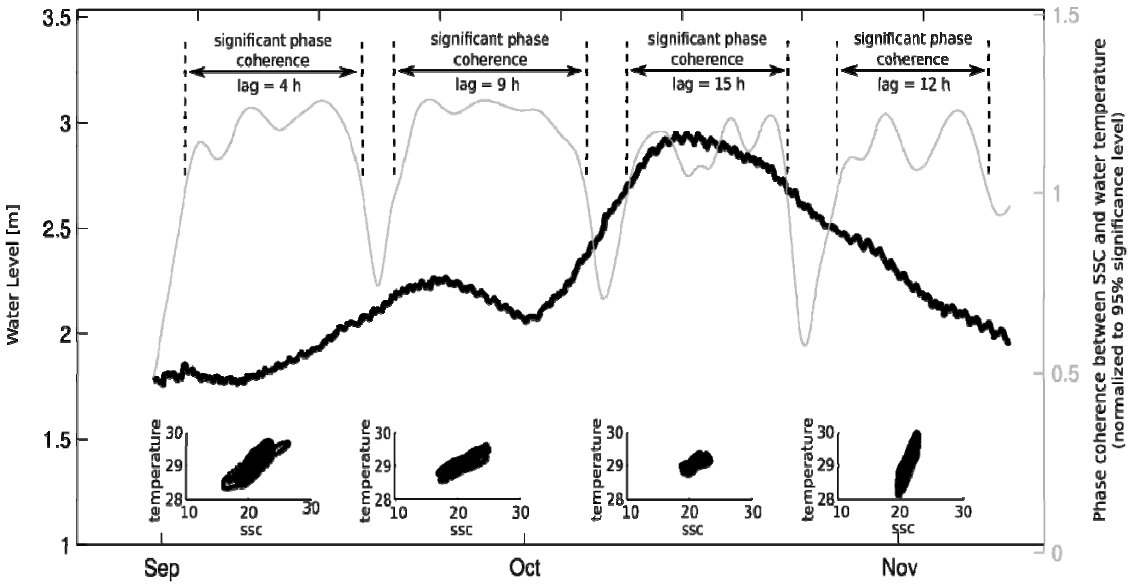

Figure 5.2. Water level and phase coherence of the daily cycle between SSC and water temperature in compartment measured at T4 in 2009. The different relationships between SSC

and temperature for different stages of the hydrograph are shown by the scatter plots. Unit for SSC is mg/l and for temperature is degree Celsius (^{o}C).

The process responsible for this dependency is the change of water density and viscosity with temperature. This, in turn, influences the settling velocity of the suspended particles. Temperature changes in the water column follow a daily cycle. The different time lags between SSC and temperature as illustrated in Figure 5.2 correspond to different water depths. In general the time lag is caused by differences in the temperature perturbation of the water column and the time required for the suspended particles to settle form the upper water layers to the lower layers, i.e. the difference between the vertical temperature changes in the water column to the settling velocity. This difference increases with higher water levels causing the detected longer time lags at periods of higher water levels (cf. Figure 5.2).

In conclusion, these findings showed that the water temperature has a strong influence on the suspended sediment concentration. Hence, temperature should be used as a parameter to improve the applicability of the rating curve approach discussed in section 4.5.

5.3.2 Dispersed grain size distribution

In floodplain sedimentation studies, one of the challenges is to determine the sediment grain sizes, since the sediment is either clay (<2µm) or silt (2-63µm). Many authors used LISST instruments for measuring the particle distribution (e.g Williams et al., 2004; Thonon et al., 2005). In some cases, there was no *in-situ* measurement of the grain size, the sediment retrieved from the sediment traps could also be used for grain size analysis (e.g Asselman and Middelkoop, 1995; Thonon et al., 2007).

In addition, in the case of the Mekong Delta, the dike system works like a vertical wall to stop the entering of coarser sediment into paddy compartments. The lower concentration and finer particles near the surface of the water body can enter the compartment by the overflow of the dike system. The coarser particles could enter through a culvert system, but this depends on the capacity of the culvert. Figure 5.3 shows the dispersed grain size from twelve traps in different locations in the floodplains during the flood season 2010 (see also Figure 5.9 for trap locations). Sediment retrieved from the traps was used for grain size analysis. The sedimentation method was applied, and grain size was determined based on a Hydrometer. The median size is about 10 to 15 µm, and it is rather homogenous across the twelve traps, although the samples were collected from low dike rings and high dike rings in different locations.

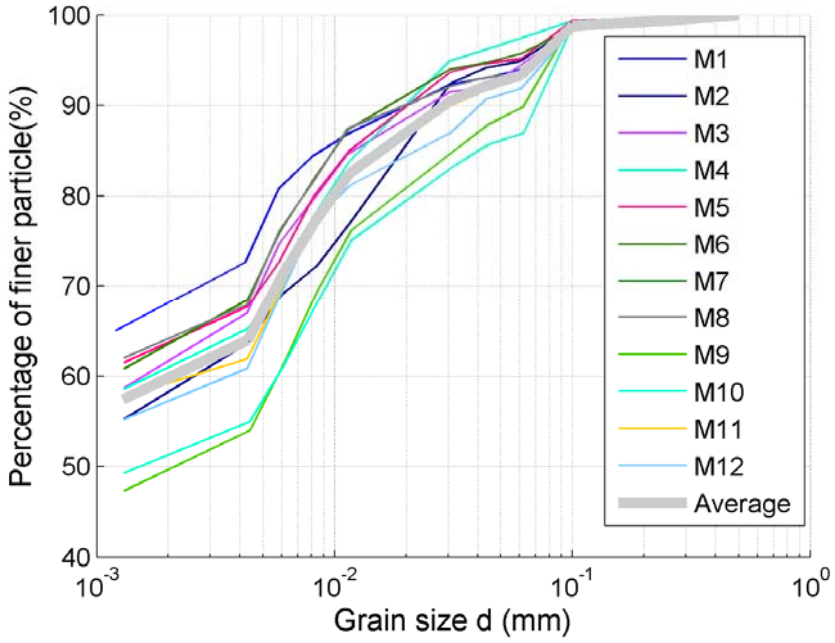

Figure 5.3.The median dispersed grain size distribution according to a Hydrometer analysis in the study area based on twelve traps in the 2010 flood, see figure 5.9 for locations.

It should be noted that this grain size is derived based on the assumption of dispersed grains of a sphere shape based on Stokes's law. However, in reality, fresh water flocculation occurs depending on biological and hydrological conditions (Lick and Lick, 1988; Droppo, 2001). Therefore, the grain size could be larger than the dispersed size.

In present study, there is no information about flocculation, therefore we used the context of effective grain size, so-called flocculated grain size. Moreover, the dispersed median size (D_{50}) given here is the lower boundary of the actual grain size. The sediment samples contain clay fraction of about 50 to 70 percent of finer particles. This is higher than the relatively small fraction of clay (15-20%) found by Wolanski et al (1996) for rivers and channels in the Mekong Estuary. This difference is explainable by the differentiation of sediments on the floodplains, usually resulting in floodplain sediments with higher proportion of fine sediment compared to the source rivers.

Regarding information on the particle size distribution of bed material, the reader should refer to Luu et al., 2004 for the Delta. They collected samples from the riverbanks and river bed for the grain size analysis at the Tan Chau bend, a river bend located upstream of the study area at a distance of about 15km. The river bank material varied from 10 to 80µm with presence of cohesive and non-cohesive material.

Because, the flocculated grain size will larger than the dispersed grain size, therefore, we used the range of median grain size from 10µm up to 80µm (river bed) for calculating the deposition and erosion rate. Finally, the flocculated grain size was found through trial-and-error and is discussed in the next chapters.

5.3.3 Sediment settling velocity

In fine sediment, the settling velocity of particles is very small and very sensitive to external or internal changes in fluid properties. Regardless of its size, it is an important factor that directly influences the prediction of erosion and deposition. There are many experimental equations to estimate the settling velocity of sediment particles (e.g van Rijn, 1993; Dietrich, 1982; Cheng 1997; Zhiyao et al., 2008). In particular, in the case of floodplain application, Thonon et al (2005) recommended calculating the settling velocity as a power relationship using flocculated grain size. However, the results from a test of this equation (not shown) for our study area were less applicable than the settling velocity based on Stokes's law (Vanoni, 1975). We assume that the reason lies in the dike ring of the floodplain compartment where the flow velocity is relatively small, about 10 to 26 (cm/s). Because of this, a settling velocity computed by Stokes's law is still valid.

$$w_s(t) = \frac{(s-1)gd^2}{18v(t)} \qquad 5.1$$

where

$w_s(t)$, settling velocity of sediment particle, varying in time (m/s);

s, specific gravity of sediment particles (s=2.65, for quartz-rich sediment);

g, acceleration of gravity, g=9.81 (m/s^2)

$\upsilon(t)$, kinematic viscosity coefficient, varying in time with water temperature (m^2/s)

According to Van Rijn (1993), kinematic viscosity could be computed based on water temperature, which is measured from the sensors:

$$\vartheta(t) = 10^{-6} * [1.14 - 0.031 * (T(t) - 15) + 0.00068 * (T(t) - 15)^2] \qquad 5.2$$

where

T, water temperature (^oC) measured from sensors

t, indicating time varying

Another alternative approach to estimate the particle settling velocity in floodplains use the term of apparent settling velocity (Thonon et al., 2007) which is calculated as:

$$w_s = D/(SSC.\Delta T) \quad 5.3$$

where w_s, apparent settling velocity (m/s);

D, deposition volume, derived from the retrieved traps (g/ m^2);

SSC, average sediment concentration during the inundation period, derived from the optical sensors (mg/l)

ΔT, duration of inundation period, determine from the Seba probe (s)

Table 5.2 shows the settling velocity calculated according to equation 5.1 and 5.2 with the dispersed grain size D_{50}=15 μm and the estuary flocculation grain size according to Wolanski et al (1996), D_{50}= 40 μm. These results are compared with the apparent settling velocity based on equation 5.3. The apparent settling velocity is around ten times smaller than the result from the Stokes's law with D_{50}=15 μm. Because of the water temperature was varying in time, the calculated settling velocity in equation 5.1 differs from 2008 to 2010, as well as from one location to another (T3 to T6).

According to Thonnon et al (2007), the apparent settling velocity should give a rough estimation of the trapping efficiency in each floodplain compartment. However, if we use the very small values of the apparent settling velocity for computing the deposition volume by the method of Krone (1962), we strongly underestimate the measurements. Using the flocculated grain size in the range between 10 to 80 μm, results in a good agreement between the calculated and the measured deposition volume. Further discussion regarding this issue will be found in the next chapter.

Table 5.2.Summary of settling velocity

Station name	Flood year	Apparent falling velocity (m/s)	Settling velocity of dispersed grain size D_{50}=15μm (m/s)		Settling velocity of estuary floc grain size D_{50}=40μm (m/s)	
			Max	Min	Max	Min
T3	2008	1.05E-05	2.59E-04	2.25E-04	1.84E-03	1.60E-03
T4		8.59E-05	2.54E-04	2.18E-04	1.80E-03	1.55E-03
T5		4.24E-05	2.56E-04	2.16E-04	1.82E-03	1.54E-03
T6		5.40E-07	2.54E-04	2.16E-04	1.81E-03	1.53E-03
T4	2009	3.74E-05	2.56E-04	2.16E-04	1.82E-03	1.54E-03
T5		4.08E-06	2.56E-04	2.32E-04	1.82E-03	1.65E-03
T6	2010	5.16E-06	2.60E-04	2.19E-04	1.85E-03	1.56E-03
Mean		2.66E-05	2.56E-04	2.20E-04	1.82E-03	1.57E-03
Standard deviation (SD)		3.10E-05	2.28E-06	6.00E-06	1.62E-05	4.3E-05

5.4 Computation of sediment deposition and erosion rate - Parameters estimation

The present study used the concepts of Krone (1962) for calculating the deposition rate, and Partheniades (1965) for calculating the erosion rate. The idea is that, by applying these twin methods, one can compute the deposition volume, determined from the retrieved sediment trap. If this idea is implemented successfully, not only can the volume in the sediment trap be computed, but the dynamics of deposition and erosion during flood season is also predicted. In other words, neither the sediment trap, the erosion pin nor the load cell sensor can presently produce insight into the deposition and erosion dynamics related to the hydraulic conditions as this approach does. In addition, the results will contribute to the development of a mathematical model for the Delta.

Since 1962, Krone studied the deposition process of cohesive sediments in the laboratory. He found that the deposition occurs when the bed shear stress is lower than a certain threshold. His work is considered as the first estimation of cohesive sediment deposition according to the exclusive paradigm. He introduced an equation for calculating the deposition rate, and this equation is widely used in engineering, especially coastal and port engineering.

$$D = \begin{cases} w_s . C_b . \left(1 - \frac{\tau_b}{T_d}\right) \; if \; \tau_b \leq T_d \\ \\ 0 \quad if \; \tau_b > T_d \end{cases} \tag{5.4}$$

where

D, deposition rate (kg/m^2/s);

w_s , particle settling velocity (m/s);

C_b , near bed suspended sediment concentration (mg/l);

τ_b , bed shear stress (N/m^2);

T_d, critical bed shear stress for deposition (N/m^2), has to be estimated

In equation (5.4), the question of how to determine the threshold for the deposition process - Td arises. Many investigators have tried to estimate this value, but the answers varied depending on the circumstance of the field conditions, laboratory capacity, and sediment properties (Van Rijn, 1993; Tolhust et al., 2009). In fact, when Krone did his study with cohesive sediment from San Fransico Bay, he observed the suspended concentration in a straight flume. He found T_d=0.06N/m^2 to be the threshold, where the cohesive sediment San Fransico Bay started to deposit. Later on, many studies applied his approach, and they found different value of critical bed shear stress for deposition (Partheniades, 1965; Mehta et al., 1982; Krone, 1993, Ha and Maa, 2009). Overall, they concluded that a deposition threshold existed with its values ranged widely depending on local hydraulic conditions and sediment type.

Furthermore, for the case of cohesive sediment erosion published by Partheniades (1965) via equation:

$$E = \begin{cases} M_{se} . \left(\frac{\tau_b}{Te} - 1\right) \; if \; \tau_b \geq T_e \\ \\ 0 \quad if \; \tau_b < T_e \end{cases} \tag{5.5}$$

τ_b , bed shear stress (N/m^2);

T_e, critical bed shear stress for erosion (N/m^2), has to be estimated

M_{se} , surface erosion rate constant (kg/m^2/s), has to be estimated

Equation (5.5) also includes two experimental parameters for erosion - T_e and M_{se}. Depending on these values, the deposition threshold varies from 0.06N/m^2 to 1.1 N/m^2

(Krone, 1962; Mehta, 1975), and even more in other case studies. The critical bed shear stress for erosion varies even more between 0.05N/m^2 to 3N/m^2 and the surface erosion rate constant M_{se} varies from 0.00000013 to 0.2827 (Bureau of Reclamation, 2006). These variations reflect local conditions, hence they were estimated based on the own measurements for the Mekong Delta.

According to the exclusive paradigm, erosion and deposition do not occur at the same time and there is a threshold for deposition and erosion. Therefore, the amount of sediment trapped results from accumulative deposition minus accumulative erosion.

$$S_{cal} = \sum_{T1}^{T2} D(t) - \sum_{T1}^{T2} E(t) \tag{5.6}$$

$$S_{cal} = 0, if\ Scal < 0 \tag{5.7}$$

where

S_{cal}, the accumulative deposition in the trap (kg/m^2);

D(t), deposition rate at time t, calculated based on equation 5.4;

E(t), erosion rate at time t, calculated based on equation 5.5;

T_1, the time of setting up the trap;

T_2, the time of collecting the trap.

In summary, to estimate the critical bed shear stress for deposition (T_d) in equation (5.4), for erosion (T_e) and M_{se} in equation (5.5), one should compare the accumulative sedimentation calculated from equation (5.6) and the measured deposition volume from the trap.

The six datasets at different places in different flood year are used to estimate the parameter sets (T3 in 2008, T4 in 2008, T5 in 2008, T6 in 2008, T5 in 2009, T6 in 2009), and one data set for validate the finding parameter sets (T6 in 2010). One complete data set includes time series of suspended sediment concentration, water depth, water temperatures, and the volume of deposition derived from the sediment trap. Using these data sets the parameters of equations (5.4) and (5.5) were estimated by minimizing the difference between calculated and measured deposition using equation (5.6). However, a unique solution of the parameter estimation problem does not exist, because the degrees of freedom in the estimation problem exceed the number of equations. Therefore several sets of parameter values of equal validity using a Gauss-Newton algorithm were estimated with the given constraints: $0<T_e<T_{e0}=0.08$

N/m^2, $0 < T_d < T_{d0}=0.08$ N/m^2, and M_{se} =0.00000013 to 0.2827 (Bureau of Reclamation, 2006). The value $T_{e0,}$ and T_{d0} is the maximum bed shear stress corresponding with maximum water depth of three meters in the study area.

These sets of valid parameters were consequently used for the calculation of deposition and erosion. The scheme for estimating parameters is outlined in Figure 5.4.

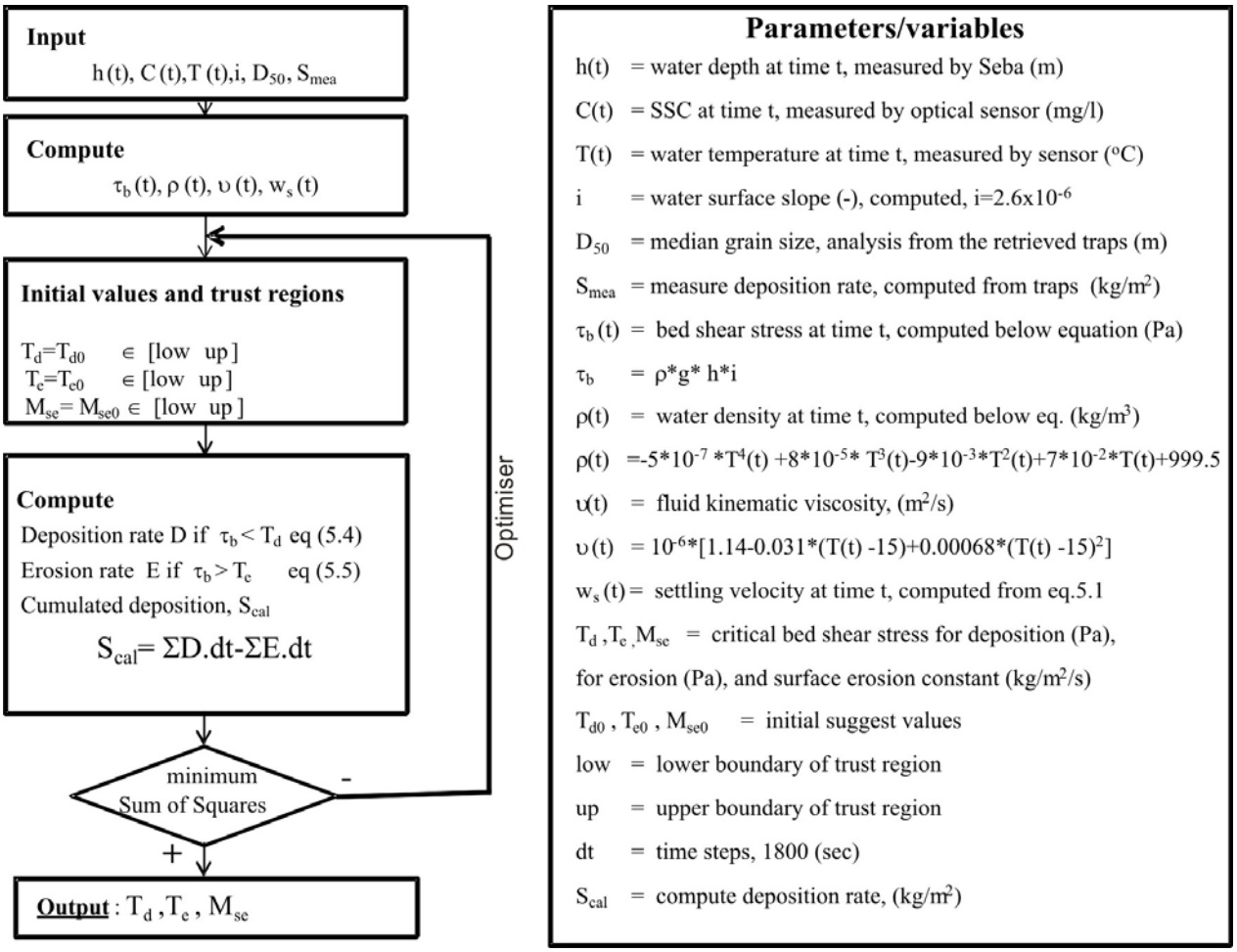

Figure 5.4.The scheme for estimating the parameters of sediment deposition and erosion

5.5 Predicted deposition and erosion dynamics

In order to maximise sediment trapping to fertilise the soils in paddy fields, the prediction of deposition and erosion in the floodplains of the Mekong Delta is crucially important information for optimising the operation of sluice gates. If one knew the period of time when sediment deposition will occur and how much will be deposited into the paddy field, the sluice gate system could be opened for sediment trapping. Conversely, they could be closed when erosion would occur. For that reason, this section is dealing with the deposition and

erosion dynamics during the flood season, especial with the magnitude and time of the deposition/erosion rate.

As mentioning above, six data sets were used for estimating the critical bed shear stress for deposition (T_d), for erosion(T_e), and the constant surface erosion rate (M_{se}): in the 2008 flood (T3, T4, T5, T6), and in the 2009 flood (T4, T5), see Figure 1.2 for their locations. One data set of the flood 2010 was used for validation (T6). In the flood season 2009, the measurement was conducted at all stations, however, the data at station T3 and T6 had some gaps because of hardware failures. In flood 2010 the monitoring scheme was reduced, only two stations were working (T5, T6) because of limited resources in the project. Unfortunately, T5 failed because of lightning struck leaving only T6 for validation.

Because no unique solution of the parameter estimation problem exist, set of equally valid parameters were estimated by running the optimization numerous times with different initial values of T_d, T_e, M_{se} covering the whole valid parameter space. With different initial values the optimizer converged at different optimal parameter sets yielding different sums of squared residuals. This procedure was repeated for different flocculation grains sizes in the possible range of 10µm to 80µm. The final parameter sets were selected for every flocculation grain size by selecting the parameter sets with the same minimum sum of squared residuals over all data sets (SS_{err}) used for the estimation. Since there are several data sets yielding identical residuals, several parameter sets are selected for each flocculation grain size.

Figure 5.5 depicts the relationship between the possible flocculated grain size and the sum of squared residuals. It shows that the deposition is estimated best with flocculated grain sizes in the range of 30 to 42µm. The corresponding parameter sets of T_d, T_e, M_{se} are in the range of T_d=[0.021-0.029] N/m^2, T_e= [0.028-0.044] N/m^2, M_{se}= [5.13x10^{-6} - 8.80x10^{-5}] kg/m^2/s.

The minimum SS_{err} occurs at the grain size D_{50}=35µm with SS_{err}=13. Eighty-three parameter sets of T_d, T_e, M_{se} yielded this result (Appendix II). Within this parameter sets T_d is always constant at 0.025 N/m^2 T_e= [0.032-0.042] N/m^2, M_{se}= [6.29x10^{-6} - 5.95x10^{-5}] kg/m^2/s. These parameters are smaller than a range published by Krone (1962), but all in a range published by Van Rijn (1993) and Tolhurst (2009). The identified best flocculated grain size (D_{50}=35µm) in this study is in agreement with Wolanski et al.(1996), who quantified the flocculation grain size at D_{50}=40µm.

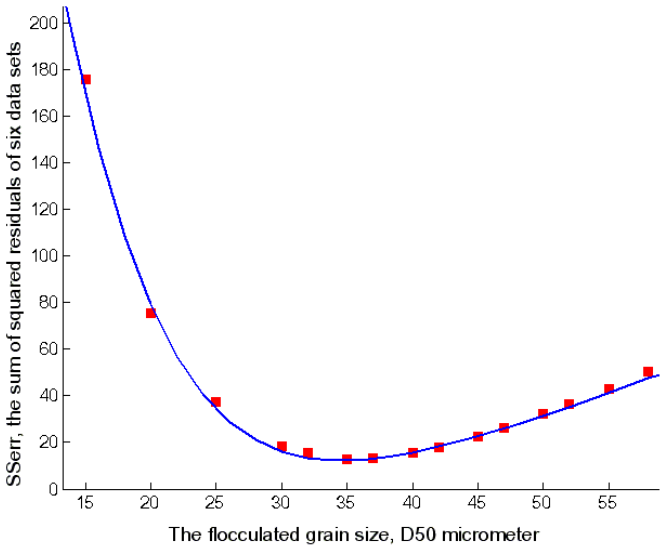

Figure 5.5. The sum of squared residuals and the flocculated size

Figure 5.6 shows the comparison between measured and calculated deposition volume assuming a flocculation grain size of 35µm and the best parameter sets. It shows a very good agreement of measurement and simulation with an R^2 of 0.95. In particular, stations T4 and T5 with two years of measurements, the results show very good agreement. Especially at station T4, the difference between calculated and measured deposition volume is in the order of 1kg/m^2 in two years.

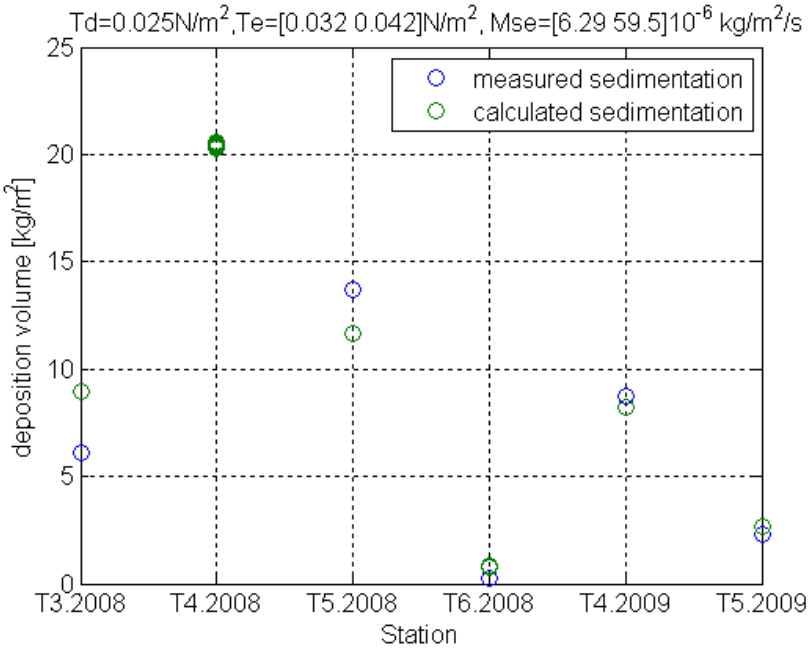

Figure 5.6. Comparison of measured and calculated deposition volume using the best equally performing parameter sets with flocculation grain size of 35µm; R^2=0.95

The data set at T6 in flood season 2010 was used to validate these parameters. The 2010 flood is a very low flood, therefore, the average hydraulic gradient in the study area is $1.1*10^{-5}$ which is higher than the gradients of the other floods used for parameter estimation in section 5.4 ($i=2.6x10^{-6}$). The hydraulic gradient is higher for lower flood levels because of the tide influence. Using the 83 parameter sets for a flocculation grain size of 35µm the deposition was always calculated at $S_{calculation}$=2.24kg/m^2, which is acceptable given the measured deposition of $S_{measure}$=1.88kg/m^2. This indicates that the identified equally valid parameter sets can be used to calculate the overall sedimentation budgets. However, the calculation of deposition and erosion over time differs with different parameter sets. Figure 5.7 shows the 83 different erosion rates calculated for four stations for a flocculation grain size of 35 µm The deposition rate does not differ between the different calculations, because T_d is constant in the 83 parameter sets.

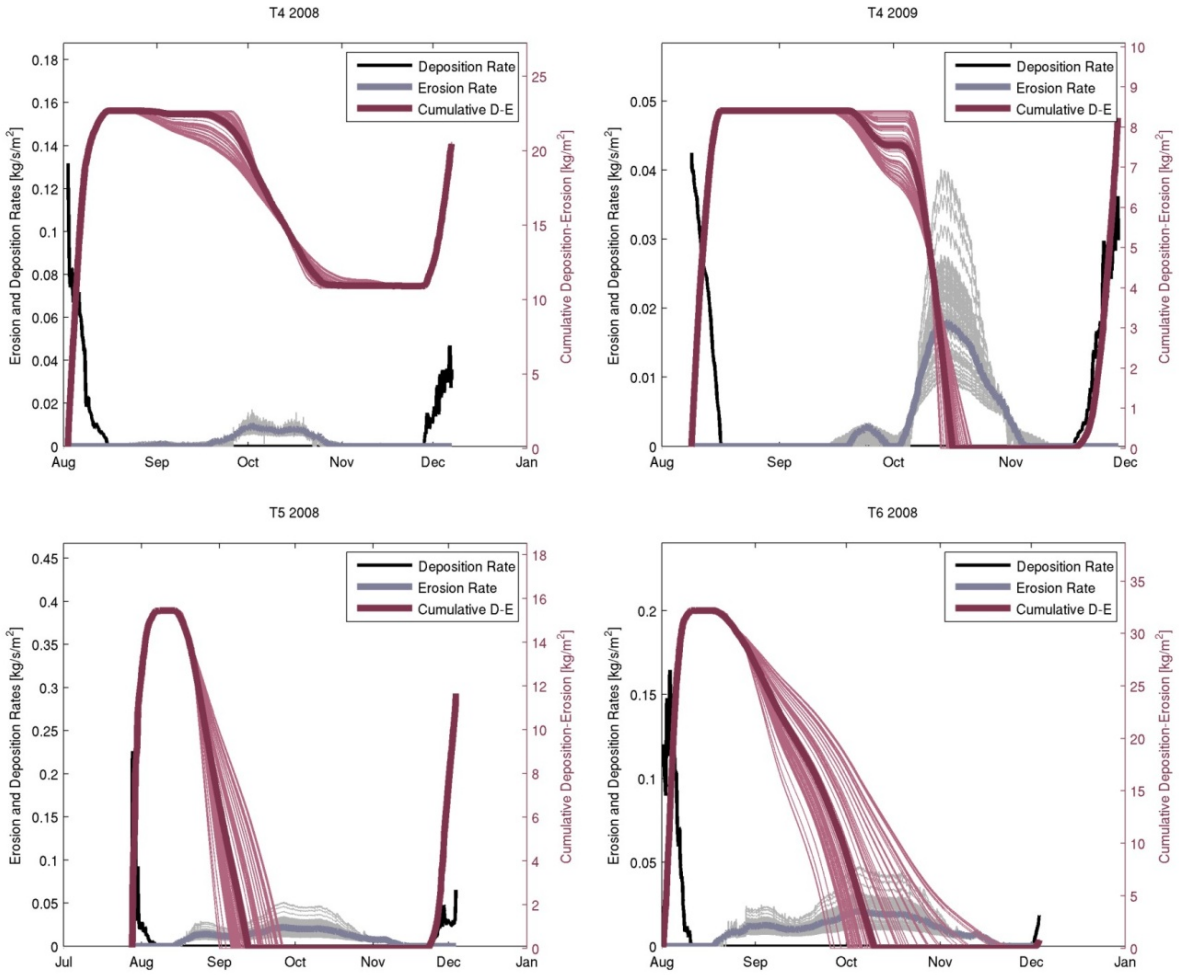

Figure 5.7.The dynamics of deposition and erosion derived from 83 parameter sets

Figure 5.7 shows that the sediment deposition in the floodplain occurs in two periods: at the beginning of flood season (August) and at the ending of flood season (November and December). The maximum deposition rate is about 0.2kg/m^2/s, and this deposition rate occurs only in a very short time. The maximum of erosion rate is about 0.05kg/m^2/s and the duration of erosion process is much longer, about two months (Sept, October). The deposition at the end of flood season depicts the anthropogenic influence by cultivating paddy rice, increasing the suspended sediment in the study area, as discussed in section 4.3. However, this period of deposition can be acknowledged as re-distributed deposition, because the primary sediment source from upstream conveyed by the flood is almost finished. Again in the context of maximizing sediment trapping, in general, the sluice gate system should open for capturing more sediment into the paddy fields in August and they should close during the erosion period in September and October. However, when operating and managing such a complex hydraulic network in the Mekong Delta, the trade-off between sediment trapping benefit and flood hazard has to be taken into account.

5.6 Quantification of sediment deposition in the study area

5.6.1 General information

This section estimates the amount of sediment deposited in the study area. Moreover, it discusses which approaches can be used to estimate the annual sediment budget for the whole Delta. As it appeared in the state of the art, there are many experimental approaches to estimate and interpolate sediment budget in the floodplain. In addition, the Delta has a complex topography and hydrodynamic conditions. For those reasons, we will discuss several approaches with examples from the study area.

Table 5.3 shows a very short summary of the three year measurements as an overview. Flood inundation lasts about 113.7 days on average with a standard deviation of 16.3 days. The mean suspended sediment concentration in three years for four stations is about 40mg/l, and the three year average of deposition is 6.86kg/m^2 (≈6.0mm/yr). The maximum water depth in the study area in three years is about 2m, with the average being 1.38m. The average hydraulic gradient for 2008 and 2009 is $2.6*10^{-6}$, and $1.1*10^{-5}$ for 2010. This information will be used in the next section to estimate the deposition in the study area.

Table 5.3. The summary of three year measurements

Station name	Flood year	Deposition rate (kg/m^2)	Max Depth (m)	Average depth (m)	Average SSC (mg/l)	Inundated duration (days)
T3	2008	6.13	1.84	1.42	65.87	102.7
T4		20.47	1.94	1.35	20.91	132.0
T5		13.73	2.47	1.72	28.00	133.9
T6		0.29	2.42	1.79	43.11	129.3
T4	2009	8.74	2.30	1.38	23.13	117.0
T5		2.30	2.62	1.76	67.80	96.3
T5	2010	1.34	1.39	0.85	-	97.7
T6		1.88	1.39	0.80	30.84	100.4
Average		6.86	2.04	1.38	39.95	113.7

The total area of study area is about $165*10^6$ m^2 with thirty-nine compartments, including fourteen compartments with high dike rings and a total area of about $51.5*10^6$ m^2, and twenty-five compartments with low dike rings and a total area of about $113.5*10^6$ m^2. Figure 5.8 shows the compartments with high dike rings and low dike rings, labelled from one to thirty nine. The black dots indicate the water level stations.

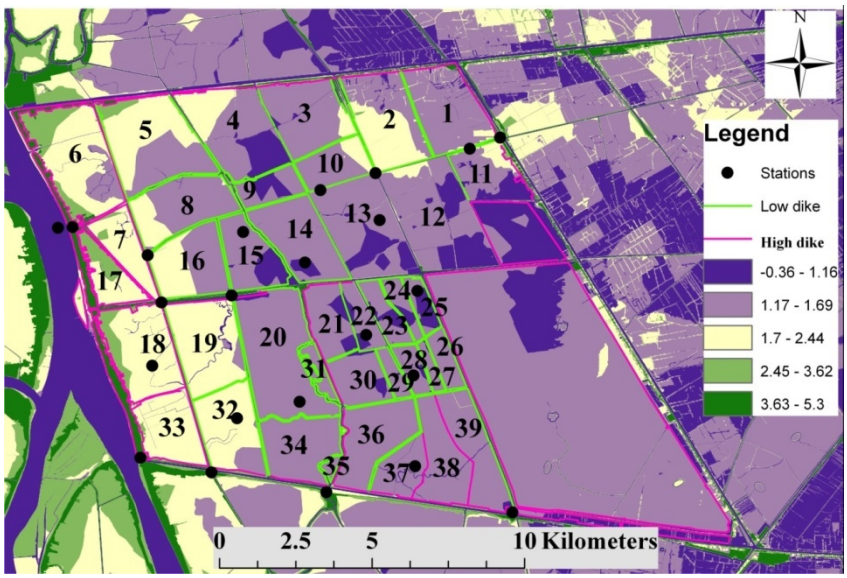

Figure 5.8. The compartments with high dike and low dike rings: blue is low dike ring, and pink is high dike ring, black dots indicate the water level stations, compartments are labeled

from one to thirty-nine for calculation of deposition/erosion. Details of each compartment are in the Appendix.

5.6.2 Sediment deposition in compartments with high and low dike rings

The hydraulic links between compartments with channels are different for low and high dike rings. The flood inundation starts in the low dike ring compartment by overflow, while the flood water is controlled by sluice gates in the compartment with high dike rings, as discussed in Chapter III. This difference makes the sediment deposition rate in each type of compartment different.

In the 2010 flood, we deployed six traps in the low dike ring compartment at station T6 and six traps in the high dike ring compartment at station T5 in different locations shown in Figure 5.9. The traps in each compartment were installed 50m away from the dike ring (M2, M3, M4, M5; M8, M9, M10, M11), in the middle of compartment (M6, M12), and at the quality stations (M1, M7). See Figure 5.9a for their locations.

The results show that, in the compartment with the low dike ring at station T6 in Figure 5.9 (or number 14 in Figure 5.8), deposition has a more homogeneous spatial distribution than that in the compartment with the high dike ring at station T5 (or number 22 in Figure 5.8). The size of compartment at station T6 is much larger than that of the compartment at station T5. Moreover, the average deposition rate in the T6 compartment (2.37kg/m^2, standard deviation =0.86) is higher than that in the T5 compartment (1.97kg/m^2, standard deviation =1.52). In the high dike ring, the rate of sedimentation is reduced by about 17%, see Figure 5.9b.

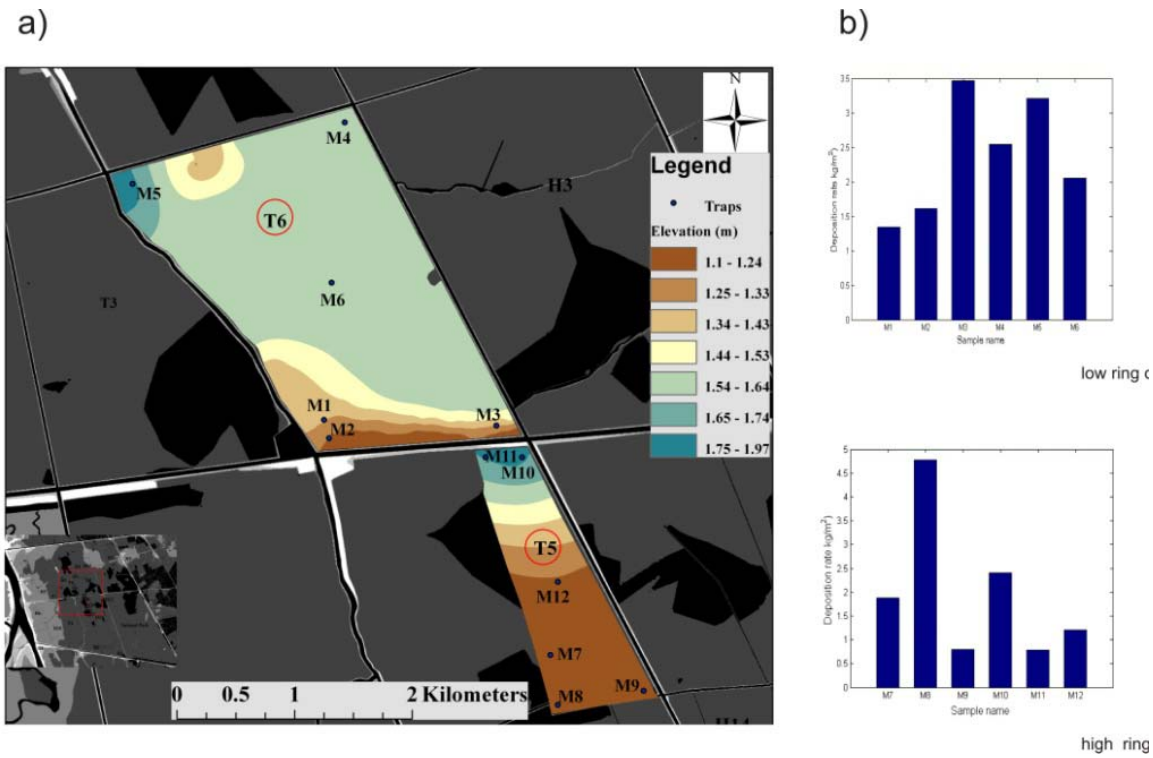

Figure 5.9 The deposition in a low dike ring compartment at station T6 and a high dike ring compartment at station T5: a) location of compartments and traps, floodplain elevation; b) sediment deposition.

In summary, the data shows how the dike elevation influences the deposition budget and its distribution in the floodplains. To estimate the deposition budget, one has to differentiate between compartments with low dike rings and high dike rings.

5.6.3 Estimation of the sediment deposition in the study area

The volume of sediment deposition can be estimated in the equation below:

$$V_d = D * A * \Delta T \qquad 5.9$$

where V_d, the volume of sediment deposition (kg);

D, deposition rate, (kg/m^2/s);

A, the inundation area, (m^2);

ΔT, duration of inundation, (s);

In equation (5.9), the inundation surface (A) is assumed to be equal to the area of the compartment, since the topography in each compartment is flat. The duration of inundation

was measured by water level probes (ΔT). The most challenging task is to define a proper deposition rate in time and space. Several ways to define the deposition rate are listed below:

- Method 1: Using the three year average value (D=6.86 kg/m^2/flooding year) defined from the retrieved sediment traps.
- Method 2: Classification of the deposition rate D_i= k*D, where D_i is the deposition rate in compartment i with high dike ring or low dike ring, k is the empirical factor used to calculate the difference between compartments with high dike or low dike (k<1 for high dike and k >1 for low dike), and D is the average deposition between high and low dike compartments. For example, in the 2010 flood, k =1.07 for the high dike ring and k =0.93 for low dike ring. Details given in Appendix.
- Method 3. Using empirical relationships between the deposition rate that was retrieved from the sediment traps with other indicators, such as: water depth, average concentration, duration of inundation, elevation of floodplain, etc;
- Method 4. Deposition rate calculated based on T_d, T_e, M_{se} as defined in section 5.4.

Method 1 and Method 2 are just a simple multiplication of the inundation area and the deposition rate. For Methods 3 and 4, however, some additional explanations are needed:

In Method 3, an attempt was made for a regression analysis with the data in Table 5.3. There were only a few traps, however, so the results are no more than a test (not shown). It shows that the deposition rate tends to correlate with the duration of inundation.

$$D=0.2879\Delta T-25.868 \qquad R^2=0.43 \qquad 5.10$$

where D, deposition rate (kg/m^2/flooding year)

ΔT, duration of inundation, ΔT>89 days (days)

In Method 4, the deposition rate in each compartment is calculated according to equation (5.4), (5.5), and (5.6). The parameters used for calculation are described below, and the details for deposition and erosion calculation are found in the Appendix.

- The water temperature used time series from measurement, selected at T4;
- The sediment grain size D_{50}=35μm, the flocculation grain size;
- The particle settling velocity, calculated from Sotes's Law, equation 5.1;
- The average hydraulic gradient i=2.6*10^{-6}, the average water surface from Seba probes;

- The bed shear stress, $\tau=\rho*g*h*i$ (N/m^2), where g is gravity acceleration, g=9.81 m/s^2; i is hydraulic gradient; h is water depth (m), We used the closest water level stations for each compartment in two years (2008, 2009),
- The author tested two options for the concentration of suspended sediment in the compartment: (1) using the average three year value C=40mg/l; (2) using the average time series of suspended sediment concentration measured in the floodplain (T3, T4, T5, and T6);
- The parameter for estimating the deposition rate is one of 83 parameter sets (because they act equally in estimating the deposition rate), we selected: T_d=0.0249 N/m^2, T_e=0.037 N/m^2, and M_{se}=$2*10^{-5}$ $kg/m^2/s$.

Table 5.4. The amount of sediment deposition in the study area

	Method 1	**Method 2**	**Method 3**	**Method 4 - Using SSC(t)**		
				C=40 mg/l	C=SSC in 2008	C=SSC in 2009
Deposition Budget (Mil.Tons)	1.051	1.082	1.080	4.053	**1.392**	**1.291**

Table 5.4 shows the total sediment deposited in the study area with different methods. The results from Methods 1, 2, and 3 are not much different because they all used the data from Table 5.3. The Method 4 shows a significant difference between using the average and the time series of the suspended sediment concentration. It shows that the average concentration does not work while using time series, the results are reliable in the 2008 and 2009 floods. This means that the temporal development of suspended sediment concentration is necessary. From this analysis, we learned that using Method 4 is reliable for estimating the deposition rate in the Mekong Delta, as it is possible to calculate the sediment deposition rate in each compartment.

In conclusion, the measurements and analyses gave insights into the sediment deposition processes in the floodplains of the Delta. Water temperature dominates the suspended sediment concentration in the paddy fields. Due to the low capacity of the hydraulic link between the channel and the paddy fields, in shallow water, heating and cooling varies the fine sediment concentration daily. The flocculation grain size in the floodplains was found

indirectly from 30 to 42µm, and the median grain size D_{50}=35µm. The combination of turbidity sensors and sediment traps makes it possible to predict the deposition and erosion process, as well as to estimate the total amount of sediment deposition in each floodplain compartment. The critical bed shear stress for deposition is about T_d= [0.021-0.029] N/m^2; the critical bed shears stress for erosion T_e= [0.028-0.044] N/m^2; and surface constant erosion rate M_{se}= [5.13 - 88] *10^{-6} kg/m^2/s.

5.7 Discussion and conclusion

5.7.1 Basic parameters and their importance in floodplain sedimentation

In the study area, the average water temperature does not vary much. However, its variation between floodplains and secondary channels is significant from location to location and from year to year. Moreover, the water temperature influences the fine particles that lead to the dynamics of suspended concentration during the flood period in floodplains. The results from the wavelet analysis proved that water temperature must be an important factor in controlling the suspended sediment dynamics in the floodplains. From this knowledge, we can improve the applicability of the sediment rating curve.

The suspended sediment in the floodplains have the dispersed sediment grain size D_{50} about 10 to 15µm, but the flocculated grain size is about 3 to 4 times larger (30 to 42µm). The apparent particles settling velocity is very small, showing no relation to the flocculation size. Despite this, the settling velocity could be computed from Stokes' Law for the paddy fields.

5.7.2 Sediment deposition in the study area

The potential deposition rates in the study area range from 0.3 to 20 kg/m^2/ flooding year, and the average three years' deposition rate is about 6.83 kg/m^2/year (≈ 6mm/yr). This amount of deposition decreases depending on location and in accordance with the reduction of suspended concentration along the secondary channel. The total amount of sediment deposition in the area is about [1.0-1.3] million tons/year. Clarifications of these values are discussed in the next part.

One should note that the topography (likely dike elevation) influences the deposition rates in the floodplains of the Delta. For example, in the 2010 flood season, the high dike ring reduced the deposition rate by 17% compared to the low dike ring. Moreover, the spatial distribution of deposition in the low dike ring was more homogeneous than in the high dike ring. We can

explain this with the discussion in section 4.6 regarding the sources and sinks of sediment in the floodplain. Because the sources and sinks of each compartment rely on the inundation processes of that compartment (time operating sluice gates or overbank flow), this leads to different deposition rates.

5.7.3 Approaches to quantify sediment deposition in the Delta

To maximize sediment trapping to fertilise paddy fields, knowledge about deposition and erosion progress is crucially important. Optimising sluice gates control intelligently requires information for trapping more sediment from the deposition process and reducing sediment erosion.

The present study demonstrates a successful combination of turbidity sensors and sediment traps for estimating the key parameters for the deposition and erosion processes. This combination is a unique field approach because it shows that it is possible to estimate deposition rates in each compartment while taking the hydraulic conditions of the compartment into account. Moreover, the method not only estimates the amount of sediment deposition, but also the dynamics of the twin key processes (erosion vs deposition) during flood season. By applying these parameters, we found that sediment deposition could not be estimated from the average suspended sediment concentration. This confirmed the importance of measuring the time series in a paddy field with turbidity sensors and sediment traps to quantify sediment deposition.

The results from field measurements and the ranges of parameters can be used to parameterize a mathematical model for quantifying the sediment dynamics in the Mekong Delta. We applied the exclusive paradigm according to Krone (1962) and Partheniades (1965) and found for the Mekong Delta: the critical bed shear stress for deposition T_d= [0.021 -0.029] N/m^2, and for erosion T_e=[0.028-0.044] N/m^2, and the constant surface erosion M_{se} = [5.13 - 88] *10^{-6} kg/m^2/s. Applying these parameters to quantify the deposition budget in the Delta is a reliable tactic, and the parameters we used for calculating the study area sediment budget were one of 83 parameter sets shows in the appendix.

In principle, we can also estimate the deposition budget by installing many more sediment traps, but the sediment traps must be linked with several practical aspects listed below:

- One must avoid anthropogenic influences in the testing space during the time between installing and retrieving the sediment traps.
- The traps must be set up in a compartment with a low dike and a high dike, in a cross-section from close to the river to further from the river and from upstream to downstream;
- The traps should be installed close to the sluice gates or pump stations where they show the hydraulic change between stagnant and high flow conditions.

6 CONCLUSIONS AND RECOMMENDATIONS

6.1 Conclusions

The annual floods provide the basis of livelihood for about 17 million people in the Mekong Delta, but they also pose a considerable hazard when extreme events exceed control levels. Therefore, a thorough understanding of the natural flood regime, benefits from the annual flood, and interaction with human control is vital not only for flood risk management, but for the economic development of the area, as well. While large-scale flood characteristics are quite well known, the influence of control measures on local floodplain inundation, as well as on the sediment dynamics, has not been studied in detail. The results of this study contribute to water resource management and the scientific understanding of the complex channel-dike-compartment system in the Delta. The conclusions are summarised in several categories below.

6.1.1 The in-situ monitoring system

In the literature, it appears that the practical difficulties in floodplain inundation studies are (1) the irregularity and unpredictability of inundation, (2) the potential of flood damage faced by the equipment and fieldwork. The *in-situ* monitoring developed in this study of the Mekong Delta was successful. In particular, the concept of this system is unique for creating a flood inundation database and for future data exploration in both spatial and temporal resolution. The *in-situ* monitoring system has been in the study area since 2008, when it started three years of monitoring flood plain inundation and suspended sediment (2008, 2009, and 2010). Until now, the system has proven to work very consistently with reliable data collection. The time series of water level, suspended sediment concentration, water temperature, electrical conductivity, and pH are unique for the Mekong Delta. The data set from the monitoring system can be regarded as the most reliable and comprehensive for the Mekong Delta, and can be used to fill the knowledge gaps about sediment dynamics in the floodplains.

6.1.2 The floodplain inundation processes

The flood season can be distinguished into three phases with their own specific hydraulic features: A rising stage, where the inundation starts in the floodplains and is controlled by dike elevation and sluice gates; a high stage, where floodplains and channels are hydraulically

linked, and the inundation dynamics are governed by the natural flood regime; and, finally, a falling stage, where human control of inundation levels is resumed by pumping water out of the floodplains, prematurely disconnecting the floodplains from the channels.

The human impact on floodplain inundation through sluice gate operation and pumping can be described quantitatively. The hydraulic linkage between channels and floodplains differs between different types of floodplains. Floodplains in high dike rings have a weaker hydraulic linkage; this link is governed by the capacity of the sluice gates. Other floodplains are more directly linked to the channels. Today's inundation patterns are, therefore, patchy compared to the more continuous patterns resulting from pristine floodplain processes. Hydraulic models of floodplain processes often neglect these human controls. When implementing a hydraulic model, it is necessary to check if these human controls must be considered.

Today, remote sensing data are extensively used for analysing hydrological and hydraulic systems. For the Mekong Delta, high resolution and high accuracy data are necessary, since the dike lines and channel networks are very thin line objects, though they are still key factors for flood inundation processes. This study used TerraSAR-X which has the advantages of high accuracy and high resolution (up to 3 m). This data set proved to be a very valuable information source for the study. However, a problem with the X-band radar is that the short wave length cannot penetrate high and dense altocumulus clouds with the high water contents typical for tropical convective thunderstorms in the Delta.

6.1.3 Suspended sediment dynamics

The suspended sediment dynamics in the floodplain of the Mekong Delta relies on two mechanisms: flood waves and the higher-frequency tidal waves. The results from the three-year monitoring of suspended sediment in our study area show that: (1) during low flow, the SSC is approximately 50mg/l with a tidal variation of about 20mg/l, (2) during high flow, the maximum SSC is about 200mg/l.

One important aspect not often taken into account by mathematical models is the anthropogenic influence on the suspended sediment. It proved possible to detect this influence qualitatively in the data. This influence increases the suspended concentration in two periods: opening sluice gates in August and pumping extra water out of the paddy field between November and December.

Further, the reduction of sediment along the channel was quantified. This exponential decrease happened within 10km of the Mekong River, while outside this distance, the concentration tended to stabilize. Moreover, in the paddy field, not all suspended sediment entering the floodplain compartment deposited. Because the flocculation is weak and the particles are very fine, the background of SSC in the floodplain was about 20mg/l.

The sediment rating curve approach showed a poor relationship between discharge and suspended sediment concentration. Instead, other influence factors (e.g. the water level, the water temperature, distance from the river, anthropogenic influence) have to be taken into consideration for constructing useful sediment rating curves. We learned that that using the sediment rating curve in the same year but for different location worked better than using it in the same location but for different years. This means that, eventually, the overall suspended sediment inflow from upstream, different from year to year during the flood season, dominates the total suspended sediment in the area.

The data and field experience show that the channels work as sediment carriers while the floodplains as sediment sinks. The sluice gates and pump station are the point source for the SSC to enter or exit floodplain compartments. They are the key factors in controlling the sediment flux to the paddy field.

6.1.4 Sediment deposition and erosion

The quantification of deposition and erosion of cohesive sediment is still a challenge, and the debate between the two paradigms is still open. Based on our measurements, the mutually-exclusive paradigm could be applied. By interpreting the data, we see that the critical bed shear stress for deposition is about T_d=[0.021-0.029]N/m^2; the critical bed shears stress for erosion T_e= [0.028-0.044]N/m^2; and surface constant erosion rate M_{se}= [5.13 - 88] *10^{-6} kg/m^2/s. The median dispersed sediment particle size in floodplain (D_{50}) is about 10 to 15µm with a clay fraction (<2µm) of about 50 to 70 percent finer particle. The flocculated grain size is indirectly estimated around 3 to 4 times larger than median of the dispersed grain size. In the study area, we recommend applying one of the 83parameter set in appendix to calculate the sediment deposition budget, and the flocculation grain size is about 35µm. In paddy fields, the deposition mainly occurs at the beginning and end of the flood season, while erosion occurs during the high flood stage. By applying the methods of Krone (1962) and Partheniades (1965) to quantify the sediment deposition and erosion, it is possible to predict the deposition in each floodplain compartment while incorporating hydraulic conditions.

The potential deposition rates in the study area range from 0.3 to 20kg/m^2/flooding year, and the average three years' deposition rate is about 6.83 kg/m^2/yr (≈6mm/yr). This amount of deposition is reduced depending on location, and according to the reduction of suspended concentration along the secondary channel. The total amount of sediment deposition in the area is about 1.0 to 1.3 million tons /year.

It is important to note that topography, likely the dike elevation, influences deposition rates and their spatial distribution. For example, in the 2010 flood season, the high dike ring's deposition rate dropped about 17% compared to the low dike ring. Moreover, the spatial distribution of deposition in the low dike ring is much more homogeneous than in the high dike ring.

Last, but not least, questions arose about the transferability of these findings to the water resource management system in the Delta. This work is part of the WISDOM project, which focuses on providing water-related information to local farmers, managers, and scientists in the Mekong Delta. Therefore, there is no doubt that the results could be translated and utilized properly by the readers.

6.2 Recommendations

There still remain many ambitious questions. Some examples are: how does the dynamics of cohesive sediments in a diked floodplain relate to pH and electrical conductivity, how sediment is re-distributed through a channel conjunction, how many nutrients, heavy metals, contaminants, etc., are contained in the suspended sediment samples, and so on. However, the time is limited for one working to identify and quantify the sediment dynamics as the first investigator. This work is but a small contribution to a burgeoning branch of studies on managing the existing complex channel-dike-compartment systems. There are many things remaining that should be taken on board for future study. They are listed below in no particular order.

- As the initial ideas of the interrelation between the *in-situ* monitoring system (single locations and high temporal resolution) and remote sensing (spatial distribution and single points in time), develop, they will enable scientists to expand the findings here in the study area to the larger spatial distribution for the entire inundated area of the Mekong Delta.

- Furthermore, data exploration of the database from the *in-situ* measurements is needed as the interaction of pH and electrical conductivity accompanied with sediment dynamics make it possible to gain more insight into the water quality of the floodplain.
- Simple sediment rating curves relating SSC to discharge do not work in the Mekong Delta due to the various factors influencing sediment transport. If sediment rating curves are to be established, they have to relate SSC to discharge, resp. water depth, water temperature, distance from main river and possibly anthropogenic influence. In any case, it has to be expected that sediment rating curves are valid for a given flood year only due to heterogeneous process in the basin of the Mekong, where the sediments origin.
- It is a wise to set up more sediment traps to investigate the budget, spatial sediment deposition, and the sediment properties (nutrient, contaminant, heavy metal,..). Moreover, they should be set in strategic locations: in compartments with low and high dike rings, from close to further away from the Mekong River. For safety reasons, installation and retrieval of sediment traps should be timed before and after the period of anthropogenic influence, as this activity could otherwise lead to the loss of traps.
- The channels, dike rings, sluice gates, pumping stations, and paddy compartments are all considered hydraulic structures that support agriculture development. They jointly form the hydrological conditions of the Mekong Delta floodplains. They, therefore, need proper treatment in terms of operation and maintenance. In other words, a proper concept in design and operation of sluice gates and pumps is an urgent requirement. To maximize sediment trapping to fertilise the soil in the paddy fields, two important points should be considered: (1) the suspended sediment concentration in the channel (magnitude and time of occurrence), and (2) the flood stage and topography of paddy field. Opening sluice gates located further from the Mekong River earlier than the ones close to the Mekong River is advisable. Moreover, the size of the sluice gates and the elevation of low dike rings should be optimised for sediment trapping. Practically, larger sluice gates may provide a better hydraulic link between the channels and compartments, sending more sediment into the compartment. However, during the high flood stage, the sluice must be closed to prevent erosion. In that sense, the trade-off between flood hazard and flood benefit should be considered.

References

Adamson PT, Rutherfurd ID, Peel MC, Conlan IA. 2009. The hydrology of the Mekong river. In *Biophysical Environment of an International River Basin*, Campbell IC (Eds) Elsevier, USA, 53-76. DOI:10.1016/B978-0-12-374026-7.00004-8

Agrawal, Y.C, Pottsmith, H.C.1994. Laser diffraction particle sizing in stress, *Continental Shelf Research*, **14** (10/11):1101-1121.

Agrawal YC, Pottsmith HC.2004. LISST Laser Diffraction Sensors *Advance Sediment Monitoring, Sea Technology* [Sea Technol.]. **45 (8)** 33-38 vp. Aug 2004.

Agrawal YC, Amanda W, Mikkelsen OA, Pottsmith HC.2008. Light scattering by random shaped particles and consequences on measuring suspended sediments by laser diffraction. *Journal of Geophysical Research*. **113. C04023**, DOI: 10.1029/2007JC004403

Apel H, Hung NN, Thoss H, Schöne T. 2011. GPS buoys for stage monitoring of large rivers. *Journal of Hydrology*, accepted.

Anderson, CA .2005. Turbidity, in National Field Manual for the Collection of Water-Quality Data, *U.S. Geol. Surv. Tech. of Water Resour. Invest*., Book 9, U. S. Geol. Surv., Reston, Va.
(Available at : http://water.usgs.gov/owq/FieldManual/Chapter6/6.7_contents.html)

Asselman NEM, Middelkoop H.1995. Floodplain sedimentation: quantities, Patterns and Processes. *Earth Surface Processes and Landforms*, **20**, 481-499

Asselman, N. E. M.1997. Suspended sediment in the Rhine River, The impact of climate change on ero- sion, transport and deposition, *University of Utrecht*, The Netherlands, Ph.D. thesis, 341 pp.

Asselman, N. 2000. Fitting and interpretation of sediment rating curves. *Journal of Hydrology*. **234** . 228-248

Asselman AEM, Vanwijngaarden M.2002. Development and application of a 1D floodplain sedimentation model for the River Rhine in The Netherlands. *Journal of Hydrology*. **268**. 127-142

Baborowski M, Büttner O, Morgenstern P, Krüger F, Lobe I, Rupp H, Tümpling Wv.2007. Spatial and temporal variability of sediment deposition on artificial-lawn traps in a floodplain of the River Elbe. *Environmental Pollution*. **148**. 770-778. DOI: 10.1016/j.envpol.2007.01.032

Black P.K, Resenberg M.A. 1994. Suspended sand measurements in a turbulent environment: field comparison of optical and pump sampling techniques, *Coastal Engineering* **24**:137-150.

Bloesch J, Burns NM. 1980. A critical review of sedimentation trap technique. *Schweizerische Zeitschrift für Hydrologie*. **42**. 15-55.

Bureau of Reclamation. 2006. Erosion and sedimentation manual. Eds. Chid Ted Yang, 2006, USA, 601

Campbell IC. 2007. Perceptions, data, and river management: Lessons from the Mekong River. *Water Resour. Res*. 2007. **43. W02407**, Doi:10.1029/2006WR005130

Carpenter MC. Field trials monitoring sand deposition and erosion on a razorback sucker spawning bar on the green river near jensen, utah, and operational description of load-cell scour sensors. USGS http://water.usgs.gov/osw/indirects/Carpenter.pdf

Chen, Zhimin , Hanson, Jim D. and Curran, Paul J. 1991.The form of the relationship between suspended sediment concentration and spectral reflectance: its implications for the use of Daedalus 1268 data. *International Journal of Remote Sensing*, **12(1)**, 215- 222

Cheng NS. 1997. A simplified settling velocity formula for sediment particle. *Journal of Hydraulic Engineering*, ASCE, **123(2),** 149-152.

Clifford NJ, Richards KS, Brown RA, LaneS.N .1995. Laboratory and field assessment of an infrared turbidity probe and its respone to particle size and variation in suspended sediment concentration, *Hydrological Sciences*, **40(6),** 771-791.

Curran PJ, Novo EMM. 1988. The relationship between suspended sediment concentration and remotely sensed spectral radiance: A review. *Journal of Coastal Research*. **4(3).** 351-368

David EB .2005. A guide to the proper selection and use of federally approved sediment and water-quality samplers, *Federal Interagency Sedimentation Project*, 2005,USGS.

Delgado JM, Apel H, and Merz B. 2010. Flood trends and variability in the Mekong river. *Hydrology and Earth System Sciences*: **14**, 407–418.

Dietrich W. 1982. Settling Velocity of Natural Particles. Water Resources. **18(6).** 1615-1626

Dieu NT.1999. The Mekong River and the struggle for Indochina: Water, War and Peace, Praeger, USA; 280

Doyle TW, Day RH, and Michot TC.2010. Development of sea level rise scenarios for climate change assessments of the Mekong Delta, Vietnam. U.S. *Geological Survey Open-File Report* 2010–1165, 110.

Doxaran, D, Froidefond J, Lavender S, Castaing P. 2002. Spectral signature of highly turbid waters Application with SPOT data to quantify suspended particulate matter concentrations. *Remote Sensing of Environment* : **81** 149– 161.

Dung N V, Merz B, Bárdossy A, Thang T D, and Apel H.2011. Multi-objective automatic calibration of hydrodynamic models utilizing inundation maps and gauge data, *Hydrology and Earth System Sciences*: **15** 1339-1354, Doi:10.5194/hess-15-1339-2011

Droppo IG.2001. Rethinking what constitutes suspended sediment, *Hydrol. Process*. **15**, 1551–1564

Edwards TK, and Glysson G.D. 1999. Field Methods for Measurement of Fluvial Sediment, Book 3 Application of Hydraulics, Chater 2, *U.S. Geological Survey Techniques of Water-Resources Investigations*, USGS, 1999.

Jansen, PP, Bendegom L, Van den Berg, De Vries, Zanen (Eds).1979. Principles of River Engineering The non-tidal alluvial river. *Pitman*. London, UK. 505

Gray JR, Glysson GD.2003. Proceedings of the Federal Interagency Workshop on Turbidity and Other Sediment Surrogates. *U.S. Geological Survey*: available http://water.usgs.gov/osw/techniques/sediment/sedsurrogate2003workshop.html

Gray JR, Gartner JW.2009. Technological advances in suspended-sediment surrogate monitoring. *Water Resources*. **45.W00D29**, doi: 10.1029/2008WR007063

Gooding DJ.2001. Photo-optical sedimentation tube: *Proceedings of the 7th Federal Interagency Sedimentation Conference*, March 25-29, 2001, Reno, Nevada, **1**, Poster 29-30.

Ha HK, Maa JPY.2009. Evaluation of two conflicting paradigms for cohesive sediment deposition. *Marine Geology*. **265** : 120-129

Huy SN. 2010. Methodology and adapted measures in Mekong delta for sustainable development in the climate change scenarios, Technical Report, *National Research Project, Water Resource University*, MARD, 2010, In Vietnamese;

Hung LM .2004. Research on the causes and solutions to prevent river bank erosion and deposition for the lower Mekong River system, Vietnam, *Ministry of Science and Technology*, code KC08-15 [in Vietnamese].

Hung NN, Delgado JM, Tri VK, Hung LM, Merz B, Bárdossy A, Apel H. 2011. Floodplain hydrology of the Mekong Delta, Vietnam. *Hydrol. Process*. DOI: 10.1002/hyp.8183.

Houwing EJ. 1999. Determination of the Critical Erosion Threshold of Cohesive Sediments on Intertidal Mudflats Along the Dutch Wadden Sea Coast. *Estuarine, Coastal and Shelf Science*. **49(4)**: 545-555.

Hwang KN, Mehta AJ.1989. Fine sediment erodibility in Lake Okeechobee. Report UFLICOEL-891019, *Coastal and Oceanographic Engineering Dept.*, Univ. of Florida, Gainesville, Florida.

Junk WJ, Bayley PB, Sparks RE. 1989. The flood pulse concept in river- floodplain systems, p 110-127. In D.P. Dodge [ed.] *Proceedings of the International large river symposium, Can.Spec*. Publ. Fish. Aquat. Sci. 106

Kim NQ, Trung NN, Khiet DV. 2007. Studies on fine sediment dynamics for developing of the Plains of Reeds, Tech Report. *Water Resource University*, Ministry of Agriculture and Rural Development [in Vietnamese]

Kummu M, Varis O. 2007. Sediment-related impacts due to upstream reservoir trapping, the Lower Mekong River. *Geomorphology*. **85**

Kummu M, Sarkkula J.2008. Impact of the Mekong River Flow Alteration on the Tonle Sap Flood Pulse. *In Royal Swedish Academy of Sciences*, Ambio **37**: 185-192.

Kummu M, Penny D, Sarkkula J, Koponen J. 2008. Sediment: Curse or Blessing for Tonle Sap Lake? *In Royal Swedish Academy of Sciences*, Ambio **37**: 158-163.

Krone, R.B. 1962. Flume studies of the transport of sediment in estuarial shoaling processes. Final Report, *Hydraulic Engineering Laboratory and Sanitary Engineering Research Laboratory, University of California*, Berkeley, USA.

Krone, R.B. 1993. Sedimentation revisited. In: Nearshore and Estuarine Cohesive Sediment Transport. Mehta, A.1. (ed.), *American Geophysical Union, Coastal and Estuarine Studies*, 108-125

Lambert CP, Walling DE.1987. Floodplain sedimentation: a preliminary investigation of contemporary deposition within the lower reaches of the river Culm. Devon, UK. *Geografiska Annaler*. **69A**. 393- 404.

Larsen MC, Alamo CF, Gray JR, William F. 2001. Continuous automated sensing of streamflow density as a surrogate for suspended-sediment concentration sampling: *Proceedings of the 7th Federal Interagency Sedimentation Conference*, Reno, Nevada, March 25-29. Vol. I, III-102 to III-109.

Lawer DM. 1992. Design and installation of a novel automatic erosion monitoring system. *Earth surface processes and landforms*. **17**, 455-463.

Lawler DM. 2004. The importance of high-resolution monitoring in erosion and deposition dynamics studies : examples from estuarine and fluvial systems. *Geomorphology*. **64**:1-23.

Lawler DM. 2008. Advances in the continuous monitoring of erosion and deposition dynamics: Developments and applications of the new PEEP-3T system. *Geomorphology* **93** 17–39

Lewis AJ, Rasmussen TC. 1996. A New, Passive Technique for the In Situ Measurement of Total Suspended Solids Concentrations in Surface Water, Technical Completion Report for Project 14-08-001-G-2013 (07), *U.S. Department of the Interior, Geological Survey*. August 1996

Lick W, Lick J.1988. Aggregation and disaggregation of fine-grained lake sediments. *Journal of Great Lakes Research*. **14(4)**. 514-523

Liew SC, Saengtuksin B, Keong L. 2009. Monitoring turbidity and suspended sediment concentration of coastal and inland waters using satellite data. *Geosciences and Remote Sensing Symposium*,2009 IEEE International, IGARSS 2009 , 12-17 July 2009

Lu X X, Siew R Y.2006. Water discharge and sediment flux changes over the past decades inthe Lower Mekong River: possible impacts of the Chinese dams. *Hydrology Earth System Sciences*, **10**: 181–195.

Luu XL, Egashira S, Takebayashi H. 2004. Investigation of Tan Chau reach in lower Mekong using field data and numerical simulation. *Annual Journal of Hydraulic Engineering*: **48** 1058-1062.

McHenry JR, Coleman, N L, Willis JC, Murphree CE, Bolton GC, Sansom OW, Gill A C.1967. Performance of Nuclear-Sediment Concentration Gauges, From Symposium: Isotopes in Hydrology. Vienna, Austria. *International Atomic Energy Agency*. SM83/17 pp. 207-225.

Mehta, AJ.1975. Depositional behavior of cohesive sediments. Ph.D. Dissertation, *University of Florida,* Gainesville.

Mehta, AJ., E. Partheniades, J.O. Dixit and W.H. McAnally. 1982. Properties of deposited kaolinite in a long flume. In: *Proceedings of the ASCE Hydraulics Division Conference on Applied Research to Hydrodynamic Practice*, 594-603.

Mehta AJ, Hayter EJ, Parker WR, Krone RB, Teeter AM.1989. Cohesive Sediment Transport I: Process Description. *Journal of Hydraulic Engineering*.**115(8)**. 1076-1093;

Mehta AJ, McAnally WH, Hayter EJ, Teer M, Schoellhamer D, Heltzel SB, Carey WP. 1989. Cohesive Sediment transport part II: Application. *Journal of Hydraulic Engineering* .**115 (8)**. 1094-1112.

Middelkoop H. 1997. Embanked floodplains in The Netherlands, Geomorphological evolution over various time scale, *University Utrecht*, The Netherlands. 341pp.

Middelkoop H, Van der Berg. 1998 . Modelling spatial patterns of overbank sedimentation on embanked floodplains. *Geografiska Annaler Series A Physical Geography* (1998) **80**(2): 95-109 DOI: 10.1111/j.0435-3676.1998.00029.x

Middelkoop H.2005. Floodplain Sedimentation- Methods, Patterns, and Processes: A Review with Examples from the Lower Rhine , the Netherlands. *Encyclopedia of Hydrological Sciences*. 1241-1282

Minella JPG, Merten GH, Reichert JM, Clarke R. 2008. Estimating suspended sediment concentrations from turbidity measurements and the calibration problem. *Hydrol. Process*. **22**, 1819–1830, DOI: 10.1002/hyp.6763.

MRC .2007. Diagnostic study of water quality in the Lower Mekong Basin, Tech.Pap. No. 15, *Mekong River Commission*, Vientiane.

MRC.2008. Regional Workshop on Discharge and Sediment Monitoring and Geomorphological Tools for the Lower-Mekong Basin. *Mekong River Commission* Secretariat Vientiane, Lao PDR, 21-22 October 2008: Available on-line at http://www.mrcmekong.org/free_download/sediment-monitoring-ppt.htm

MRCS/WUP-FIN. 2007. Final Report – Part 2: Research findings and recommendations. WUP-FIN Phase 2 – Hydrological, Environmental and Socio- Economic Modelling Tools for the Lower Mekong Basin Impact Assessment. *Mekong River Commission*

and Finnish Environment Institute Consultancy Consortium, Vientiane, Lao PDR. 126 pp. Available on-line at http://www.eia.fi/wup-fin/wupfin2/ publications.htm

Nanu L, Robertson C. 1990. Estimating suspended sediment concentrations from spectral reflectance data. *International Journal of Remote Sensing* **11(5)**, 1990 .913-920.

Narinesingh P, Klaassen GJ, Ludikuize D. 1999. Floodplain sedimentation along extended river reaches. *Journal of Hydraulic Engineering*. **37 (6)**. 827-845

Nguyen AD, Savenije HHG. 2006. Salt intrusion in multi-channel estuaries: a case study in the Mekong Delta, Vietnam. *Hydrology and Earth System Sciences*: **10**, 743–754.

Nicholas AP, Walling D E.1997. Modelling Flood Hydraulics and Overbank Deposition on River Floodplains. *Earth Surface Processes and Landforms:* **22**: 59-77

Oanh TTK, Nguyen VL, Tateishi M, Kobayashi I, Tanabe S, Saito Y. 2002. Holocene delta evolution and sediment discharge of the Mekong River, southern Vietnam. *Quaternary Science Reviews:* **21**, 1807–1819.

Papadopoulos, J. and Ziegler, C. A. (1966). "Radioisotope Technique for Monitoring Sediment Concentration in Rivers and Streams." *In Proceedings. on Radioisotope Instruments in Industry and Geophysics*. IAEA, Vienna, Austria. SM-68/26:pp. 381-394.

Partheniades, E. 1965. Erosion and deposition of cohesive solid. *Journal of the Hydraulics Division*, ASCE, **(91)** HYl, 105-139

Partheniades E. 2007. Engineering properties and hydraulic behavior of cohesive sediments, *Taylor & Francis Group*, USA; 338

Phillips,J.M., and Walling, D.E. (1995) Measurement in situ of the effective particle size characteristics of fluvial suspended sediment by means of a field portable laser backscatter probe: Some preliminary results. *Mar.Freshwater Res*.**46**: 349-357

Pizzuto JE.1987. Sediment diffusion during overbank flows. Sedimentology. **34**. 301-317

Poole GC. 2002. Fluvial landscape ecology: addressing uniqueness within the river discontinuum. *Freshwater Biology* **47**, 641–660

Proceedings of the Federal Interagency Workshop. 1998. Sediment technology for the 21st Century", Feb.17-19. 1998. St. Peterburg, Florida, USA. http://water.usgs.gov/osw/techniques/sedtech21/index.html

Proceedings of the Federal Interagency Workshop on Turbidity and other Sediment Surrogates, April 30-May 2, 2002, Reno, Nevada, USA. http://pubs.usgs.gov/circ/2003/circ1250/

Rouse H. 1937 Modern conceptions of the mechanics of fluid turbulence. *Transactions of the American Society of Civil Engineers*, **102**, 463–541.

Roux GL, Marshall WA, 2010, Constructing recent peat accumulation chronologies using atsmospheric fall-out radionuclides, *Mires and Peat*, **7** (2010/2011). 1-14. Available at: http://www.mires-and-peat.net/map07/map_07_08.pdf

Sam L. 2004 Research on salt intrusion for socio-economic development in the coastal zone of the Mekong Delta, Vietnam, *Ministry of Science and Technology*, code KC08-18, [in Vietnamese].

Sanford L, Halka J. 1993. Assessing the paradigm of mutually exclusive erosion and deposition of mud, with examples from upper Chesapeake Bay. *Marine Geology*. **114** 37-57

Sutherland .T.F., Lane P.M., Amos C.L., Downing J. (2000) The calibration of optical backscatter sensors for suspended sediment of varying darkness levels, *Marine Geology*. **162** 587–597

Sung C.C, Huang Y. J., Lai J. S., and Hwang G. W. (2007) Ultrasonic measurement of suspended sediment concentrations: an experimental validation of the approach using kaolin suspensions and reservoir sediments under variable thermal conditions *Hydrol. Process*. (2007).

Sumi T, Morita S, Ochi T and Komiya H. 2002. Development of the suspended-sediment concentration measuring system with differential pressure transmitter in rivers and reservoirs. *Tokyo University*. (Available at: http://ecohyd.dpri.kyoto-u.ac.jp/data/sumi/2002/200211.pdf)

Szalona JJ. 1986. Description and test of a straight- tube-fluid- density gage for measuring suspended sediment concentration in streams. *Federal Inter Agency sedimentation project. Progress report*. US. Army Engineer District, St. Paul. 33p

Steiger J, Gurnell AM, Goodson JM. 2003. Quantifying and characterizing contemporary riparian sedimentation. *River Research and Applications*: **19(4)**: 335-352 DOI: 10.1002/rra.708

Thoms MC, Foster J M, Gawne B. 2000. Flood-plain sedimentation in a dryland river: the River Murray, Australia. In Proceeding. The role of erosion and sediment transport in nutrient and contaminant transfer. *Waterloo, Canada, IAHS Publ*. no. **263**, pp 227-236.

Thonon I, Roberti JR, Middelkoop H, Van der Perk M, Burrough PA.2005. In situ measurements of sediment settling characteristics in floodplains using a LISST-ST. *Earth Surf. Process. Landforms* **30**, 1327–1343 DOI: 10.1002/esp.1239

Thonon I, Middelkoop H, Van Der Perk M. 2007. The influence of floodplain morphology and river works on spatial patterns of overbank deposition. *Netherlands Journal of Geosciences*. **86(1),** 63-75.

Thorn and Hanes, 2002 A review of acoustic measurement of small-scale sediment processes. *Continental Shelf Research*. **22,** 603–632.

Thuyen LX, Tran NN, Tuan BD, Bay NT. 2000. Transportation and deposition of fine sediment during flood season in Long Xuyen Quadrangle, Tech Report. *Ministry of Science and Technology*. [in Vietnamese]

Turton and Wigington, 1984 a Stage-Activated Triggering Device for Automatic Pumping Samplers. *Journal of the American Water Resources Association*. **20(3).** 443-448: DOI: 10.1111/j.1752-1688.1984.tb04727.x

Tolhurst TJ, Black KS, Paterson DM, 2009, Muddy sediment erosion: Insights from field studies, *Journal of Hydraulic Engineering*, Feb, 2009. 73-87.

Torrence C, and Compo G P. 1998. A practical guide to wavelet analysis. *Bulletin of the American Meteorological Society* **79**: 61-78.

van Rijn LC. 1993. Principles of sediment transport in rivers, estuaries and coastal seas. *Amsterdam Aqua Publication* 111, NUGI 186/831.

Vannote, R L, Minshall GW, Cummins KW, Sedell JR, Cushing CE. 1980. The River Continuum Concept. *Canadian Journal of Fisheries and Aquatic Sciences*.**37**. 130-137.

Vanoni, VA. 1975. Sedimentation Engineering. Report of Engineering Practice, No. **54**, *American Society of Civil Engineers*, New York, USA.

Västilä K, Kummu M, Sangmanee, C Chinvanno, S.: Modelling climate change impacts on the flood pulse in the Lower Mekong floodplains, *Journal of water and Climate Change*, 01.1,2010, doi: 10.2166/wcc.2010.008

Wang J, Lu X X, Kummu M. 2009. Sediment load estimates and variations in the lower Mekong River. *River Research and Applications*. DOI: 10.1002/rra.1337

Walling and Teer, 1971 A simple pumping sampler for research into suspended sediment transport in small catchments. *Journal of Hydrology*. **13** 325-337.

Walling DE, Bradley SB, Lambert CP. 1986. Conveyance losses of suspended sedimen1 within a flood plain system. In Drainage Basin Sediment Delivery. Hadley R.F. (Ed.), *IAHS Publication 159*. IAHS pp. 119-132.

Walling DE, He Q . 1993. Use of caesium-137 as a tracer in a study of rates and patterns of floodplain sedimentation. In: Tracers in Hydrology. *Proceedings of the Yokohama Symposium*.. IAHS Publ. no. **215**, 319-328pp

Walling DE, He Q. 1998. The spatial variability of overbank sedimentation on river floodplains. *Geomorphology*. **24**: 209-223.

Walling DE . 1999. Using fallout radionuclides in investigations of contemporary overbank sedimentation on the floodplains of British rivers. *Geological Society*, London, Special Publications. **163**: 41-59 DOI: 10.1144/GSL.SP.1999.163.01.04

Walling DE. 2005a. Evaluation and analysis of sediment data from the Lower Mekong River, Report prepared for the Mekong River Commission, *Mekong River Commission*: 61 pp.

Walling, D. E.2005b. "Tracing suspended sediment sources in catchments and river systems." *The Science of the total environment* **344,** 159-184.

Walling D E.2008. The Changing Sediment Load of the Mekong River, *In Royal Swedish Academy of Sciences*, Ambio Vol. **37**: 150-157.

Webb BW, Hannah DM, Moore RD, Brown LE, Nobilis F. 2008. Recent advances in stream and river temperature research. *Hydrological Processes* 02/2008: 902- 918 DOI: 10.1002/hyp

Winterwerp, J.C., 2007. On the sedimentation rate of cohesive sediment. In: Maa, J.P.-Y., Sanford, L.P., Schoellhamer, D.H. (Eds.), Estuarine and Coastal Fine Sediment Dynamics. *Elsevier, Amsterdam*, pp. 209–226.

Williams ND, Walling DE, Leeks GJL.2004. The settling behaviour of fine sediment particles: some preliminary results from LISST instruments. *Sediment Transfer through the Fluvial System* (in Proceedings of a symposium held in, Moscow. August 2004) IAHS Publ. 288. 2004. 283-290.

WMO.2003. Manual on sediment management and measurement, Edited by Xiaoqing.Y, *World Meteorological Oganization*, WMO-No **948**, 2003, Geneva, Switzerland.

Wolanski E, Huan NN, Dao LT, Nhan NH, Thuy NN.1996. Fine-sediment Dynamics in the Mekong River Estuary, Vietnam. Estuarine, *Coastal and Shelf Science*: **43**, 565-582

Wolanski E, Nhan NH, Spagnol S.1998. Sediment dynamics during low flow condition in the Mekong River Estuary, Vietnam. *Journal of Coastal Research*: **14(2),** 472-482.

Wolman MG, Leopold LB. 1957. River Flood Plains : Some Observations On Their Formation. *Geological survey professional paper*. 282-c.United States Government Printing office, Washington, 87-109.

Wolman M G. 1977. Changing needs and opportunities in the sediment field. *Water Resources Research*. **13(1).** 50-54.

Woo HS, Julien PY, Richardson EV. Washload and Fine Sediment Load. *Journal of Hydraulic Engineering*. **112**. No 6. June. 1986. 541-545

WTW, 2006 ViSolid® 700 IQ, Operating manual, WTW, available at: http://www.wtw.com/downloads/manuals/ba57302e04_ViSolid_700_IQ.pdf

Wren DG, Barkdoll BD, Kuhnle RA, Derrow RW.2000. Field techniques for suspended sediment measurement. *Journal of Hydraulic Engineering* **126 (2)**. 97-104

Wren and Kuhnle. 2002. Surrogate techniques for suspended-sediment measurement. *Proceedings of the Federal Interagency Workshop on Turbidity and other Sediment Surrogates*, April 30-May 2, 2002, Reno, Nevada, USA.

Xue Z, Liu J P, Ge Q.2010. Changes in hydrology and sediment delivery of the Mekong River in the last 50 years: connection to damming, monsoon, and ENSO, *Earth Surf. Process. Landforms*, DOI: 10.1002/esp.2036.

Yasuyuki K.2001. Canal development and intensification of rice cultivation in the Mekong delta: A Case study in Can Tho province, Vietnam, *Southeast Asian Studies*, **39**:70-85.

Ziegler AC. 2002. Issues related to use of turbidity measurements as a surrogate for suspended sediment. Turbidity and Other Sediment Surrogates Workshop, April 30 – May 2, 2002, Reno, NV available at: http://water.usgs.gov/osw/techniques/TSS/ZieglerT.pdf

Zhiyao S, Tingting W, Fumin X, Ruijie L. 2008. A simple formula for predicting settling velocity of sediment particles. *Water Science and Engineering*, **1(1)**: 37-43 DOI: 10.3882/j. issn. 1674-2370.2008.01.005

Appendix I: Calculation of sediment deposition and erosion

A.1 Method 1

We used the three year average of deposition rate (D=6.86 kg/m^2/year) that was defined from the retrieved sediment traps, and assuming this deposition rate is constant for everywhere in three year (2008, 2009, 2010), this is very roughly estimation method;

The total area of the study area is A= 165*10^6 m^2, and we used the average deposition rate D= D=6.86 kg/m^2/year, the volume of deposition V_d = A *D= 1.13 million tons/ year.

A.2 Method 2

This approach is practically simple and easy to handle, by classifying the total area of compartment with low dike and high dike, and their deposition rates. The volume of sediment deposition, therefore, should be computed. This is an example from our study area, we could setup more and more traps indifferent places and estimate the deposition more accuracy for the Delta. Classification the deposition rate D_i= k*D, where D_i is deposition rate in compartment i with high dike ring or low dike ring, k is empirical factor that used for calculate the different between compartment with high dike or low dike (k<1 for high dike and k >1 for low dike), and D is the average of deposition between high and low dike compartment. For example, in the 2010 flood, k≈1.07 for the high dike ring and k≈0.93 for low dike ring, a proper estimation in comparison with method 1;

In flood 2010, twelve traps were deployed in the compartments with low and high dike. The detailed data shows in table A.1 and table A.2. The average deposition rate in low dike compartment D_1=2.37 kg /m^2/year, and the average deposition rate in high dike compartment D_2=2.06.

$k_1 = \frac{2*D_1}{D_{2+}D_1}$ = 1.07 for low dike case

$k_2 = \frac{2*D_2}{D_{2+}D_1}$ = 0.93 for high dike case

We use the data in 2010 for define the empirical factor k, and the average deposition rate in three year is D=6.86 kg/m^2/year for estimate the deposition volume, and the total area of low dike compartment A_1=113.5*10^6 m^2 and high dike compartments A_2= 51.5*10^6 m^2;

The total volume of deposition $V_d = k_1*A_1*D+k_2*A_2*D$=1.16 (million tons/year).

Table A.1 The traps from low dike compartment T6

Sample number	Wet weight (kg)	*Dry weight (kg)	Trap dimension (cm) / Area (m^2)	Deposition rate (kg/m^2)
M1	1.70	0.31	60 x 38 / 0.228	1.36
M2	1.80	0.37	60 x 38 / 0.228	1.62
M3	2.6	0.79	60 x 38 / 0.228	3.46
M4	2.62	0.58	60 x 38 / 0.228	2.54
M5	3.52	0.73	60 x 38 / 0.228	3.20
M6	2.45	0.47	60 x 38 / 0.228	2.06
Average (D_1)	2.45	0.54		2.37

* *Dry weight was defined in laboratory by constant heating at 60 degree of Celsius until unchangeable weight.*

Table A.2 The traps from high dike compartment T5

Sample number	Wet weight (kg)	Dry weight (kg)	Trap dimension (cm) / Area (m^2)	Deposition rate (kg/m^2)
M7	1.20	0.43	60 x 38 / 0.228	1.89
M8	3.60	1.09	60 x 38 / 0.228	4.78
M9	1.20	0.18	60 x 38 / 0.228	1.32
M10	2.80	0.55	60 x 38 / 0.228	2.41
M11	1.41	0.18	60 x 38 / 0.228	0.79
M12	1.50	0.27	60 x 38 / 0.228	1.18
Average (D_2)	1.95	0.45		2.06

* *Dry weight was defined in laboratory by constant heating at 60 degree of Celsius until weight unchangeable.*

A.3 Method 3

In Method 3, an attempt was made for regression analysis with the data in Table 5.3. There were only a few traps, however, so the results are no more than a test (not shown). It shows that the deposition rate tends to correlate with the duration of inundation.

$$D=0.2879\Delta T-25.868 \qquad R^2=0.43$$

where D, deposition rate (kg/m2/flooding year)

ΔT, duration of inundation (days)

Data from table 5.3 shows that, ΔT=113.7 days, it is, therefore, the deposition rate could be computed D=7.048 kg/m^2, though, the volume of sediment deposition is V_d=D*A=1.16 million tons.

A.4 Method 4

In Method 4, the deposition rate in each compartment is calculated according to equation (5.4), (5.5), and (5.6). The parameters used for calculation are described below, and the details for deposition and erosion calculation are found in the Appendix.

- The water temperature used time series from measurement;
- The sediment grain size D_{50}=35μm, the flocculation grain size;
- The particle settling velocity, calculated from Sotes's Law, equation 5.1;
- The average hydraulic gradient i=2.6*10^{-6}, the average water surface from Seba probes;
- The bed shear stress, τ=ρ*g*h*i (N/m^2), where g is gravity acceleration, g=9.81 m/s^2; i is hydraulic gradient; h is water depth (m), We used the closest water level stations for each compartment in two years (2008, 2009),
- The author tested two options for the concentration of suspended sediment in the compartment: (1) using the average three year value C=40mg/l; (2) using the average time series of suspended sediment concentration measured in the floodplain;
- The parameter for estimating the deposition rate is: T_d=0.0249 N/m2, T_e=0.037 N/m^2, and M_{se}=2x10-5 kg/m^2/s, which was calibrated in the flood 2010.

The results of sediment deposition according to this methods shows in table A .3

Compartment number	Surface Area (m^2)	2008 Deposition (kg/m^2)	2008 Deposition (ton)	2009 Deposition (kg/m^2)	2009 Deposition (ton)	Deposition (kg/m^2)	Deposition (ton)
		C=40mg/l		C=SCC(t) average T3, T4, T5, T6			
1	5455782.5	43.94	239,706.59	1.47	7,996.10	18.59	101,444.61
2	6155106.1	46.83	288,242.02	19.46	119,785.44	14.91	91,755.87
3	5526091.6	43.94	242,796.17	0.48	2,662.53	18.59	102,752.12
4	7044776.1	13.05	91,954.78	1.03	7,249.63	3.52	24,815.55
5	8224485.5	13.20	108,525.67	19.10	157,110.67	3.70	30,429.71
6	7782536.8	26.35	205,046.82	26.21	204,016.24	8.22	63,964.60
7	2862407.0	54.81	156,886.84	28.12	80,493.86	18.70	53,525.26
8	5257875.9	13.93	73,245.07	19.91	104,700.66	3.94	20,725.66
9	2015714.0	9.78	19,707.34	0.07	134.16	2.60	5,243.40
10	2821403.7	11.47	32,367.01	6.16	17,373.43	3.20	9,036.98
11	3390645.1	17.65	59,856.68	22.45	76,120.03	5.31	18,008.77
12	8723116.4	17.65	153,993.81	22.45	195,835.11	5.31	46,331.35
13	7305506.2	66.79	487,929.19	0.17	1,241.94	16.48	120,362.82
14	5388557.5	9.78	52,683.13	0.07	358.66	2.60	14,017.06
15	3702024.0	5.44	20,155.73	8.51	31,503.34	1.45	5,369.43
16	4856706.9	16.96	82,380.64	0.22	1,068.48	5.02	24,398.50
17	2531029.2	54.81	138,724.22	28.12	71,175.17	18.70	47,328.69
18	6119614.6	19.11	116,916.20	0.50	3,059.81	8.50	52,032.60
19	6251636.9	24.72	154,509.83	0.33	2,063.04	7.76	48,515.55
20	9021684.1	26.04	234,903.60	2.93	26,418.69	8.29	74,815.21
21	3041875.4	13.73	41,760.14	1.33	4,058.54	3.73	11,342.88
22	1637597.7	10.65	17,442.05	3.14	5,137.60	2.83	4,638.88
23	1807643.9	7.65	13,825.69	0.75	1,356.12	2.02	3,655.13

Compartment number	Surface Area (m^2)	Deposition (kg/m^2)	Deposition (ton) C=40mg/l	Deposition (kg/m^2)	2008 Deposition (ton)	Deposition (kg/m^2)	2009 Deposition (ton) C=SCC(t) average T3, T4, T5, T6
24	1041765.7	16.46	17,152.52	3.35	3,487.33	4.64	4,838.06
25	1139376.5	16.46	18,759.67	3.35	3,814.08	4.64	5,291.37
26	1288716.3	21.39	27,565.28	6.39	8,228.72	5.91	7,622.22
27	600673.5	16.91	10,159.61	16.63	9,987.94	4.68	2,810.20
28	1211290.5	21.39	25,909.16	24.82	30,067.05	5.91	7,164.28
29	866766.3	21.39	18,539.89	24.84	21,528.29	5.91	5,126.56
30	2884491.4	10.65	30,722.71	3.28	9,449.77	2.83	8,170.99
31	788633.0	26.04	20,534.16	8.39	6,614.46	8.29	6,539.99
32	5043288.5	41.64	210,025.62	0.56	2,824.24	13.86	69,898.96
33	4237189.1	27.77	117,661.54	0.77	3,262.64	9.30	39,416.49
34	4885210.0	26.41	128,994.72	10.36	50,630.44	9.25	45,181.13
35	267694.3	26.04	6,970.13	5.29	1,417.21	8.29	2,219.94
36	5098331.9	29.85	152,171.10	5.29	26,991.22	9.29	47,358.94
37	2548421.1	21.39	54,510.01	8.50	21,661.51	5.91	15,072.84
38	4072245.0	21.39	87,104.18	8.50	34,613.98	5.91	24,085.62
39	4378149.4	21.39	93,647.39	8.50	37,214.16	5.91	25,894.92
Total	**157,276,059.62**		**4,053,986.91**		**1,392,712.28**		**1,291,203.15**

Appendix II: The eighty-three parameter sets

No	T_d	T_e	M_{se}	SS_{er}	No	T_d	T_e	M_{se}	SS_{er}
1	0.02494	0.0368	1.60E-05	13.00	43	0.02494	0.0345	9.99E-06	13.00
2	0.02494	0.0395	2.78E-05	13.00	44	0.02494	0.0390	2.50E-05	13.00
3	0.02494	0.0369	1.61E-05	13.00	45	0.02494	0.0389	2.43E-05	13.00
4	0.02494	0.0377	1.89E-05	13.00	46	0.02494	0.0414	4.33E-05	13.00
5	0.02494	0.0380	2.04E-05	13.00	47	0.02494	0.0357	1.27E-05	13.00
6	0.02494	0.0400	3.08E-05	13.00	48	0.02494	0.0396	2.81E-05	13.00
7	0.02494	0.0326	7.12E-06	13.00	49	0.02494	0.0424	5.82E-05	13.00
8	0.02494	0.0341	9.22E-06	13.00	50	0.02494	0.0358	1.29E-05	13.00
9	0.02494	0.0320	6.45E-06	13.00	51	0.02494	0.0379	1.98E-05	13.00
10	0.02494	0.0374	1.81E-05	13.00	52	0.02494	0.0390	2.48E-05	13.00
11	0.02494	0.0393	2.63E-05	13.00	53	0.02494	0.0393	2.64E-05	13.00
12	0.02494	0.0354	1.18E-05	13.00	54	0.02494	0.0387	2.35E-05	13.00
13	0.02494	0.0319	6.29E-06	13.00	55	0.02494	0.0381	2.08E-05	13.00
14	0.02494	0.0329	7.50E-06	13.00	56	0.02494	0.0393	2.65E-05	13.00
15	0.02494	0.0341	9.22E-06	13.00	57	0.02494	0.0396	2.82E-05	13.00
16	0.02494	0.0356	1.22E-05	13.00	58	0.02494	0.0397	2.90E-05	13.00
17	0.02494	0.0372	1.73E-05	13.00	59	0.02494	0.0389	2.42E-05	13.00
18	0.02494	0.0383	2.17E-05	13.00	60	0.02494	0.0386	2.30E-05	13.00
19	0.02494	0.0327	7.21E-06	13.00	61	0.02494	0.0388	2.36E-05	13.00
20	0.02494	0.0319	6.32E-06	13.00	62	0.02494	0.0388	2.39E-05	13.00
21	0.02494	0.0327	7.26E-06	13.00	63	0.02494	0.0387	2.35E-05	13.00
22	0.02494	0.0341	9.22E-06	13.00	64	0.02494	0.0390	2.49E-05	13.00
23	0.02494	0.0387	2.36E-05	13.00	65	0.02494	0.0370	1.63E-05	13.00
24	0.02494	0.0374	1.80E-05	13.00	66	0.02494	0.0346	1.01E-05	13.00
25	0.02494	0.0319	6.34E-06	13.00	67	0.02494	0.0350	1.10E-05	13.00
26	0.02494	0.0341	9.22E-06	13.00	68	0.02494	0.0351	1.11E-05	13.00
27	0.02494	0.0369	1.61E-05	13.00	69	0.02494	0.0402	3.22E-05	13.00
28	0.02494	0.0398	2.96E-05	13.00	70	0.02494	0.0354	1.18E-05	13.00
29	0.02494	0.0341	9.22E-06	13.00	71	0.02494	0.0402	3.24E-05	13.00
30	0.02494	0.0369	1.61E-05	13.00	72	0.02494	0.0352	1.14E-05	13.00
31	0.02494	0.0420	5.19E-05	13.00	73	0.02494	0.0372	1.72E-05	13.00
32	0.02494	0.0405	3.48E-05	13.00	74	0.02494	0.0358	1.27E-05	13.00
33	0.02494	0.0339	8.99E-06	13.00	75	0.02494	0.0355	1.21E-05	13.00
34	0.02494	0.0375	1.81E-05	13.00	76	0.02494	0.0378	1.96E-05	13.00
35	0.02494	0.0340	9.09E-06	13.00	77	0.02494	0.0395	2.77E-05	13.00
36	0.02494	0.0405	3.44E-05	13.00	78	0.02494	0.0394	2.69E-05	13.00
37	0.02494	0.0335	8.32E-06	13.00	79	0.02494	0.0322	6.59E-06	13.00
38	0.02494	0.0363	1.42E-05	13.00	80	0.02494	0.0331	7.72E-06	13.00
39	0.02494	0.0337	8.53E-06	13.00	81	0.02494	0.0377	1.91E-05	13.00
40	0.02494	0.0377	1.92E-05	13.00	82	0.02494	0.0425	5.95E-05	13.00
41	0.02494	0.0404	3.36E-05	13.00	83	0.02494	0.0319	6.29E-06	13.00
42	0.02494	0.0425	5.95E-05	13.00					

Curriculum vitae

Nguyen Nghia Hung was born on the 25th of October, 1976, in Nghe An Province, Vietnam. He earned his high school diploma at Ha Huy Tap Secondary School in 1994 (Nghe An). During his time at secondary school, he won the first prize at the Mathematical Olympics of Nghe An Province in 1992, and the third prize at the Biology Olympics of Nghe An Province in 1994. Hung started university in Hanoi University of Civil Engineering (HUCE). While there, he received the Vietnamese government's university student scholarship from 1994-1999.

After graduation, he was employed as a researcher at the Institute of Water Resource Research in Ha Noi (1999-2001) and worked for the Southern Institute of Water Resource Research in Ho Chi Minh City (2001-2004). From 2004 to 2006, he granted his Master of Science in Hydraulic Engineering and River basin development at the UNESCO-IHE Institute for Water Education in Delft, Netherlands, with the thesis "Bank erosion prediction and mitigation measures along the Mekong River" by Rijkswaterstraat and Public Work Ministry of the Netherlands. He came back and worked for the Southern Institute of Water Resource Research (2006). In September 2007, he has granted a scholarship from the WISDOM project for his PhD program, which led to this thesis. Currently, Hung works as a researcher for the Southern Institute of Water Resource Research in Ho Chi Minh, Vietnam.

Institut für Wasserbau
Universität Stuttgart

Pfaffenwaldring 61
70569 Stuttgart (Vaihingen)
Telefon (0711) 685 - 64717/64749/64752/64679
Telefax (0711) 685 - 67020 o. 64746 o. 64681
E-Mail: iws@iws.uni-stuttgart.de
http://www.iws.uni-stuttgart.de

Verzeichnis der Mitteilungshefte

1 Röhnisch, Arthur: *Die Bemühungen um eine Wasserbauliche Versuchsanstalt an der Technischen Hochschule Stuttgart*, und
Fattah Abouleid, Abdel: *Beitrag zur Berechnung einer in lockeren Sand gerammten, zweifach verankerten Spundwand*, 1963

2 Marotz, Günter: *Beitrag zur Frage der Standfestigkeit von dichten Asphaltbelägen im Großwasserbau*, 1964

3 Gurr, Siegfried: *Beitrag zur Berechnung zusammengesetzter ebener Flächentragwerke unter besonderer Berücksichtigung ebener Stauwände, mit Hilfe von Randwert- und Lastwertmatrizen*, 1965

4 Plica, Peter: *Ein Beitrag zur Anwendung von Schalenkonstruktionen im Stahlwasserbau*, und Petrikat, Kurt: *Möglichkeiten und Grenzen des wasserbaulichen Versuchswesens*, 1966

5 Plate, Erich: *Beitrag zur Bestimmung der Windgeschwindigkeitsverteilung in der durch eine Wand gestörten bodennahen Luftschicht*,
und
Röhnisch, Arthur; Marotz, Günter: *Neue Baustoffe und Bauausführungen für den Schutz der Böschungen und der Sohle von Kanälen, Flüssen und Häfen; Gestehungskosten und jeweilige Vorteile*, sowie Unny, T.E.: *Schwingungsuntersuchungen am Kegelstrahlschieber*, 1967

6 Seiler, Erich: *Die Ermittlung des Anlagenwertes der bundeseigenen Binnenschiffahrtsstraßen und Talsperren und des Anteils der Binnenschiffahrt an diesem Wert*, 1967

7 *Sonderheft anläßlich des 65. Geburtstages von Prof. Arthur Röhnisch mit Beiträgen von* Benk, Dieter; Breitling, J.; Gurr, Siegfried; Haberhauer, Robert; Honekamp, Hermann; Kuz, Klaus Dieter; Marotz, Günter; Mayer-Vorfelder, Hans-Jörg; Miller, Rudolf; Plate, Erich J.; Radomski, Helge; Schwarz, Helmut; Vollmer, Ernst; Wildenhahn, Eberhard; 1967

8 Jumikis, Alfred: *Beitrag zur experimentellen Untersuchung des Wassernachschubs in einem gefrierenden Boden und die Beurteilung der Ergebnisse*, 1968

9 Marotz, Günter: *Technische Grundlagen einer Wasserspeicherung im natürlichen Untergrund*, 1968

10 Radomski, Helge: *Untersuchungen über den Einfluß der Querschnittsform wellenförmiger Spundwände auf die statischen und rammtechnischen Eigenschaften*, 1968

11 Schwarz, Helmut: *Die Grenztragfähigkeit des Baugrundes bei Einwirkung vertikal gezogener Ankerplatten als zweidimensionales Bruchproblem*, 1969

12 Erbel, Klaus: *Ein Beitrag zur Untersuchung der Metamorphose von Mittelgebirgsschneedecken unter besonderer Berücksichtigung eines Verfahrens zur Bestimmung der thermischen Schneequalität*, 1969

13 Westhaus, Karl-Heinz: *Der Strukturwandel in der Binnenschiffahrt und sein Einfluß auf den Ausbau der Binnenschiffskanäle*, 1969

14 Mayer-Vorfelder, Hans-Jörg: *Ein Beitrag zur Berechnung des Erdwiderstandes unter Ansatz der logarithmischen Spirale als Gleitflächenfunktion*, 1970

15 Schulz, Manfred: *Berechnung des räumlichen Erddruckes auf die Wandung kreiszylindrischer Körper*, 1970

16 Mobasseri, Manoutschehr: *Die Rippenstützmauer. Konstruktion und Grenzen ihrer Standsicherheit*, 1970

17 Benk, Dieter: *Ein Beitrag zum Betrieb und zur Bemessung von Hochwasserrückhaltebecken*, 1970

18 Gàl, Attila: *Bestimmung der mitschwingenden Wassermasse bei überströmten Fischbauchklappen mit kreiszylindrischem Staublech*, 1971, vergriffen

19 Kuz, Klaus Dieter: *Ein Beitrag zur Frage des Einsetzens von Kavitationserscheinungen in einer Düsenströmung bei Berücksichtigung der im Wasser gelösten Gase*, 1971, vergriffen

20 Schaak, Hartmut: *Verteilleitungen von Wasserkraftanlagen*, 1971

21 *Sonderheft zur Eröffnung der neuen Versuchsanstalt des Instituts für Wasserbau der Universität Stuttgart mit Beiträgen von* Brombach, Hansjörg; Dirksen, Wolfram; Gàl, Attila; Gerlach, Reinhard; Giesecke, Jürgen; Holthoff, Franz-Josef; Kuz, Klaus Dieter; Marotz, Günter; Minor, Hans-Erwin; Petrikat, Kurt; Röhnisch, Arthur; Rueff, Helge; Schwarz, Helmut; Vollmer, Ernst; Wildenhahn, Eberhard; 1972

22 Wang, Chung-su: *Ein Beitrag zur Berechnung der Schwingungen an Kegelstrahlschiebern*, 1972

23 Mayer-Vorfelder, Hans-Jörg: *Erdwiderstandsbeiwerte nach dem Ohde-Variationsverfahren*, 1972

24 Minor, Hans-Erwin: *Beitrag zur Bestimmung der Schwingungsanfachungsfunktionen überströmter Stauklappen*, 1972, vergriffen

25 Brombach, Hansjörg: *Untersuchung strömungsmechanischer Elemente (Fluidik) und die Möglichkeit der Anwendung von Wirbelkammerelementen im Wasserbau*, 1972, vergriffen

26 Wildenhahn, Eberhard: *Beitrag zur Berechnung von Horizontalfilterbrunnen*, 1972

27 Steinlein, Helmut: *Die Eliminierung der Schwebstoffe aus Flußwasser zum Zweck der unterirdischen Wasserspeicherung, gezeigt am Beispiel der Iller*, 1972

28 Holthoff, Franz Josef: *Die Überwindung großer Hubhöhen in der Binnenschiffahrt durch Schwimmerhebewerke*, 1973

29 Röder, Karl: *Einwirkungen aus Baugrundbewegungen auf trog- und kastenförmige Konstruktionen des Wasser- und Tunnelbaues*, 1973

30 Kretschmer, Heinz: *Die Bemessung von Bogenstaumauern in Abhängigkeit von der Talform*, 1973

31 Honekamp, Hermann: *Beitrag zur Berechnung der Montage von Unterwasserpipelines*, 1973

32 Giesecke, Jürgen: *Die Wirbelkammertriode als neuartiges Steuerorgan im Wasserbau*, und Brombach, Hansjörg: *Entwicklung, Bauformen, Wirkungsweise und Steuereigenschaften von Wirbelkammerverstärkern*, 1974

33 Rueff, Helge: *Untersuchung der schwingungserregenden Kräfte an zwei hintereinander angeordneten Tiefschützen unter besonderer Berücksichtigung von Kavitation*, 1974

34 Röhnisch, Arthur: *Einpreßversuche mit Zementmörtel für Spannbeton - Vergleich der Ergebnisse von Modellversuchen mit Ausführungen in Hüllwellrohren*, 1975

35 *Sonderheft anläßlich des 65. Geburtstages von Prof. Dr.-Ing. Kurt Petrikat mit Beiträgen von*: Brombach, Hansjörg; Erbel, Klaus; Flinspach, Dieter; Fischer jr., Richard; Gàl, Attila; Gerlach, Reinhard; Giesecke, Jürgen; Haberhauer, Robert; Hafner Edzard; Hausenblas, Bernhard; Horlacher, Hans-Burkhard; Hutarew, Andreas; Knoll, Manfred; Krummet, Ralph; Marotz, Günter; Merkle, Theodor; Miller, Christoph; Minor, Hans-Erwin; Neumayer, Hans; Rao, Syamala; Rath, Paul; Rueff, Helge; Ruppert, Jürgen; Schwarz, Wolfgang; Topal-Gökceli, Mehmet; Vollmer, Ernst; Wang, Chung-su; Weber, Hans-Georg; 1975

36 Berger, Jochum: *Beitrag zur Berechnung des Spannungszustandes in rotationssymmetrisch belasteten Kugelschalen veränderlicher Wandstärke unter Gas- und Flüssigkeitsdruck durch Integration schwach singulärer Differentialgleichungen*, 1975

37 Dirksen, Wolfram: *Berechnung instationärer Abflußvorgänge in gestauten Gerinnen mittels Differenzenverfahren und die Anwendung auf Hochwasserrückhaltebecken*, 1976

38 Horlacher, Hans-Burkhard: *Berechnung instationärer Temperatur- und Wärmespannungsfelder in langen mehrschichtigen Hohlzylindern*, 1976

39 Hafner, Edzard: *Untersuchung der hydrodynamischen Kräfte auf Baukörper im Tiefwasserbereich des Meeres*, 1977, ISBN 3-921694-39-6

40 Ruppert, Jürgen: *Über den Axialwirbelkammerverstärker für den Einsatz im Wasserbau*, 1977, ISBN 3-921694-40-X

41 Hutarew, Andreas: *Beitrag zur Beeinflußbarkeit des Sauerstoffgehalts in Fließgewässern an Abstürzen und Wehren*, 1977, ISBN 3-921694-41-8, vergriffen

42 Miller, Christoph: *Ein Beitrag zur Bestimmung der schwingungserregenden Kräfte an unterströmten Wehren*, 1977, ISBN 3-921694-42-6

43 Schwarz, Wolfgang: *Druckstoßberechnung unter Berücksichtigung der Radial- und Längsverschiebungen der Rohrwandung*, 1978, ISBN 3-921694-43-4

44 Kinzelbach, Wolfgang: *Numerische Untersuchungen über den optimalen Einsatz variabler Kühlsysteme einer Kraftwerkskette am Beispiel Oberrhein*, 1978, ISBN 3-921694-44-2

45 Barczewski, Baldur: *Neue Meßmethoden für Wasser-Luftgemische und deren Anwendung auf zweiphasige Auftriebsstrahlen*, 1979, ISBN 3-921694-45-0

46 Neumayer, Hans: *Untersuchung der Strömungsvorgänge in radialen Wirbelkammerverstärkern*, 1979, ISBN 3-921694-46-9

47 Elalfy, Youssef-Elhassan: *Untersuchung der Strömungsvorgänge in Wirbelkammerdioden und -drosseln*, 1979, ISBN 3-921694-47-7

48 Brombach, Hansjörg: *Automatisierung der Bewirtschaftung von Wasserspeichern*, 1981, ISBN 3-921694-48-5

49 Geldner, Peter: *Deterministische und stochastische Methoden zur Bestimmung der Selbstdichtung von Gewässern*, 1981, ISBN 3-921694-49-3, vergriffen

50 Mehlhorn, Hans: *Temperaturveränderungen im Grundwasser durch Brauchwassereinleitungen*, 1982, ISBN 3-921694-50-7, vergriffen

51 Hafner, Edzard: *Rohrleitungen und Behälter im Meer*, 1983, ISBN 3-921694-51-5

52 Rinnert, Bernd: *Hydrodynamische Dispersion in porösen Medien: Einfluß von Dichteunterschieden auf die Vertikalvermischung in horizontaler Strömung*, 1983, ISBN 3-921694-52-3, vergriffen

53 Lindner, Wulf: *Steuerung von Grundwasserentnahmen unter Einhaltung ökologischer Kriterien*, 1983, ISBN 3-921694-53-1, vergriffen

54 Herr, Michael; Herzer, Jörg; Kinzelbach, Wolfgang; Kobus, Helmut; Rinnert, Bernd: *Methoden zur rechnerischen Erfassung und hydraulischen Sanierung von Grundwasserkontaminationen*, 1983, ISBN 3-921694-54-X

55 Schmitt, Paul: *Wege zur Automatisierung der Niederschlagsermittlung*, 1984, ISBN 3-921694-55-8, vergriffen

56 Müller, Peter: *Transport und selektive Sedimentation von Schwebstoffen bei gestautem Abfluß*, 1985, ISBN 3-921694-56-6

57 El-Qawasmeh, Fuad: *Möglichkeiten und Grenzen der Tropfbewässerung unter besonderer Berücksichtigung der Verstopfungsanfälligkeit der Tropfelemente*, 1985, ISBN 3-921694-57-4, vergriffen

58 Kirchenbaur, Klaus: *Mikroprozessorgesteuerte Erfassung instationärer Druckfelder am Beispiel seegangsbelasteter Baukörper*, 1985, ISBN 3-921694-58-2

59 Kobus, Helmut (Hrsg.): *Modellierung des großräumigen Wärme- und Schadstofftransports im Grundwasser*, Tätigkeitsbericht 1984/85 (DFG-Forschergruppe an den Universitäten Hohenheim, Karlsruhe und Stuttgart), 1985, ISBN 3-921694-59-0, vergriffen

60 Spitz, Karlheinz: *Dispersion in porösen Medien: Einfluß von Inhomogenitäten und Dichteunterschieden*, 1985, ISBN 3-921694-60-4, vergriffen

61 Kobus, Helmut: *An Introduction to Air-Water Flows in Hydraulics*, 1985, ISBN 3-921694-61-2

62 Kaleris, Vassilios: *Erfassung des Austausches von Oberflächen- und Grundwasser in horizontalebenen Grundwassermodellen*, 1986, ISBN 3-921694-62-0

63 Herr, Michael: *Grundlagen der hydraulischen Sanierung verunreinigter Porengrundwasserleiter*, 1987, ISBN 3-921694-63-9

64 Marx, Walter: *Berechnung von Temperatur und Spannung in Massenbeton infolge Hydratation*, 1987, ISBN 3-921694-64-7

65 Koschitzky, Hans-Peter: *Dimensionierungskonzept für Sohlbelüfter in Schußrinnen zur Vermeidung von Kavitationsschäden*, 1987, ISBN 3-921694-65-5

66 Kobus, Helmut (Hrsg.): *Modellierung des großräumigen Wärme- und Schadstofftransports im Grundwasser*, Tätigkeitsbericht 1986/87 (DFG-Forschergruppe an den Universitäten Hohenheim, Karlsruhe und Stuttgart) 1987, ISBN 3-921694-66-3

67 Söll, Thomas: *Berechnungsverfahren zur Abschätzung anthropogener Temperaturanomalien im Grundwasser*, 1988, ISBN 3-921694-67-1

68 Dittrich, Andreas; Westrich, Bernd: *Bodenseeufererosion, Bestandsaufnahme und Bewertung*, 1988, ISBN 3-921694-68-X, vergriffen

69 Huwe, Bernd; van der Ploeg, Rienk R.: *Modelle zur Simulation des Stickstoffhaushaltes von Standorten mit unterschiedlicher landwirtschaftlicher Nutzung*, 1988, ISBN 3-921694-69-8, vergriffen

70 Stephan, Karl: *Integration elliptischer Funktionen*, 1988, ISBN 3-921694-70-1

71 Kobus, Helmut; Zilliox, Lothaire (Hrsg.): *Nitratbelastung des Grundwassers, Auswirkungen der Landwirtschaft auf die Grundwasser- und Rohwasserbeschaffenheit und Maßnahmen zum Schutz des Grundwassers*. Vorträge des deutsch-französischen Kolloquiums am 6. Oktober 1988, Universitäten Stuttgart und Louis Pasteur Strasbourg (Vorträge in deutsch oder französisch, Kurzfassungen zweisprachig), 1988, ISBN 3-921694-71-X

72 Soyeaux, Renald: *Unterströmung von Stauanlagen auf klüftigem Untergrund unter Berücksichtigung laminarer und turbulenter Fließzustände*,1991, ISBN 3-921694-72-8

73 Kohane, Roberto: *Berechnungsmethoden für Hochwasserabfluß in Fließgewässern mit überströmten Vorländern*, 1991, ISBN 3-921694-73-6

74 Hassinger, Reinhard: *Beitrag zur Hydraulik und Bemessung von Blocksteinrampen in flexibler Bauweise*, 1991, ISBN 3-921694-74-4, vergriffen

75 Schäfer, Gerhard: *Einfluß von Schichtenstrukturen und lokalen Einlagerungen auf die Längsdispersion in Porengrundwasserleitern*, 1991, ISBN 3-921694-75-2

76 Giesecke, Jürgen: *Vorträge, Wasserwirtschaft in stark besiedelten Regionen; Umweltforschung mit Schwerpunkt Wasserwirtschaft*, 1991, ISBN 3-921694-76-0

77 Huwe, Bernd: *Deterministische und stochastische Ansätze zur Modellierung des Stickstoffhaushalts landwirtschaftlich genutzter Flächen auf unterschiedlichem Skalenniveau*, 1992, ISBN 3-921694-77-9, vergriffen

78 Rommel, Michael: *Verwendung von Kluftdaten zur realitätsnahen Generierung von Kluftnetzen mit anschließender laminar-turbulenter Strömungsberechnung*, 1993, ISBN 3-92 1694-78-7

79 Marschall, Paul: *Die Ermittlung lokaler Stofffrachten im Grundwasser mit Hilfe von Einbohrloch-Meßverfahren*, 1993, ISBN 3-921694-79-5, vergriffen

80 Ptak, Thomas: *Stofftransport in heterogenen Porenaquiferen: Felduntersuchungen und stochastische Modellierung*, 1993, ISBN 3-921694-80-9, vergriffen

81 Haakh, Frieder: *Transientes Strömungsverhalten in Wirbelkammern,* 1993, ISBN 3-921694-81-7

82 Kobus, Helmut; Cirpka, Olaf; Barczewski, Baldur; Koschitzky, Hans-Peter: *Versucheinrichtung zur Grundwasser und Altlastensanierung VEGAS, Konzeption und Programmrahmen*, 1993, ISBN 3-921694-82-5

83 Zang, Weidong: *Optimaler Echtzeit-Betrieb eines Speichers mit aktueller Abflußregenerierung*, 1994, ISBN 3-921694-83-3, vergriffen

84 Franke, Hans-Jörg: *Stochastische Modellierung eines flächenhaften Stoffeintrages und Transports in Grundwasser am Beispiel der Pflanzenschutzmittelproblematik*, 1995, ISBN 3-921694-84-1

85 Lang, Ulrich: *Simulation regionaler Strömungs- und Transportvorgänge in Karstaquiferen mit Hilfe des Doppelkontinuum-Ansatzes: Methodenentwicklung und Parameteridentifikation*, 1995, ISBN 3-921694-85-X, vergriffen

86 Helmig, Rainer: *Einführung in die Numerischen Methoden der Hydromechanik*, 1996, ISBN 3-921694-86-8, vergriffen

87 Cirpka, Olaf: *CONTRACT: A Numerical Tool for Contaminant Transport and Chemical Transformations - Theory and Program Documentation* -, 1996, ISBN 3-921694-87-6

88 Haberlandt, Uwe: *Stochastische Synthese und Regionalisierung des Niederschlages für Schmutzfrachtberechnungen*, 1996, ISBN 3-921694-88-4

89 Croisé, Jean: *Extraktion von flüchtigen Chemikalien aus natürlichen Lockergesteinen mittels erzwungener Luftströmung*, 1996, ISBN 3-921694-89-2, vergriffen

90 Jorde, Klaus: *Ökologisch begründete, dynamische Mindestwasserregelungen bei Ausleitungskraftwerken*, 1997, ISBN 3-921694-90-6, vergriffen

91 Helmig, Rainer: *Gekoppelte Strömungs- und Transportprozesse im Untergrund - Ein Beitrag zur Hydrosystemmodellierung*-, 1998, ISBN 3-921694-91-4, vergriffen

92 Emmert, Martin: *Numerische Modellierung nichtisothermer Gas-Wasser Systeme in porösen Medien,* 1997, ISBN 3-921694-92-2

93 Kern, Ulrich: *Transport von Schweb- und Schadstoffen in staugeregelten Fließgewässern am Beispiel des Neckars*, 1997, ISBN 3-921694-93-0, vergriffen

94 Förster, Georg: *Druckstoßdämpfung durch große Luftblasen in Hochpunkten von Rohrleitungen 1997*, ISBN 3-921694-94-9

95 Cirpka, Olaf: *Numerische Methoden zur Simulation des reaktiven Mehrkomponententransports im Grundwasser*, 1997, ISBN 3-921694-95-7, vergriffen

96 Färber, Arne: *Wärmetransport in der ungesättigten Bodenzone: Entwicklung einer thermischen In-situ-Sanierungstechnologie*, 1997, ISBN 3-921694-96-5

97 Betz, Christoph: *Wasserdampfdestillation von Schadstoffen im porösen Medium: Entwicklung einer thermischen In-situ-Sanierungstechnologie*, 1998, ISBN 3-921694-97-3

98 Xu, Yichun: *Numerical Modeling of Suspended Sediment Transport in Rivers*, 1998, ISBN 3-921694-98-1, vergriffen

99 Wüst, Wolfgang: *Geochemische Untersuchungen zur Sanierung CKW-kontaminierter Aquifere mit Fe(0)-Reaktionswänden,* 2000, ISBN 3-933761-02-2

100 Sheta, Hussam: *Simulation von Mehrphasenvorgängen in porösen Medien unter Einbeziehung von Hysterese-Effekten*, 2000, ISBN 3-933761-03-4

101 Ayros, Edwin: *Regionalisierung extremer Abflüsse auf der Grundlage statistischer Verfahren*, 2000, ISBN 3-933761-04-2, vergriffen

102 Huber, Ralf: *Compositional Multiphase Flow and Transport in Heterogeneous Porous Media*, 2000, ISBN 3-933761-05-0

103 Braun, Christopherus: *Ein Upscaling-Verfahren für Mehrphasenströmungen in porösen Medien*, 2000, ISBN 3-933761-06-9

104 Hofmann, Bernd: *Entwicklung eines rechnergestützten Managementsystems zur Beurteilung von Grundwasserschadensfällen*, 2000, ISBN 3-933761-07-7

105 Class, Holger: *Theorie und numerische Modellierung nichtisothermer Mehrphasenprozesse in NAPL-kontaminierten porösen Medien,* 2001, ISBN 3-933761-08-5

106 Schmidt, Reinhard: *Wasserdampf- und Heißluftinjektion zur thermischen Sanierung kontaminierter Standorte*, 2001, ISBN 3-933761-09-3

107 Josef, Reinhold:, *Schadstoffextraktion mit hydraulischen Sanierungsverfahren unter Anwendung von grenzflächenaktiven Stoffen*, 2001, ISBN 3-933761-10-7

108 Schneider, Matthias: *Habitat- und Abflussmodellierung für Fließgewässer mit unscharfen Berechnungsansätzen*, 2001, ISBN 3-933761-11-5

109 Rathgeb, Andreas: *Hydrodynamische Bemessungsgrundlagen für Lockerdeckwerke an überströmbaren Erddämmen*, 2001, ISBN 3-933761-12-3

110 Lang, Stefan: *Parallele numerische Simulation instätionärer Probleme mit adaptiven Methoden auf unstrukturierten Gittern*, 2001, ISBN 3-933761-13-1

111 Appt, Jochen; Stumpp Simone: *Die Bodensee-Messkampagne 2001, IWS/CWR Lake Constance Measurement Program 2001*, 2002, ISBN 3-933761-14-X

112 Heimerl, Stephan: *Systematische Beurteilung von Wasserkraftprojekten,* 2002, ISBN 3-933761-15-8, vergriffen

113 Iqbal, Amin: *On the Management and Salinity Control of Drip Irrigation,* 2002, ISBN 3-933761-16-6

114 Silberhorn-Hemminger, Annette: *Modellierung von Kluftaquifersystemen: Geostatistische Analyse und deterministisch-stochastische Kluftgenerierung,* 2002, ISBN 3-933761-17-4

115 Winkler, Angela: *Prozesse des Wärme- und Stofftransports bei der In-situ-Sanierung mit festen Wärmequellen,* 2003, ISBN 3-933761-18-2

116 Marx, Walter: *Wasserkraft, Bewässerung, Umwelt - Planungs- und Bewertungsschwerpunkte der Wasserbewirtschaftung,* 2003, ISBN 3-933761-19-0

117 Hinkelmann, Reinhard: *Efficient Numerical Methods and Information-Processing Techniques in Environment Water,* 2003, ISBN 3-933761-20-4

118 Samaniego-Eguiguren, Luis Eduardo: *Hydrological Consequences of Land Use / Land Cover and Climatic Changes in Mesoscale Catchments*, 2003, ISBN 3-933761-21-2

119 Neunhäuserer, Lina: *Diskretisierungsansätze zur Modellierung von Strömungs- und Transportprozessen in geklüftet-porösen Medien*, 2003, ISBN 3-933761-22-0

120 Paul, Maren: *Simulation of Two-Phase Flow in Heterogeneous Poros Media with Adaptive Methods*, 2003, ISBN 3-933761-23-9

121 Ehret, Uwe: *Rainfall and Flood Nowcasting in Small Catchments using Weather Radar*, 2003, ISBN 3-933761-24-7

122 Haag, Ingo: *Der Sauerstoffhaushalt staugeregelter Flüsse am Beispiel des Neckars - Analysen, Experimente, Simulationen -,* 2003, ISBN 3-933761-25-5

123 Appt, Jochen: *Analysis of Basin-Scale Internal Waves in Upper Lake Constance,* 2003, ISBN 3-933761-26-3

124 Hrsg.: Schrenk, Volker; Batereau, Katrin; Barczewski, Baldur; Weber, Karolin und Koschitzky, Hans-Peter: *Symposium Ressource Fläche und VEGAS - Statuskolloquium 2003, 30. September und 1. Oktober 2003,* 2003, ISBN 3-933761-27-1

125 Omar Khalil Ouda: *Optimisation of Agricultural Water Use: A Decision Support System for the Gaza Strip,* 2003, ISBN 3-933761-28-0

126 Batereau, Katrin: *Sensorbasierte Bodenluftmessung zur Vor-Ort-Erkundung von Schadensherden im Untergrund*, 2004, ISBN 3-933761-29-8

127 Witt, Oliver: *Erosionsstabilität von Gewässersedimenten mit Auswirkung auf den Stofftransport bei Hochwasser am Beispiel ausgewählter Stauhaltungen des Oberrheins*, 2004, ISBN 3-933761-30-1

128 Jakobs, Hartmut: *Simulation nicht-isothermer Gas-Wasser-Prozesse in komplexen Kluft-Matrix-Systemen*, 2004, ISBN 3-933761-31-X

129 Li, Chen-Chien: *Deterministisch-stochastisches Berechnungskonzept zur Beurteilung der Auswirkungen erosiver Hochwasserereignisse in Flussstauhaltungen,* 2004, ISBN 3-933761-32-8

130 Reichenberger, Volker; Helmig, Rainer; Jakobs, Hartmut; Bastian, Peter; Niessner, Jennifer: *Complex Gas-Water Processes in Discrete Fracture-Matrix Systems: Upscaling, Mass-Conservative Discretization and Efficient Multilevel Solution,* 2004, ISBN 3-933761-33-6

131 Hrsg.: Barczewski, Baldur; Koschitzky, Hans-Peter; Weber, Karolin; Wege, Ralf: *VEGAS - Statuskolloquium 2004,* Tagungsband zur Veranstaltung am 05. Oktober 2004 an der Universität Stuttgart, Campus Stuttgart-Vaihingen, 2004, ISBN 3-933761-34-4

132 Asie, Kemal Jabir: *Finite Volume Models for Multiphase Multicomponent Flow through Porous Media*. 2005, ISBN 3-933761-35-2

133 Jacoub, George: *Development of a 2-D Numerical Module for Particulate Contaminant Transport in Flood Retention Reservoirs and Impounded Rivers,* 2004, ISBN 3-933761-36-0

134 Nowak, Wolfgang: *Geostatistical Methods for the Identification of Flow and Transport Parameters in the Subsurface,* 2005, ISBN 3-933761-37-9

135 Süß, Mia: *Analysis of the influence of structures and boundaries on flow and transport processes in fractured porous media*, 2005, ISBN 3-933761-38-7

136 Jose, Surabhin Chackiath: *Experimental Investigations on Longitudinal Dispersive Mixing in Heterogeneous Aquifers,* 2005, ISBN: 3-933761-39-5

137 Filiz, Fulya: *Linking Large-Scale Meteorological Conditions to Floods in Mesoscale Catchments,* 2005, ISBN 3-933761-40-9

138 Qin, Minghao: *Wirklichkeitsnahe und recheneffiziente Ermittlung von Temperatur und Spannungen bei großen RCC-Staumauern*, 2005, ISBN 3-933761-41-7

139 Kobayashi, Kenichiro: *Optimization Methods for Multiphase Systems in the Subsurface - Application to Methane Migration in Coal Mining Areas*, 2005, ISBN 3-933761-42-5

140 Rahman, Md. Arifur: *Experimental Investigations on Transverse Dispersive Mixing in Heterogeneous Porous Media,* 2005, ISBN 3-933761-43-3

141 Schrenk, Volker: *Ökobilanzen zur Bewertung von Altlastensanierungsmaßnahmen,* 2005, ISBN 3-933761-44-1

142 Hundecha, Hirpa Yeshewatesfa: *Regionalization of Parameters of a Conceptual Rainfall-Runoff Model*, 2005, ISBN: 3-933761-45-X

143 Wege, Ralf: *Untersuchungs- und Überwachungsmethoden für die Beurteilung natürlicher Selbstreinigungsprozesse im Grundwasser,* 2005, ISBN 3-933761-46-8

144 Breiting, Thomas: *Techniken und Methoden der Hydroinformatik - Modellierung von komplexen Hydrosystemen im Untergrund*, 2006, 3-933761-47-6

145 Hrsg.: Braun, Jürgen; Koschitzky, Hans-Peter; Müller, Martin: *Ressource Untergrund: 10 Jahre VEGAS: Forschung und Technologieentwicklung zum Schutz von Grundwasser und Boden,* Tagungsband zur Veranstaltung am 28. und 29. September 2005 an der Universität Stuttgart, Campus Stuttgart-Vaihingen, 2005, ISBN 3-933761-48-4

146 Rojanschi, Vlad: *Abflusskonzentration in mesoskaligen Einzugsgebieten unter Berücksichtigung des Sickerraumes,* 2006, ISBN 3-933761-49-2

147 Winkler, Nina Simone: *Optimierung der Steuerung von Hochwasserrückhaltebecken-systemen,* 2006, ISBN 3-933761-50-6

148 Wolf, Jens: *Räumlich differenzierte Modellierung der Grundwasserströmung alluvialer Aquifere für mesoskalige Einzugsgebiete*, 2006, ISBN: 3-933761-51-4

149 Kohler, Beate: *Externe Effekte der Laufwasserkraftnutzung*, 2006, ISBN 3-933761-52-2

150 Hrsg.: Braun, Jürgen; Koschitzky, Hans-Peter; Stuhrmann, Matthias: *VEGAS-Statuskolloquium 2006,* Tagungsband zur Veranstaltung am 28. September 2006 an der Universität Stuttgart, Campus Stuttgart-Vaihingen, 2006, ISBN 3-933761-53-0

151 Niessner, Jennifer: *Multi-Scale Modeling of Multi-Phase - Multi-Component Processes in Heterogeneous Porous Media*, 2006, ISBN 3-933761-54-9

152 Fischer, Markus: *Beanspruchung eingeerdeter Rohrleitungen infolge Austrocknung bindiger Böden,* 2006, ISBN 3-933761-55-7

153 Schneck, Alexander: *Optimierung der Grundwasserbewirtschaftung unter Berücksichtigung der Belange der Wasserversorgung, der Landwirtschaft und des Naturschutzes*, 2006, ISBN 3-933761-56-5

154 Das, Tapash: *The Impact of Spatial Variability of Precipitation on the Predictive Uncertainty of Hydrological Models,* 2006, ISBN 3-933761-57-3

155 Bielinski, Andreas: *Numerical Simulation of CO_2 sequestration in geological formations*, 2007, ISBN 3-933761-58-1

156 Mödinger, Jens: *Entwicklung eines Bewertungs- und Entscheidungsunterstützungssystems für eine nachhaltige regionale Grundwasserbewirtschaftung*, 2006, ISBN 3-933761-60-3

157 Manthey, Sabine: *Two-phase flow processes with dynamic effects in porous media - parameter estimation and simulation,* 2007, ISBN 3-933761-61-1

158 Pozos Estrada, Oscar: *Investigation on the Effects of Entrained Air in Pipelines,* 2007, ISBN 3-933761-62-X

159 Ochs, Steffen Oliver: *Steam injection into saturated porous media – process analysis including experimental and numerical investigations*, 2007, ISBN 3-933761-63-8

160 Marx, Andreas: *Einsatz gekoppelter Modelle und Wetterradar zur Abschätzung von Niederschlagsintensitäten und zur Abflussvorhersage, 2007,* ISBN 3-933761-64-6

161 Hartmann, Gabriele Maria: *Investigation of Evapotranspiration Concepts in Hydrological Modelling for Climate Change Impact Assessment*, 2007, ISBN 3-933761-65-4

162 Kebede Gurmessa, Tesfaye: *Numerical Investigation on Flow and Transport Characteristics to Improve Long-Term Simulation of Reservoir Sedimentation*, 2007, ISBN 3-933761-66-2

163 Trifković, Aleksandar: *Multi-objective and Risk-based Modelling Methodology for Planning, Design and Operation of Water Supply Systems*, 2007, ISBN 3-933761-67-0

164 Götzinger, Jens: *Distributed Conceptual Hydrological Modelling - Simulation of Climate, Land Use Change Impact and Uncertainty Analysis*, 2007, ISBN 3-933761-68-9

165 Hrsg.: Braun, Jürgen; Koschitzky, Hans-Peter; Stuhrmann, Matthias: *VEGAS – Kolloquium 2007,* Tagungsband zur Veranstaltung am 26. September 2007 an der Universität Stuttgart, Campus Stuttgart-Vaihingen, 2007, ISBN 3-933761-69-7

166 Freeman, Beau: *Modernization Criteria Assessment for Water Resources Planning; Klamath Irrigation Project, U.S.*, 2008, ISBN 3-933761-70-0

167 Dreher, Thomas: *Selektive Sedimentation von Feinstschwebstoffen in Wechselwirkung mit wandnahen turbulenten Strömungsbedingungen*, 2008, ISBN 3-933761-71-9

168 Yang, Wei: *Discrete-Continuous Downscaling Model for Generating Daily Precipitation Time Series*, 2008, ISBN 3-933761-72-7

169 Kopecki, Ianina: *Calculational Approach to FST-Hemispheres for Multiparametrical Benthos Habitat Modelling,* 2008*,* ISBN 3-933761-73-5

170 Brommundt, Jürgen: *Stochastische Generierung räumlich zusammenhängender Niederschlagszeitreihen*, 2008, ISBN 3-933761-74-3

171 Papafotiou, *Alexandros: Numerical Investigations of the Role of Hysteresis in Heterogeneous Two-Phase Flow Systems*, 2008, ISBN 3-933761-75-1

172 He, Yi: *Application of a Non-Parametric Classification Scheme to Catchment Hydrology*, 2008, ISBN 978-3-933761-76-7

173 Wagner, Sven: *Water Balance in a Poorly Gauged Basin in West Africa Using Atmospheric Modelling and Remote Sensing Information*, 2008, ISBN 978-3-933761-77-4

174 Hrsg.: Braun, Jürgen; Koschitzky, Hans-Peter; Stuhrmann, Matthias; Schrenk, Volker: *VEGAS-Kolloquium 2008 Ressource Fläche III*, Tagungsband zur Veranstaltung am 01. Oktober 2008 an der Universität Stuttgart, Campus Stuttgart-Vaihingen, 2008, ISBN 978-3-933761-78-1

175 Patil, Sachin: *Regionalization of an Event Based Nash Cascade Model for Flood Predictions in Ungauged Basins*, 2008, ISBN 978-3-933761-79-8

176 Assteerawatt, Anongnart: *Flow and Transport Modelling of Fractured Aquifers based on a Geostatistical Approach,* 2008, ISBN 978-3-933761-80-4

177 Karnahl, Joachim Alexander: *2D numerische Modellierung von multifraktionalem Schwebstoff- und Schadstofftransport in Flüssen*, 2008, ISBN 978-3-933761-81-1

178 Hiester, Uwe: *Technologieentwicklung zur In-situ-Sanierung der ungesättigten Bodenzone mit festen Wärmequellen,* 2009, ISBN 978-3-933761-82-8

179 Laux, Patrick: *Statistical Modeling of Precipitation for Agricultural Planning in the Volta Basin of West Africa,* 2009, ISBN 978-3-933761-83-5

180 Ehsan, Saqib: *Evaluation of Life Safety Risks Related to Severe Flooding,* 2009, ISBN 978-3-933761-84-2

181 Prohaska, Sandra: *Development and Application of a 1D Multi-Strip Fine Sediment Transport Model for Regulated Rivers,* 2009, ISBN 978-3-933761-85-9

182 Kopp, Andreas: *Evaluation of CO_2 Injection Processes in Geological Formations for Site Screening,* 2009, ISBN 978-3-933761-86-6

183 Ebigbo, Anozie: *Modelling of biofilm growth and its influence on CO_2 and water (two-phase) flow in porous media,* 2009, ISBN 978-3-933761-87-3

184 Freiboth, Sandra: *A phenomenological model for the numerical simulation of multiphase multicomponent processes considering structural alterations of porous media*, 2009, ISBN 978-3-933761-88-0

185 Zöllner, Frank: *Implementierung und Anwendung netzfreier Methoden im Konstruktiven Wasserbau und in der Hydromechanik*, 2009, ISBN 978-3-933761-89-7

186 Vasin, Milos: *Influence of the soil structure and property contrast on flow and transport in the unsaturated zone*, 2010, ISBN 978-3-933761-90-3

187 Li, Jing: *Application of Copulas as a New Geostatistical Tool*, 2010, ISBN 978-3-933761-91-0

188 AghaKouchak, Amir: *Simulation of Remotely Sensed Rainfall Fields Using Copulas*, 2010, ISBN 978-3-933761-92-7

189 Thapa, Pawan Kumar: *Physically-based spatially distributed rainfall runoff modelling for soil erosion estimation*, 2010, ISBN 978-3-933761-93-4

190 Wurms, Sven: *Numerische Modellierung der Sedimentationsprozesse in Retentionsanlagen zur Steuerung von Stoffströmen bei extremen Hochwasserabflussereignissen*, 2011, ISBN 978-3-933761-94-1

191 Merkel, Uwe: *Unsicherheitsanalyse hydraulischer Einwirkungen auf Hochwasserschutzdeiche und Steigerung der Leistungsfähigkeit durch adaptive Strömungsmodellierung*, 2011, ISBN 978-3-933761-95-8

192 Fritz, Jochen: *A Decoupled Model for Compositional Non-Isothermal Multiphase Flow in Porous Media and Multiphysics Approaches for Two-Phase Flow*, 2010, ISBN 978-3-933761-96-5

193 Weber, Karolin (Hrsg.): *12. Treffen junger WissenschaftlerInnen an Wasserbauinstituten*, 2010, ISBN 978-3-933761-97-2

194 Bliefernicht, Jan-Geert: *Probability Forecasts of Daily Areal Precipitation for Small River Basins,* 2011, ISBN 978-3-933761-98-9

195 Hrsg.: Koschitzky, Hans-Peter; Braun, Jürgen: *VEGAS-Kolloquium 2010 In-situ-Sanierung - Stand und Entwicklung Nano und ISCO -,* Tagungsband zur Veranstaltung am 07. Oktober 2010 an der Universität Stuttgart, Campus Stuttgart-Vaihingen, 2010, ISBN 978-3-933761-99-6

196 Gafurov, Abror: *Water Balance Modeling Using Remote Sensing Information - Focus on Central Asia,* 2010, ISBN 978-3-942036-00-9

197 Mackenberg, Sylvia: *Die Quellstärke in der Sickerwasserprognose: Möglichkeiten und Grenzen von Labor- und Freilanduntersuchungen,* 2010, ISBN 978-3-942036-01-6

198 Singh, Shailesh Kumar: *Robust Parameter Estimation in Gauged and Ungauged Basins,* 2010, ISBN 978-3-942036-02-3

199 Doğan, Mehmet Onur: *Coupling of porous media flow with pipe flow,* 2011, ISBN 978-3-942036-03-0

200 Liu, Min: *Study of Topographic Effects on Hydrological Patterns and the Implication on Hydrological Modeling and Data Interpolation,* 2011, ISBN 978-3-942036-04-7

201 Geleta, Habtamu Itefa: *Watershed Sediment Yield Modeling for Data Scarce Areas,* 2011, ISBN 978-3-942036-05-4

202 Franke, Jörg: *Einfluss der Überwachung auf die Versagenswahrscheinlichkeit von Staustufen,* 2011, ISBN 978-3-942036-06-1

203 Bakimchandra, Oinam: *Integrated Fuzzy-GIS approach for assessing regional soil erosion risks,* 2011, ISBN 978-3-942036-07-8

204 Alam, Muhammad Mahboob: *Statistical Downscaling of Extremes of Precipitation in Mesoscale Catchments from Different RCMs and Their Effects on Local Hydrology,* 2011, ISBN 978-3-942036-08-5

205 Hrsg.: Koschitzky, Hans-Peter; Braun, Jürgen: *VEGAS-Kolloquium 2011 Flache Geothermie - Perspektiven und Risiken,* Tagungsband zur Veranstaltung am 06. Oktober 2011 an der Universität Stuttgart, Campus Stuttgart-Vaihingen, 2011, ISBN 978-3-933761-09-2

206 Haslauer, Claus: *Analysis of Real-World Spatial Dependence of Subsurface Hydraulic Properties Using Copulas with a Focus on Solute Transport Behaviour,* 2011, ISBN 978-3-942036-10-8

207 Dung, Nguyen Viet: *Multi-objective automatic calibration of hydrodynamic models – development of the concept and an application in the Mekong Delta,* 2011, ISBN 978-3-942036-11-5

208 Hung, Nguyen Nghia: *Sediment dynamics in the floodplain of the Mekong Delta, Vietnam,* 2011, ISBN 978-3-942036-12-2

Die Mitteilungshefte ab der Nr. 134 (Jg. 2005) stehen als pdf-Datei über die Homepage des Instituts: www.iws.uni-stuttgart.de zur Verfügung.